Online ISSN: 2249-4596
Print ISSN: 0975-5861
DOI: 10.17406/GJRE

GLOBAL JOURNAL

OF RESEARCHES IN ENGINEERING: C

Chemical Engineering

Highlights

- Austenitic Stainless Steels
- Oxygen Atoms in Ceria-Zirconia
- Artificial Oil Field Formation
- Catalyst Particle Membrane Filter

Discovering Thoughts, Inventing Future

VOLUME 23 ISSUE 1 VERSION 1.0

GLOBAL JOURNAL OF RESEARCHES IN ENGINEERING: C

CHEMICAL ENGINEERING

GLOBAL JOURNAL OF RESEARCHES IN ENGINEERING: C
CHEMICAL ENGINEERING

VOLUME 23 ISSUE 1 (VER. 1.0)

OPEN ASSOCIATION OF RESEARCH SOCIETY

© Global Journal of
Researches in Engineering.
2023.

All rights reserved.

This is a special issue published in version 1.0 of "Global Journal of Researches in Engineering." By Global Journals Inc.

All articles are open access articles distributed under "Global Journal of Researches in Engineering"

Reading License, which permits restricted use. Entire contents are copyright by of "Global Journal of Researches in Engineering" unless otherwise noted on specific articles.

No part of this publication may be reproduced or transmitted in any form or by any means, electronic or mechanical, including photocopy, recording, or any information storage and retrieval system, without written permission.

The opinions and statements made in this book are those of the authors concerned. Ultraculture has not verified and neither confirms nor denies any of the foregoing and no warranty or fitness is implied.

Engage with the contents herein at your own risk.

The use of this journal, and the terms and conditions for our providing information, is governed by our Disclaimer, Terms and Conditions and Privacy Policy given on our website http://globaljournals.us/terms-and-condition/menu-id-1463/.

By referring / using / reading / any type of association / referencing this journal, this signifies and you acknowledge that you have read them and that you accept and will be bound by the terms thereof.

All information, journals, this journal, activities undertaken, materials, services and our website, terms and conditions, privacy policy, and this journal is subject to change anytime without any prior notice.

Incorporation No.: 0423089
License No.: 42125/022010/1186
Registration No.: 430374
Import-Export Code: 1109007027
Employer Identification Number (EIN):
USA Tax ID: 98-0673427

Global Journals Inc.

*(A Delaware USA Incorporation with "Good Standing"; **Reg. Number: 0423089**)*
Sponsors: *Open Association of Research Society*
Open Scientific Standards

Publisher's Headquarters office

Global Journals® Headquarters
945th Concord Streets,
Framingham Massachusetts Pin: 01701,
United States of America
USA Toll Free: +001-888-839-7392
USA Toll Free Fax: +001-888-839-7392

Offset Typesetting

Global Journals Incorporated
2nd, Lansdowne, Lansdowne Rd., Croydon-Surrey,
Pin: CR9 2ER, United Kingdom

Packaging & Continental Dispatching

Global Journals Pvt Ltd
E-3130 Sudama Nagar, Near Gopur Square,
Indore, M.P., Pin:452009, India

Find a correspondence nodal officer near you

To find nodal officer of your country, please email us at *local@globaljournals.org*

eContacts

Press Inquiries: *press@globaljournals.org*
Investor Inquiries: *investors@globaljournals.org*
Technical Support: *technology@globaljournals.org*
Media & Releases: *media@globaljournals.org*

Pricing (Excluding Air Parcel Charges):

Yearly Subscription (Personal & Institutional)
250 USD (B/W) & 350 USD (Color)

EDITORIAL BOARD

GLOBAL JOURNAL OF RESEARCH IN ENGINEERING

Dr. Ren-Jye Dzeng

Professor Civil Engineering, National Chiao-Tung University, Taiwan Dean of General Affairs, Ph.D., Civil & Environmental Engineering, University of Michigan United States

Dr. Iman Hajirasouliha

Ph.D. in Structural Engineering, Associate Professor, Department of Civil and Structural Engineering, University of Sheffield, United Kingdom

Dr. Ye Tian

Ph.D. Electrical Engineering The Pennsylvania State University 121 Electrical, Engineering East University Park, PA 16802, United States

Dr. Eric M. Lui

Ph.D., Structural Engineering, Department of Civil & Environmental Engineering, Syracuse University United States

Dr. Zi Chen

Ph.D. Department of Mechanical & Aerospace Engineering, Princeton University, US Assistant Professor, Thayer School of Engineering, Dartmouth College, Hanover, United States

Dr. T.S. Jang

Ph.D. Naval Architecture and Ocean Engineering, Seoul National University, Korea Director, Arctic Engineering Research Center, The Korea Ship and Offshore Research Institute, Pusan National University, South Korea

Dr. Ephraim Suhir

Ph.D., Dept. of Mechanics and Mathematics, Moscow University Moscow, Russia Bell Laboratories Physical Sciences and Engineering Research Division United States

Dr. Pangil Choi

Ph.D. Department of Civil, Environmental, and Construction Engineering, Texas Tech University, United States

Dr. Xianbo Zhao

Ph.D. Department of Building, National University of Singapore, Singapore, Senior Lecturer, Central Queensland University, Australia

Dr. Zhou Yufeng

Ph.D. Mechanical Engineering & Materials Science, Duke University, US Assistant Professor College of Engineering, Nanyang Technological University, Singapore

Dr. Pallav Purohit

Ph.D. Energy Policy and Planning, Indian Institute of Technology (IIT), Delhi Research Scientist, International Institute for Applied Systems Analysis (IIASA), Austria

Dr. Balasubramani R

Ph.D., (IT) in Faculty of Engg. & Tech. Professor & Head, Dept. of ISE at NMAM Institute of Technology

Dr. Sofoklis S. Makridis

B.Sc(Hons), M.Eng, Ph.D. Professor Department of Mechanical Engineering University of Western Macedonia, Greece

Dr. Steffen Lehmann

Faculty of Creative and Cultural Industries Ph.D., AA Dip University of Portsmouth United Kingdom

Dr. Wenfang Xie

Ph.D., Department of Electrical Engineering, Hong Kong Polytechnic University, Department of Automatic Control, Beijing University of Aeronautics and Astronautics China

Dr. Hai-Wen Li

Ph.D., Materials Engineering, Kyushu University, Fukuoka, Guest Professor at Aarhus University, Japan

Dr. Saeed Chehreh Chelgani

Ph.D. in Mineral Processing University of Western Ontario, Adjunct professor, Mining engineering and Mineral processing, University of Michigan United States

Belen Riveiro

Ph.D., School of Industrial Engineering, University of Vigo Spain

Dr. Adel Al Jumaily

Ph.D. Electrical Engineering (AI), Faculty of Engineering and IT, University of Technology, Sydney

Dr. Maciej Gucma

Assistant Professor, Maritime Univeristy of Szczecin Szczecin, Ph.D.. Eng. Master Mariner, Poland

Dr. M. Meguellati

Department of Electronics, University of Batna, Batna 05000, Algeria

Dr. Haijian Shi

Ph.D. Civil Engineering Structural Engineering Oakland, CA, United States

Dr. Chao Wang

Ph.D. in Computational Mechanics Rosharon, TX, United States

Dr. Joaquim Carneiro

Ph.D. in Mechanical Engineering, Faculty of Engineering, University of Porto (FEUP), University of Minho, Department of Physics Portugal

Dr. Wei-Hsin Chen

Ph.D., National Cheng Kung University, Department of Aeronautics, and Astronautics, Taiwan

Dr. Bin Chen

B.Sc., M.Sc., Ph.D., Xian Jiaotong University, China. State Key Laboratory of Multiphase Flow in Power Engineering Xi?an Jiaotong University, China

Dr. Charles-Darwin Annan

Ph.D., Professor Civil and Water Engineering University Laval, Canada

Dr. Jalal Kafashan

Mechanical Engineering Division of Mechatronics KU Leuven, Belglum

Dr. Alex W. Dawotola

Hydraulic Engineering Section, Delft University of Technology, Stevinweg, Delft, Netherlands

Dr. Shun-Chung Lee

Department of Resources Engineering, National Cheng Kung University, Taiwan

Dr. Gordana Colovic

B.Sc Textile Technology, M.Sc. Technical Science Ph.D. in Industrial Management. The College of Textile? Design, Technology and Management, Belgrade, Serbia

Dr. Giacomo Risitano

Ph.D., Industrial Engineering at University of Perugia (Italy) "Automotive Design" at Engineering Department of Messina University (Messina) Italy

Dr. Maurizio Palesi

Ph.D. in Computer Engineering, University of Catania, Faculty of Engineering and Architecture Italy

Dr. Salvatore Brischetto

Ph.D. in Aerospace Engineering, Polytechnic University of Turin and in Mechanics, Paris West University Nanterre La D?fense Department of Mechanical and Aerospace Engineering, Polytechnic University of Turin, Italy

Dr. Wesam S. Alaloul

B.Sc., M.Sc., Ph.D. in Civil and Environmental Engineering, University Technology Petronas, Malaysia

Dr. Ananda Kumar Palaniappan

B.Sc., MBA, MED, Ph.D. in Civil and Environmental Engineering, Ph.D. University of Malaya, Malaysia, University of Malaya, Malaysia

Dr. Hugo Silva

Associate Professor, University of Minho, Department of Civil Engineering, Ph.D., Civil Engineering, University of Minho Portugal

Dr. Fausto Gallucci

Associate Professor, Chemical Process Intensification (SPI), Faculty of Chemical Engineering and Chemistry Assistant Editor, International J. Hydrogen Energy, Netherlands

Dr. Philip T Moore

Ph.D., Graduate Master Supervisor School of Information Science and engineering Lanzhou University China

Dr. Cesar M. A. Vasques

Ph.D., Mechanical Engineering, Department of Mechanical Engineering, School of Engineering, Polytechnic of Porto Porto, Portugal

Dr. Jun Wang

Ph.D. in Architecture, University of Hong Kong, China Urban Studies City University of Hong Kong, China

Dr. Stefano Invernizzi

Ph.D. in Structural Engineering Technical University of Turin, Department of Structural, Geotechnical and Building Engineering, Italy

Dr. Togay Ozbakkaloglu

B.Sc. in Civil Engineering, Ph.D. in Structural Engineering, University of Ottawa, Canada Senior Lecturer University of Adelaide, Australia

Dr. Zhen Yuan

B.E., Ph.D. in Mechanical Engineering University of Sciences and Technology of China, China Professor, Faculty of Health Sciences, University of Macau, China

Dr. Jui-Sheng Chou

Ph.D. University of Texas at Austin, U.S.A. Department of Civil and Construction Engineering National Taiwan University of Science and Technology (Taiwan Tech)

Dr. Houfa Shen

Ph.D. Manufacturing Engineering, Mechanical Engineering, Structural Engineering, Department of Mechanical Engineering, Tsinghua University, China

Prof. (LU), (UoS) Dr. Miklas Scholz

Cand Ing, BEng (equiv), PgC, MSc, Ph.D., CWEM, CEnv, CSci, CEng, FHEA, FIEMA, FCIWEM, FICE, Fellow of IWA, VINNOVA Fellow, Marie Curie Senior, Fellow, Chair in Civil Engineering (UoS) Wetland Systems, Sustainable Drainage, and Water Quality

Dr. Yudong Zhang

B.S., M.S., Ph.D. Signal and Information Processing, Southeast University Professor School of Information Science and Technology at Nanjing Normal University, China

Dr. Minghua He

Department of Civil Engineering Tsinghua University Beijing, 100084, China

Dr. Philip G. Moscoso

Technology and Operations Management IESE Business School, University of Navarra Ph.D. in Industrial Engineering and Management, ETH Zurich M.Sc. in Chemical Engineering, ETH Zurich, Spain

Dr. Stefano Mariani

Associate Professor, Structural Mechanics, Department of Civil and Environmental Engineering, Ph.D., in Structural Engineering Polytechnic University of Milan Italy

Dr. Ciprian Lapusan

Ph. D in Mechanical Engineering Technical University of Cluj-Napoca Cluj-Napoca (Romania)

Dr. Francesco Tornabene

Ph.D. in Structural Mechanics, University of Bologna Professor Department of Civil, Chemical, Environmental and Materials Engineering University of Bologna, Italy

Dr. Kitipong Jaojaruek

B. Eng, M. Eng, D. Eng (Energy Technology, Asian Institute of Technology). Kasetsart University Kamphaeng Saen (KPS) Campus Energy Research Laboratory of Mechanical Engineering

Dr. Burcin Becerik-Gerber

University of Southern Californi Ph.D. in Civil Engineering Ddes, from Harvard University M.S. from University of California, Berkeley M.S. from Istanbul, Technical University

Hiroshi Sekimoto

Professor Emeritus Tokyo Institute of Technology Japan Ph.D., University of California Berkeley

Dr. Shaoping Xiao

BS, MS Ph.D. Mechanical Engineering, Northwestern University The University of Iowa, Department of Mechanical and Industrial Engineering Center for Computer-Aided Design

Dr. A. Stegou-Sagia

Ph.D., Mechanical Engineering, Environmental Engineering School of Mechanical Engineering, National Technical University of Athens, Greece

Diego Gonzalez-Aguilera

Ph.D. Dep. Cartographic and Land Engineering, University of Salamanca, Avilla, Spain

Dr. Maria Daniela

Ph.D in Aerospace Science and Technologies Second University of Naples, Research Fellow University of Naples Federico II, Italy

Dr. Omid Gohardani

Ph.D. Senior Aerospace/Mechanical/ Aeronautical, Engineering professional M.Sc. Mechanical Engineering, M.Sc. Aeronautical Engineering B.Sc. Vehicle Engineering Orange County, California, US

Dr. Paolo Veronesi

Ph.D., Materials Engineering, Institute of Electronics, Italy President of the master Degree in Materials Engineering Dept. of Engineering, Italy

CONTENTS OF THE ISSUE

Global Journal of Researches in Engineering: C
Chemical Engineering
Volume 23 Issue 1 Version 1.0 Year 2023
Type: Double Blind Peer Reviewed International Research Journal
Publisher: Global Journals
Online ISSN: 2249-4596 & Print ISSN: 0975-5861

Evaluation of the Corrosion Behavior on Austenitic Stainless Steels in Artificial Oil Field Formation Water using Potentiodynamic and Potentiostatic Electrochemical Techniques

By Jorge Luiz Cardoso, Luís Flávio Gaspar Herculano, Pedro de Lima Neto & Marcelo José Gomes da Silva

Federal University of Ceará

Abstract- *Objective:* The main objective of this research was to evaluate the corrosion resistance of some austenitic and super austenitic stainless steel when immersed in an aqueous solution of artificial oil field formation water saturated with CO_2 and also without CO_2. With these two simulated situations, the pH effect of the solution on the corrosion resistance of the alloys was studied.

Methods: Samples of austenitic and super austenitic stainless steels previously characterized by x-ray diffraction using synchrotron light were used in this research. Two electrochemical techniques, one potentiodynamic and the other potentiostatic were used to investigate the effect of the solution on the corrosion behavior of the samples.

Keywords: *austenitic stainless steels, CO_2 corrosion resistance, aqueous solution, pitting corrosion, potential step, passive layer.*

GJRE-C Classification: *NLM: WC 800*

Evaluation of the Corrosion Behavior on Austenitic Stainless Steels in Artificial Oil Field Formation Water using Potentiodynamic and Potentiostatic Electrochemical Techniques

Jorge Luiz Cardoso α, Luís Flávio Gaspar Herculano σ, Pedro de Lima Neto ρ
& Marcelo José Gomes da Silva Ѡ

Abstract- Objective: The main objective of this research was to evaluate the corrosion resistance of some austenitic and super austenitic stainless steel when immersed in an aqueous solution of artificial oil field formation water saturated with CO_2 and also without CO_2. With these two simulated situations, the pH effect of the solution on the corrosion resistance of the alloys was studied.

Methods: Samples of austenitic and super austenitic stainless steels previously characterized by x-ray diffraction using synchrotron light were used in this research. Two electrochemical techniques, one potentiodynamic and the other potentiostatic were used to investigate the effect of the solution on the corrosion behavior of the samples. The linear polarization test was used to evaluate the CO_2 corrosion resistance of the alloys in artificial oil field formation water. The potentiostatic technique (potential step) was used to assess the influence of the solution without CO_2 on the corrosion resistance of the alloys, thus, varying the pH of the electrolyte. Scanning Electron Microscopy (SEM) was used to observe the type of corrosion on the surface of the samples.

Results: The results indicated that the type of corrosion found on the surface of the alloys was pitting corrosion. The pH effect of the solution (artificial oil field formation water) influenced the pits' shape. The conventional austenitic steels showed to have low corrosion resistance in chloride-containing environment. The super austenitic stainless steels presented a high corrosion resistance in the solution with and without CO_2. No pits or micro pits were observed on their surfaces by SEM.

Conclusion: From the results obtained, it was evident that the conventional austenitic stainless steels are not a good choice in severe environments like those found in the pre-salt region. The super austenitic stainless steels showed to be a good option in CO2-containing environments, mainly in aqueous solution with a high content of chloride.

Keywords: austenitic stainless steels, CO_2 corrosion resistance, aqueous solution, pitting corrosion, potential step, passive layer.

I. INTRODUCTION

The discoveries made in the pre-salt region (a geological formation of continental shelves) in Brazil are among the world's most important in the past decade. In this region, there is a considerable amount of good quality oil and this reality puts Brazil in a strategic position for the global demand for energy [1]. The discovery of this region brings several technological challenges for the oil and gas exploration. The corrosion process in this region occurs under specific conditions. Some of them are high temperatures between 80°C and 150°C, the presence of gases such as carbon dioxide (CO_2) and hydrogen sulfide (H_2S), oil formation water, high pressure, leaving the operating environment very hostile[2]. The main characteristic of the pre-salt region is the high content of sodium chloride (NaCl) found there. This NaCl, CO_2 and H_2S dissolved in the oil field formation water can accelerate the corrosion of metallic materials used for the oil exploration in the pre-salt region. Another concern for this operation is the environmental impact that can occur if these materials fail. Cheaper materials such as carbon steels are a good choice but there is a problem related to them: The difficulty in adding corrosion inhibitors for carbon steel pipes in offshore oil extraction at great depths. This has led to the increased use of corrosion resistant alloys[3]. Of all types of corrosion, localized corrosion, especially pitting corrosion, is the most common in marine waters and difficult to control. Currently, the oil and gas industry is concerned about the environmental impact caused by oil leaks in the marine ecosystem. This type of accident can be prevented using materials more resistant to the environmental conditions found in the pre-salt region. There are two types of technological challenges for the exploration of oil and gas contained in the pre-salt region: the other challenge consists of drilling the well as far as the reservoir, crossing water layers, sediment, and salt. Each layer with a different behavior at temperatures ranges from 50°C to 150°C under high pressures and corrosive gases, all these conditions acting together. The way back to the surface must also be considered.

Author α σ Ѡ: Department of Metallurgical and Materials Engineering, Federal University of Ceará, Fortaleza, CE, Brazil.
e-mail: jorgeluizjlc@gmail.com
Author ρ: Department of Analytical Chemistry and Physical Chemistry, Federal University of Ceará, Fortaleza, CE, Brazil.

All the oil and natural gas extracted from the well will be transported through the pipelines, and the material from which the pipes are made must resist all adverse conditions to avoid oil leaks. The second challenge is horizontal and consists of transporting the oil and gas from the production area to the coast, localized about 300 km away from the well location [1]. In summary, it is a set of problems that begins with the well's depth, passing by the coating when drilling into soft sediments through the salt layer to reach a very high temperature and pressure environment saturated with corrosive gases already mentioned[4]. Corrosion resistant-alloys such as super austenitic stainless steels are a great choice when considering the severe conditions of pre-salt. Due to their high chromium, nickel, and molybdenum content, it is expected that this kind of material presents more corrosion resistance in the pre-salt conditions than the conventional stainless steels. Some authors have already studied the corrosion resistance of austenitic stainless steel and other materials regarding the effect of CO_2[1,5–8]. For this paper, the effect of the oil field formation water with and without CO_2 was studied, taking into account two austenitic and two super austenitic stainless steels for later comparison. Two electrochemical techniques, one potentiodynamic and the other potentiostat were used to evaluate the corrosion resistance for these materials in artificial oil formation water.

a) Materials

For this research, the materials used were the AL-6XN PLUS™ super austenitic stainless steel, the 904L super austenitic stainless steel, and the 300 series austenitic stainless steels AISI 316L and 317L. The chemical composition of the materials studied presented in Table 1 were measured in an Optical Emission Spectrometer (PDA-7000 SHIMADZU). The Pitting Resistance Equivalent Number (PRE_N) was calculated using equation 1.

$$PREN = \%Cr + 3.3\ Mo + 30\%N \qquad (Eq.1)$$

Table 1: Chemical composition (wt%) of the studied alloys and the respective Pitting Resistance Equivalent Number (PRE_N)

Alloys	C	N	Mn	Si	Cr	Ni	Mo	PRE_N
316L	0.030	0.05	1.65	0.41	17.2	10.7	2.2	26
317L	0.024	0.06	1.49	0.40	17.8	12.3	3.5	31
904L	0.027	0.10	0.74	0.66	19.5	24.3	4.5	37
AL-6XN PLUS™	0.021	0.24	0.35	0.32	21.8	25.8	7.6	54

b) Characterization of the Samples

The samples in the as-received condition were characterized using x-ray diffraction (XRD) by Synchrotron Light (energy 12 keV) to detect the phases. ICDD database (International Centre for Diffraction Data) was used to identify the peaks of the phases. A Gleeble was used to fix the samples. The measurements were carried out at the Brazilian Synchrotron Light Laboratory in the city of Campinas-SP in Brazil. For this characterization, the shape and dimensions of the samples are shown in Figure 1.

c) Electrochemical Tests used

To evaluate the corrosion behavior of the materials, two electrochemical techniques were used: a potentiodynamic technique (linear polarization test) and a potentiostatic technique (potential steptest), one complementing the other. Firstly, the linear polarization technique was used to evaluate the effect of CO_2 on the corrosion behavior of the samples. The dimensions of the samples were 5.0 mm x 5.0 mm x 3.5 mm with an average exposure area of 39 mm^2. The samples were mounted in cold resin and ground using SiC paper up to 600 mesh, washed in distilled water, and then blow-dried. An adapted cell was used with two gas inlets, one for CO_2 and one for N_2. The cell also contained an input for a pH reader, in addition to the classic inputs for the three main electrodes (reference, working, and counter electrodes) in addition to a gas outlet (see Figure 2).The electrodes used were the samples (working electrode), as counter electrode a platinum electrode (93 mm^2), and the reference electrode used was the silver chloride silver ($Ag/AgCl/Cl^-sat$) saturated with KCl. The electrolyte used (artificial oil field formation water) was named by Petrobras of TQ 3219 which composition is shown in Table 2.

Table 2: Chemical composition of the artificial oil field formation water for 1 L of distilled water

Reagents	$CaSO_4$	$MgCl_2$	$NaHCO_3$	NaCl
C (g/L)	0.516	4.566	0.425	29

First, the solution was deaerated with N_2 gas to simulate the pre-salt environment (absence of free O_2) that could interfere with the results. The N_2 gas was bubbled into the solution until a pH of 8.2 ± 0.1. After this procedure, the solution was bubbled with CO_2 until saturation (pH 5.1 ± 0.1). In this procedure, the electrolyte became acidic. CO_2 gas in contact with an aqueous solution (oil field formation water) forms acids that react with the metallic elements of the alloy [9]. A potentiostat (AUTOLAB PGSTAT302N) connected to a microcomputer was used for both techniques. The software NOVA 1.9 was used to obtain data from the linear potential curves. Before the measurements, the samples were immersed for 30 min in the solution to determine the open circuit potential (OCP). The sweep of the polarization curves was -0.5 V to 1.2 V from the OCP with a sweep rate of 1 mV/s. After linear polarization tests, the samples were washed with water and sprayed with alcohol to clean the surface. Scanning Electron Microscopy (SEM) micrographs on the surfaces of the samples were obtained after corrosion tests for later comparison. The corrosion tests were reproduced in triplicate.

The potential step technique (potentiostatic technique) was also used to evaluate the corrosion behavior of the samples for the solution of artificial oil field formation water, this time with no CO_2 and no N_2. This test was intended to evaluate only the effect of the artificial oil field formation water on the surface of the samples. For this test, the samples were mounted in cold-curing epoxy resin, ground up to 600, rinsed with ethanol, and blow-dried before each measurement. The samples had the dimensions of 8.3 mm x 8.2 mm x 3.7 mm. To reduce crevice corrosion on the epoxy/steel, the specimens were coated with a lacquer leaving an exposed area of 1 cm^2. A three-electrode cell configuration was used. A saturated silver/silver chloride (Ag/AgCl) as reference electrode and a platinum electrode as a counter electrode were used. The electrolyte used was the same used in the linear polarization test (see Table 2). A potentiostat (AUTOLAB PGSTAT302N) connected to a microcomputer along with the software NOVA 1.9 was used. Before the measurements, the samples were immersed for 30 min in the solution to determine the open circuit potential (OCP), the same procedure used before. Subsequently, the potential was increased in steps of 50 mV every one hour until a breakthrough current density was attained. The pitting corrosion initiation potential was defined when the current density reached values above 0.1 mA/cm^2 [10]. After the tests, the samples were examined by SEM to confirm the presence of pits on their surfaces. The tests were carried out in triplicate at 25°C (room temperature).

II. RESULTS AND DISCUSSION

a) Characterization of the Samples for the as-received Conditions

The X-ray diffractogram pattern for the 316L and AL-6XNPLUS™ steels can be seen in Figure 3. For both sheets of steels, the main phases detected were the matrix phase (austenite) and some ferrite peaks, indicating that both materials were not in the solution annealed condition. No other phases were detected for the analyzed angle range 2Θ (25-79°). For this measurement, a synchrotron light radiation source ($\lambda = 0.10332$ nm) was used. This measurement was not possible for the 317L and 904L steels due to a manufacturing problem of the samples.

b) pH Study of the Solution

Firstly, the solution pH used in the corrosion tests (artificial oil field formation water) was studied. The solution was deaerated by bubbling N_2 to simulate the absence of free oxygen from the pre-salt layer. Figure 4 shows the results for the pH study of the solution (called TQ3219 by Petrobras). The stabilization of pH indicates that the electrolyte is deaerated and subsequently saturated with CO_2. All the chemical reaction that happens when bubbling CO2 in the solution is described in our previous work [4].

c) CO_2 Corrosion Evaluation using a Potentiodynamic Technique

Before the linear polarization tests, the OCP of the samples was measured. The result is shown in Figure 05. The OCP of the super austenitic steels (AL-6XN PLUS™ and 904L) stabilize in 5 minutes. For the other austenitic steels (316L and 317L), the stabilization time is longer, eespecially for the 317L steel. After 30 minutes of immersion, all the OCP are stabilized. Figure 6 shows the linear polarization curves for the steels in the as-received condition. The linear polarization tests aim to verify the formation of passive film or not on the alloys surfaces[11]. For this test, all the samples were immersed in the solution used (artificial oil field formation water) saturated with CO_2. The super austenitic stainless steels AL 6XN PLUS™ and 904L showed a good CO_2 corrosion resistance. After reaching the corrosion potential (around -0.5 V), a passive film is formed and broken at -0.34 V until they reach a passivation peak around -0.20 V. After this potential, there is the formation of another passive layer that remains until the potential of +0.89 V where there is a slight breakdown of this layer and another passivation. After reaching a potential of +1.02V (pitting potential), there is an increase in current density, the transmissive region, since the potential is too high (above +1.0 V). It is possible to observe that the electrochemical behavior for the super austenitic steels studied in this work is very similar. Their passive regions are quite stable. The increase of current density after +1,0 V can be associated with oxygen evolution, reported in the literature[12]. The 317L steel also showed a good CO_2 corrosion resistance. The formation of its passive layer is not so stable as the passive layers of the super austenitic steels; even so, the current density in the passive region remains low, in the order of 10^{-6} A/cm^2. Its pitting potential is around +0.61 V. The 316L steel did not present any passivation since the anodic current increased with time. This steel presented the highest anodic current rate (in the order of 10^{-5} A/cm^2) if compared with the other steels. Its corrosion potential is similar to the corrosion potential of 317L steel (+0.40 V). 316L steel presented the lowest pitting potential (+0.30 V), indicating that its CO_2 corrosion resistance is not very efficient. The reduction in anodic current density is associated with the passive film as a protective barrier against corrosion. The super austenitic steels AL-6XN PLUS™ and 904L showed a reduction in their anodic current, while the austenitic steels 316L and 317L showed an increase in anodic current with time. This result shows that the passive film of super austenitic steels is more stable. This effect can be attributed to the high levels of alloying elements such as Cr, Mo, and Ni. According to Sedriks, on a polarization curve, the greater the difference between the pitting potential and the corrosion potential ($\Delta E = E_{pit} - E_{corr}$), the more resistant to corrosion the material is [13]. Table 2 shows the corrosion potential values, pitting potential, and the difference between them for the studied steels. The ΔE interval is higher for the super austenitic steels, which confirms their high performance about CO_2 corrosion. The 316L steel had the lowest value for ΔE, indicating that it is not a suitable material for applications that require good CO2 corrosion resistance. More detailed work on CO_2 corrosion using austenitic stainless steels by the authors of this research can be found in [4].

Table 2: Potentials in V (Ag/AgCl) taken from the linear polarization curves for the studied steels

Alloy	E(corr)	E(pit)	ΔE
316L	-0.41	0.30	0.71
317L	-0.41	0.61	1.02
904L	-0.49	1.02	1.51
AL-6XN PLUSTM	-0.53	0.99	1.52

After the linear polarization tests, SEM of the surfaces of the steels was carried out. The only material that presented pits on its surface was the 316L steel, as shown in Figure 7. Several factors may have influenced this form of corrosion for the 316L steel. Among them, one can mention: inefficiency of the passive film, pH of the solution, chloride content in the solution, effect of CO_2. The action of the chloride ion in an acid medium caused by the reaction of CO_2 gas in an aqueous medium can accelerate the localized corrosion process.

d) *The Corrosion Resistance of the Steels in Artificial Oil Field Formation Water by Potential Step Technique*

The samples in the as-received condition were submitted to another electrochemical technique called potential step. This time, no CO_2 or N_2 was used in the solution (artificial oil field formation water). The investigation using this technique is in agreement with the linear polarization experiments where the 904L and AL-6XN PLUS™ austenitic stainless steels had excellent pitting corrosion resistance when compared with the other austenitic steels (316L and 317L). Figure 8 shows the results of potential step for the 316L, 317L, 904L, and AL-6XN PLUS™ alloys, respectively. The graphs are of type double Y-axis, where the potential (V vs. Ag/AgCl, sat KCl) and the current density (mA/cm^2) are plotted on the Y-axis, and the time (s) is plotted on the X-axis. Every potential step was maintained for one hour. If nothing happened on the passive film, then a new step was reached by an increment of +50 mV. The pitting potential (E_p) of each alloy was achieved when the current density reached values above 0.1 mA/cm^2, as shown on the graphs. So there was an abrupt increase in the current density indicating the breakdown of the passive film. The time to achieve the pitting potential depends on the film resistance of each alloy. The more resistant the passive film, the more time is needed to reach the pitting potential. The pitting potential for the 316L steel presented the lowest value (+0.52 V), while the pitting potential for the 904L and AL-6XN PLUS™ steels presented the highest value (+1.06 V and +1.09 V, respectively). The pitting potential for the 317L steel showed an intermediate value (+0.81 V). Table 3 shows the pitting potential and the time to achieve it for each alloy. It was necessary more than one day for the sample of the AL-6XN PLUS™ steel to reach its pitting potential. This result shows how resistant this material is to the conditions used. On the other hand, the 316L steel presented the lowest time to reach its pitting potential. Even without the presence of CO_2, this steel showed susceptibility to pitting corrosion in chloride-containing environments. The 317L steel showed to be more resistant than the 316L steel in chloride-containing environments but less resistant than the other two super austenitic steels. If compared with table 2, it can be seen that the pH of the solution shifted the pitting potential of the steels. In the presence of CO_2, the solution is more aggressive, decreasing the pitting potential of the steels.

Table 3: Measured pitting potential of the studied alloys using the Potential step technique

	Potential step	
Alloy	E(pit) (V Ag/AgCl)	time (h)
316L	+0.52	13.5
317L	+0.81	16.2
904L	+1.06	23.1
AL-6XN PLUS^{TM}	+1.09	26.2

The 316L and 317L steels suffered pitting corrosion. For the 316L steel (Figure 9a), the pits possess a circular shape with a center hole. The pit propagates from the center to the edge and tries to grow with time. This effect is attributed to the chloride in the solution. The chloride ion (Cl^-) is very small and can penetrate easily in sites of the 316L surface where the film is broken. The pits on the 316L steel grow but only in the center, as shown in Figure 9a. With the absence of CO_2 in the solution, the environment is not so aggressive to permit the pits' growth. The 317L steel also suffered pitting corrosion, but its pits are so small compared with the ones of the 316L steel. The pits initiated, but they did not grow with time, as shown in Figure 9b. These pits are non-uniform. This result indicated that the 317L steel in some chloride-containing environments is also resistant, being also a good choice in some applications where the 316L cannot be used, for example, in the oil and gas industry in chloride-containing environments. The super austenitic stainless steels (904L and AL-6XN PLUS™) presented pits much smaller than the ones found on the surface of conventional austenitic steels, as seen in Figure 9 (c-d). They are micro-pits, and after initiating, they passivate again before starting to grow. The effect of CO_2 on the morphology of the pits for the 316L steel, the most affected steel in the experiments, is shown in Figure 10. In Figure 10a, one can see the pits for the potentiodynamic test using CO_2 in the solution. In Figure 10b, it can be seen a single pit formed for the potentiostatic test with no CO_2 in the solution. For the potentiostatic test (potential step), the pit did not grow as expected, leaving a hole in the center. All the micrographs of the alloys taken after the corrosion tests are in accordance by the graphs shown before. This experimental procedure has previously been used to qualify Ni-based alloys and hyper duplex stainless steel for raw seawater injection [14] and also used to study a 13% Cr supermartensitic stainless steel related to localized corrosion [15]. These results combined with the linear polarization tests in CO_2-saturated aqueous solution, show that these materials (the super austenitic stainless steels) are an excellent option for chloride-containing environments with and without CO_2 once they are cheaper than the Ni-based alloys. In some cases, the conventional 317L steel can also be a good option than the conventional 316L steel.

III. CONCLUSIONS

It can be concluded that the oil field formation water plays an important role as an aggressive substance in the pre-salt region. In chloride-containing environments, the 316L steel is not so resistant, and it is not recommended for the content of NaCl in the pre-salt region. The type of corrosion found was identified as pitting corrosion. For the 316L steel, pits were formed for both techniques used, but the pitting corrosion was more aggressive for the potentiodynamic technique due to CO_2 in the solution and the absence of free oxygen. The 317L steel presented good pitting corrosion resistance when compared to the 316L steel. The two super austenitic stainless steels studied in this research (904L and AL-6XNPLUS™) presented good pitting corrosion resistance. Both can be the solution for applications in chloride-containing environments as those found in the pre-salt region.

ACKNOWLEDGMENTS

The authors would like to thank to the Coordination for the Improvement of Higher Education Personnel (CAPES) and Cearense Foundation to Support Scientific and Technological Development (FUNCAP) for the financial support. A special thank is given to Wilman Italiano, who gave training in the electrochemical tests of potential step and also gave important contributions to this work.

REFERENCES RÉFÉRENCES REFERENCIAS

1. Race to the sea: the technological and environmental challenges of the pre-salt. Available in:<http://www.coppe.ufrj.br/sites/default/files/coppe_pre-sal.pdf>. (original in Portuguese - access: September 2020).
2. Anselmo N, May JE, Mariano NA, Nascente PAP, Kuri SE. Corrosion behavior of supermartensitic stainless steel in aerated and CO2-saturated synthetic seawater. Mater Sci Eng A 2006;428:73–9.
3. Smith L, Celant M. Martensitic stainless steels in context. Supermartensitic Stainl Steels 2002;2002: 14–20.
4. Cardoso JL, Mandel M, Krüger L, Herculano LFG, Lima Neto P de, Silva MJG da. Corrosion behavior of austenitic stainless steels in CO2-saturated synthetic oil field formation water. Mater Res 2019;22.
5. Cao G, Firouzdor V, Sridharan K, Anderson M, Allen TR. Corrosion of austenitic alloys in high temperature supercritical carbon dioxide. Corros Sci 2012;60:246–55.
6. Firouzdor V, Sridharan K, Cao G, Anderson M, Allen TR. Corrosion of a stainless steel and nickel-based alloys in high temperature supercritical carbon dioxide environment. Corros Sci 2013;69:281–91.
7. Furukawa T, Inagaki Y, Aritomi M. Corrosion behavior of FBR structural materials in high temperature supercritical carbon dioxide. J Power Energy Syst 2010;4:252–61.
8. Russick EM, Poulter GA, Adkins CLJ, Sorensen NR. Corrosive effects of supercritical carbon dioxide and cosolvents on metals. J Supercrit Fluids 1996;9:43–50.
9. Chilingar G V, Mourhatch R, Al-Qahtani GD. The fundamentals of corrosion and scaling for petroleum and environmental engineers. Elsevier; 2013.
10. Eidhagen. J Ku. Eurocorr conference. Crevice Corros. Prop. Sandvik SAF 3207TM HD Dur. Inject. Nat. chlorinated seawater, Stockholm: 2011.
11. Tait WS. An introduction to electrochemical corrosion testing for practicing engineers and scientists. PairODocs Publications; 1994.
12. Bandy R, Cahoon JR. Effect of composition on the electrochemical behavior of austenitic stainless steel in Ringer's solution. Corrosion 1977;33:204–8.

13. Sedriks AJ. Corrosion of Stainless Steels. 2nd ed. New York: John Wiley & Sons; 1996.
14. Eidhagen J, Kivisäkk U. Crevice corrosion properties for Sandvik SAF 3207TM HD during injection of natural and chlorinated seawater, EuroCorr; 2011.
15. Lima LIL, Lima MM, Ferreira M, Nolasco R, de Souza MMD, de Oliveira IA, et al. Preliminary Evaluation of Localized Corrosion Using Potentiodynamic and Potentiostatic Techniques n.d. http://sites.poli.usp.br/org/emcr2012/CD/PDF/Poster/Th-11_Lima.pdf (access: December 2020).

List of Figures

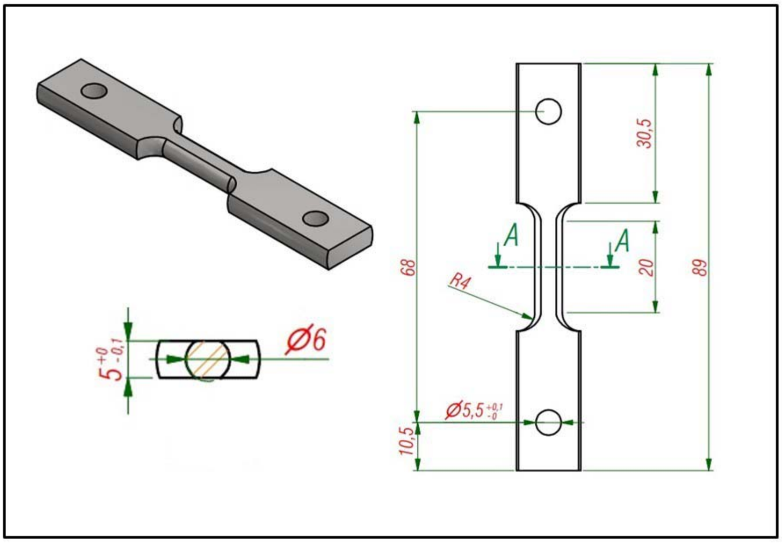

Figure 1: Shape and dimensions (mm) of the samples for the XRD measurements by synchrotron light

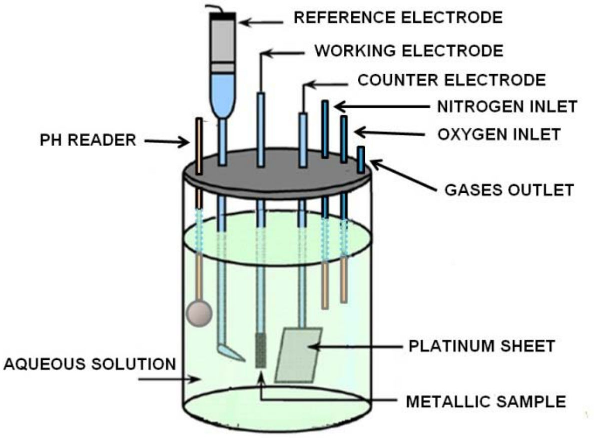

Figure 2: Cell for the CO_2 corrosion test showing all the electrodes used

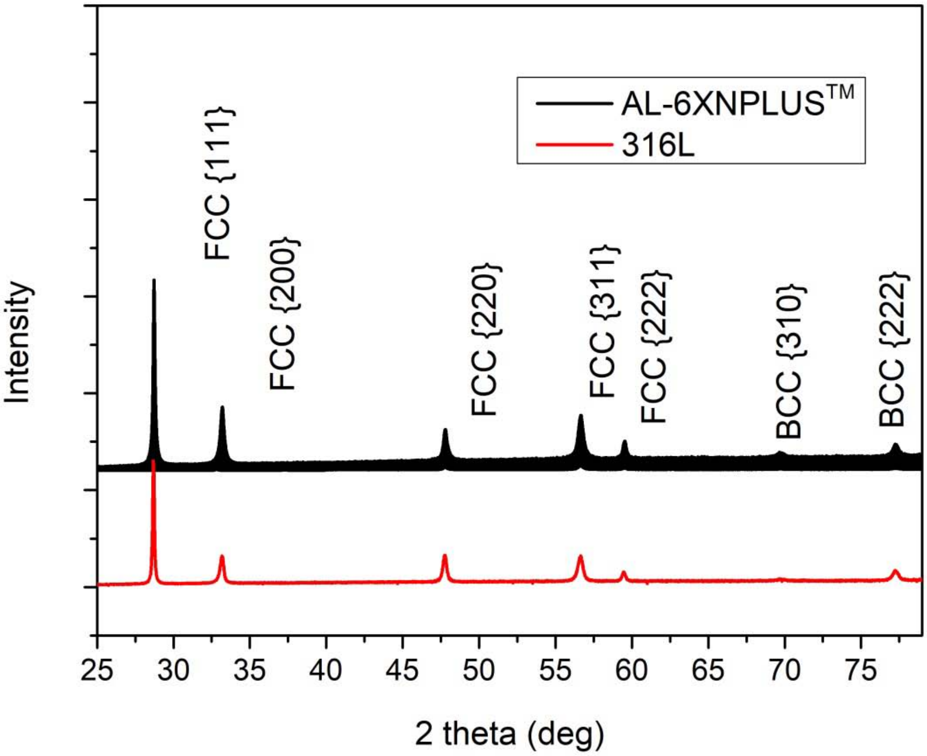

Figure 3: XRD pattern for the 316L and AL-6XNPLUS™ steels in the as-received condition (synchrotron light radiation source, λ = 0.10332 nm)

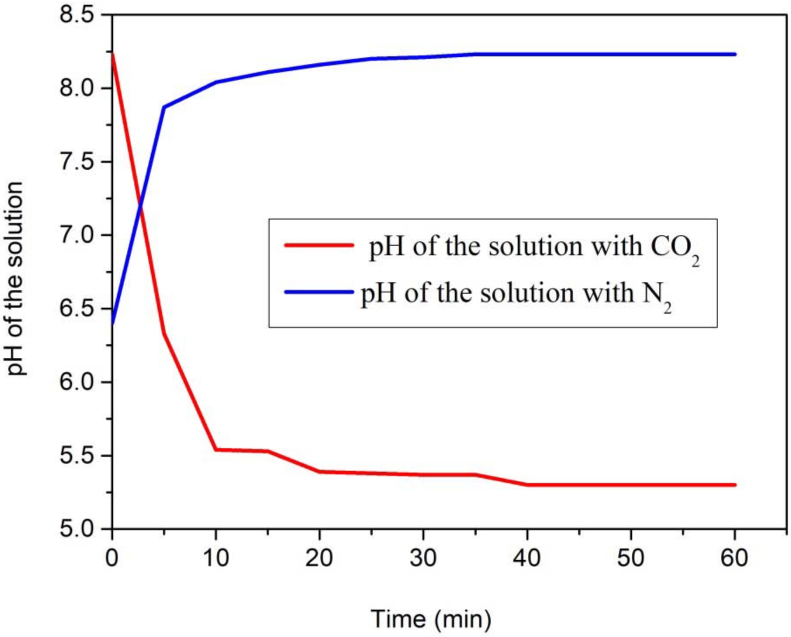

Figure 4: pH of the solution as a function of the bubbling time with N_2 and CO_2

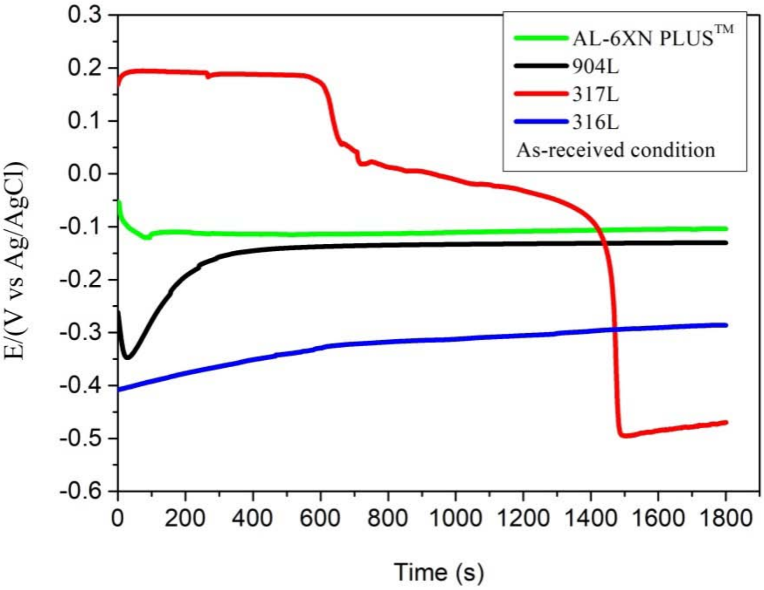

Figure 5: Open circuit potentials for the studied steels

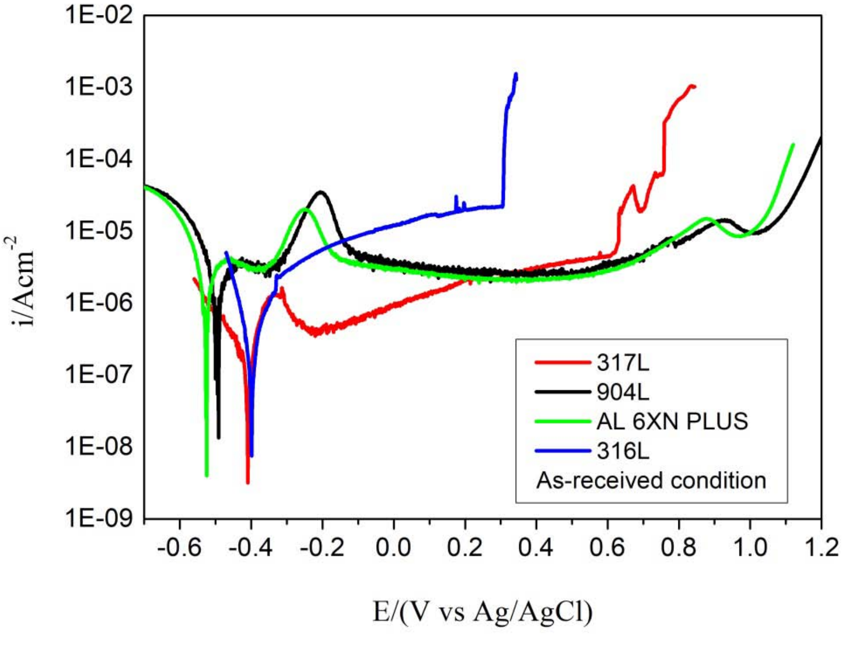

Figure 6: Linear polarization curves for the steels in the as-received condition

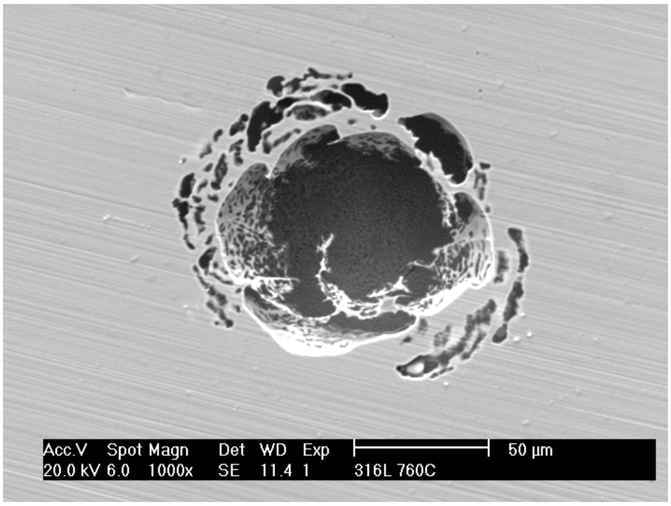

Figure 7: Pit on the surface of the 316L steel after linear polarization tests

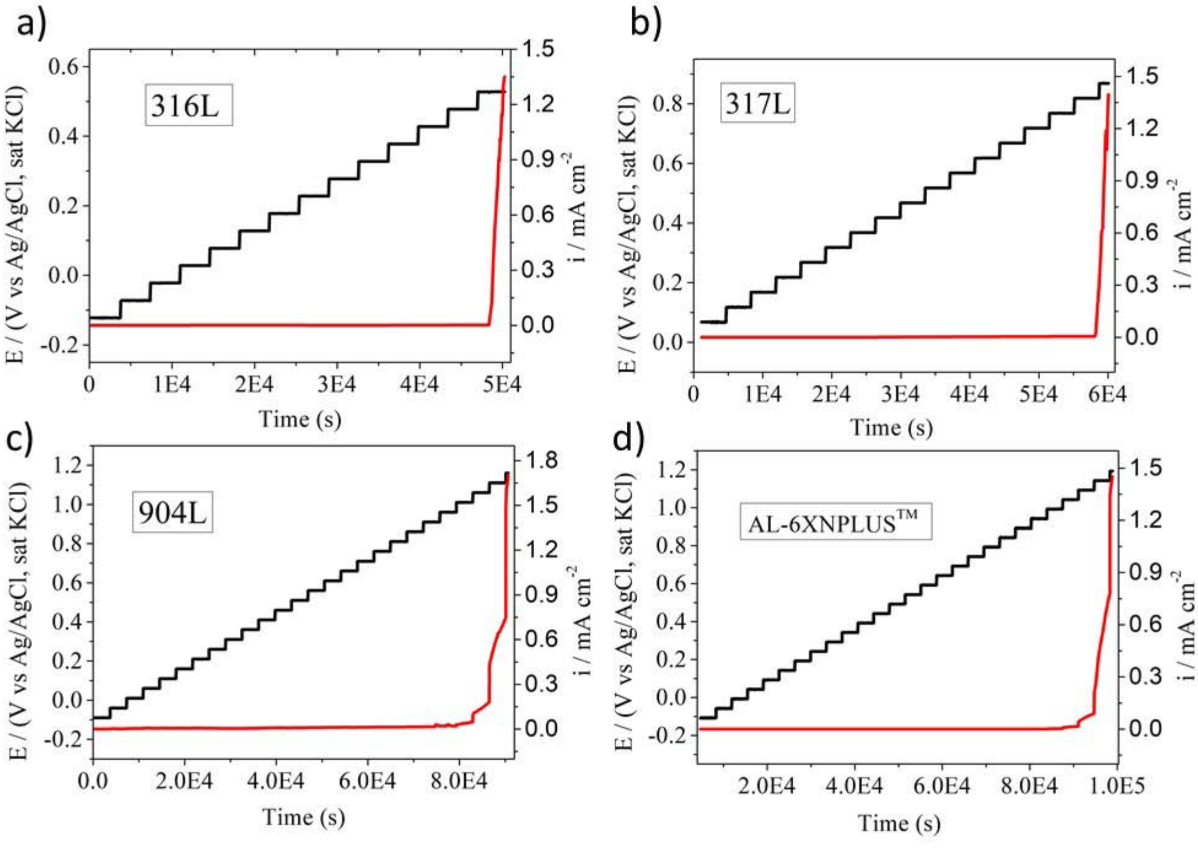

Figure 8: Plots with the potential steps, current density and time for the studied alloys in artificial oil field formation water

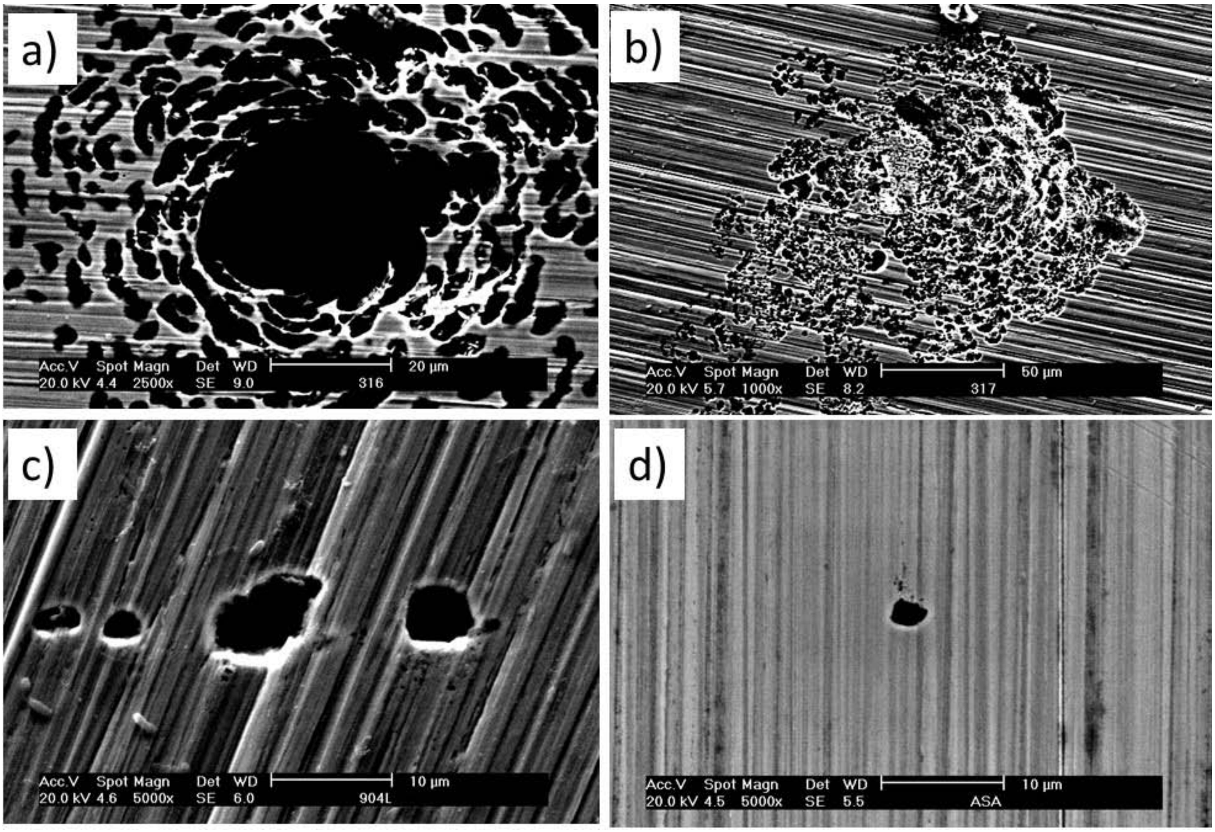

Figure 9: SEM image showing the pits formation on the surfaces of the studied alloys, a) 316L, b) 317L, c) 904L and d) AL-6XNPLUS™

Global Journal of Researches in Engineering: C
Chemical Engineering
Volume 23 Issue 1 Version 1.0 Year 2023
Type: Double Blind Peer Reviewed International Research Journal
Publisher: Global Journals
Online ISSN: 2249-4596 & Print ISSN: 0975-5861

Adsorption Kinetics and Mass Balance Mathematical Model of Monoethanolamine Surface-Modified Palm Shell Activated Carbon for Carbon Dioxide Dynamic Adsorption in Fixed Bed Column

By Saad Hashim Khalil
University of Malaya

Abstract- Dynamic adsorption kinetics results indicated that monoethanolamine-carbon dioxide (MEA-CO_2) reaction in fixed bed column packed with MEA-impregnated activated carbon (AC) particles is pseudo first order reaction. The controlling step (slow step) of adsorption is the mass transfer of CO_2 molecules form the feed gas bulk stream to the surface of the adsorbent through the boundary layer (external diffusion). A Dubinin-Astakhov and Avrami models showed that adsorption of CO_2 on MEA-impregnated activated carbon particles is homogeneous. The suggested mass balance model exhibited good agreement with the experimental results for both MEA-impregnated and non-impregnated AC, which they show also that there is no difference in adsorption rates between the two adsorption beds.

Keywords: adsorption kinetics, activated carbon, impregnation, MEA, fixed bed column.

GJRE-C Classification: LCC: TP156.A3

Adsorption Kinetics and Mass Balance Mathematical Model of Monoethanolamine Surface-Modified Palm Shell Activated Carbon for Carbon Dioxide Dynamic Adsorption in Fixed Bed Column

Saad Hashim Khalil

Abstract- Dynamic adsorption kinetics results indicated that monoethanolamine-carbon dioxide (MEA-CO_2) reaction in fixed bed column packed with MEA-impregnated activated carbon (AC) particles is pseudo first order reaction. The controlling step (slow step) of adsorption is the mass transfer of CO_2 molecules form the feed gas bulk stream to the surface of the adsorbent through the boundary layer (external diffusion). A Dubinin-Astakhov and Avrami models showed that adsorption of CO_2 on MEA-impregnated activated carbon particles is homogeneous. The suggested mass balance model exhibited good agreement with the experimental results for both MEA-impregnated and non-impregnated AC, which they show also that there is no difference in adsorption rates between the two adsorption beds.

Keywords: adsorption kinetics, activated carbon, impregnation, MEA, fixed bed column.

I. Introduction

The removal of carbon dioxide (CO_2) is significant for oil and gas industry due to its harmful acidic effects on oil and gas pipelines with no added energy value to natural gas [1]. Because of the increasing indications of CO_2 implication in global warming [2], capturing CO_2 from its emitting sources is becoming a vital topic. Adsorption is offering an effective alternative for CO_2 capturing comparing to other capture technologies [3]. There are many types of gas adsorbents; conventional, like, activated carbons, silica gel, ion-exchange resins, zeolites, and meso-porous silicates, activated alumina, metal oxides, and new like, carbon fibers and metal-organic frameworks. [4]. Adsorbent most important feature is adsorbing capacity [5], besides, good adsorbent should be selective and chemically and mechanically durable [6]. AC is cost-effective and adaptable microporous adsorbent [7] and is considered a superb adsorbent due to its high specific surface area, appropriate pore size distribution, diversity of surface chemistry [8]. It's mostly micropore structure were used extensively in liquids and gases systems. The micropores and mesopores of the AC particles were utilized to accommodate the impregnating molecules, which can be attached chemically (grafting) or physically (impregnation) to the AC particles [9]. Impregnation of AC particles with chemicals improves their natural adsorption capability to adsorb gases [10]. Alkanolamines, such as, monoethanolamine (MEA), diethanolamine (DEA), and methyldiethanolamine (MDEA) are very important absorbents for acidic gases in the field of natural gas sweetening and for mitigation the adversity of these gases on environment [11] and they are extensively used in CO_2 absorption from different gas sources [12]. MEA, which is a primary amine, has been used intensively to capture CO_2 from gas streams and from many various sources due to its fast reaction kinetics with CO_2, low coast and thermal stability, as it is more favorable than other alkanolamines [13] [14]. Because of the effectiveness of liquid amine absorption process researchers were encouraged to utilize amines in their solid state for CO_2 capture [15]. Adsorption kinetics is essential tool used to evaluate the performance of an adsorbent and to understand the mechanism of adsorption [16] and many researches had included kinetics of batch CO_2 adsorption on different adsorbents in their works [17]. They found that the restriction step is the intraparticle diffusion (pore diffusion). On contrary to the findings of this paper where the restrictive step to CO_2 adsorption was the film diffusion. In this research, dynamic adsorption experiments were conducted to investigate the adsorption kinetics of MEA-impregnated AC particles packed in adsorption column to adsorb CO_2 from gas mixture.

II. Materials and Methodology

a) Materials

1. Certified analytical reagent monoethanolamine (MEA), C_2H_7NO, molecular weight 61.

Author: Chemical Engineering Department, University of Malaya, Kuala Lumpur, Malaysia. e-mail: saadamen@yahoo.com

2. Commercial palm shell AC was purchased from Bravo Green SDN BHD (Sarawak, Malaysia).
3. Gases

a. Mixture of 15% CO_2 with 85% N_2.
b. Pure N_2.

b) *Methodology*

i. *AC Particles Characterization*

Granulated palm shell AC particles were physically activated by steam. The mostly micropore particles have total Bet surface area of 838 cm^2/g, while the micropore surface area of that total area is 675 cm^2/g and micropore volume is 0.32 cm^3/g.

ii. *AC Beds Perpetration*

A household coffee grinder crushed the AC particles. 710 and 500 μm sieves were employed to characterize the AC particles to the required particle size of 500 μm (particles passing 710 and stopping on 500 μm sieve).

iii. *Impregnation of AC Samples*

Impregnation was carried out by placing 5 g of granular AC in a beaker, 2 g of MEA added to the beaker with 10 g of deionized water as an environmentally friendly medium and to facilitate the impregnation process. The beaker contents were stirred at 500 rpm for 1 hour at room temperature. The final slurry then dried completely in Heraeus Instrument Vacuthermo oven at 70°C under 0.1 bar vacuum pressure (absolute) for 6 hours. Samples of AC particles prepared for CO_2 adsorption separation experiments are, non-impregnated AC particles and MEA-impregnated AC particles.

iv. *Working Breakthrough Time*

Working breakthrough time was utilized as a method to evaluate the performance of AC beds. Breakthrough time can be defined as the time spanning from the beginning of the adsorption experiment to the point when CO_2 molecules start to break through out of the adsorption column, which was monitored by Guardian Plus CO_2 monitor. Data Acquisition Logger was connected to the CO_2 monitor to measure the breakthrough time in minutes.

Experimental setup is presented in another work [18].

v. *Amine-CO_2 Reactions*

Amines remove CO_2 in a two-step process:

1. The gas absorbs by the liquid forming a weak acid.
2. The weak acid reacts with amines as a weak base [19].

The suggested [20] reaction path of primary and secondary unhindered amines with CO_2 is known as the carbamate formation reaction proceeds through the formation of zwitterion, which was recognized as the reaction mechanism [21].

The first step of the reaction is the formation of amine-CO_2 zwitterion as shown in Equation 1a:

$$CO_2 + R_1R_2NH \leftrightarrow R_1R_2N^+HCOO^- \text{ (Zwitterion)} \quad (1a)$$

The second step is the deprotonation of the zwitterion. For liquid amine reaction, the water would act as a base acquiring the proton released by the zwitterions. In the case of solid amine reaction, another amine molecule would acquire the released proton as the maximum theoretical amount of CO_2 reacting with amine would be 0.5 mol CO_2/1 mol N_2 as shown in equation 1. In this step, the zwitterion would be stabilized by producing carbamate as in equation 1b.

$$R_1R_2N^+HCOO^- + R_1R_2NH \leftrightarrow R_1R_2NCOO^- \text{ (Carbamate)} + R_1R_2NH_2^+ \quad (1b)$$

The overall reaction is as in equation 1:

$$CO_2 + 2R_1R_2NH \leftrightarrow R_1R_2NH_2^+ + R_1R_2NCOO^- \quad (1)$$

vi. *Rate and Mechanism of Adsorption*

To investigate the rate of adsorption two equations were explored namely, pseudo first order (SFO) and pseudo second order (PSO) equations. The mechanism of adsorption and the adsorption controlling step was determined by Weber-Morris intraparticle diffusion model.

III. RESULTS AND DISCUSSIONS

a) *Impacts of MEA Surface-Modification on AC Particles*

MEA molecules occupied the pores of the mostly micropore AC particles and blocked them, reducing significantly the micropore surface area from 675 to 36m^2/g (96%) and micropore volume from 0.32 to 0.02cm^3/g (94%). MEA-blocked AC particles adsorb selectively more CO_2 comparing to non-impregnated AC particles by 172%, as the adsorption capacity increased from 49 to 18 mg/g, respectively.

b) *Adsorption Kinetics*

i. *Adsorption Rate*

Pseudo first and second order models were investigated to find out which model is predicting the adsorption rate appropriately.

a. *Pseudo First Order Model (SFO)*

Lagergren [22] published his SFO model to describe homogenous adsorption on solid phase as in equation 2. The equation depends on the adsorption capacity of an adsorption bed rather than concentration of adsorbate as in the case of first order model equation and the adsorption rate is related to the availability of adsorption sites [23]. It had been reported that SFO model can be applied adequately for the adsorption kinetics of CO_2 on AC [24].

$$\frac{dq_t}{dt} = k_1(q_e - q_t) \tag{2}$$

The linear form of equation 1 is as in equation 3:

$$ln(q_e - q_t) = ln\, q_e - \frac{k_1}{2.303}\, t \tag{3}$$

Where,

q_e: Adsorption capacity at equilibrium, mg/g.
q_t: Adsorption capacity at any time t, mg/g.
k_1: Pseudo-first order rate constant, 1/min.
t: Time, min.

Figure 1 is a plot of ln (q_e-q_t) against t for the whole adsorption experiment showing that the straight line fitting the experimental results has good value of R^2 equal to 0.9967, which is suggesting that the SFO kinetic model is applicable for this research. The slope of the straight line from equation 3 is ($\frac{k_1}{2.303}$), where the value of the SFO rate (k_1) was found to be 0.00552721/min.

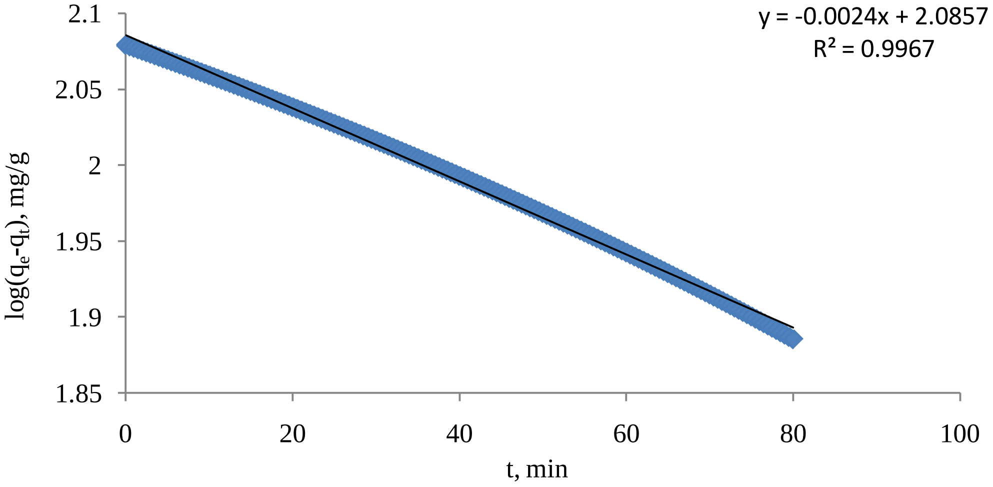

Figure 1: Plot of ln (q_e-q_t) against time

b. *Pseudo Second Order Model (PSO)*

PSO model is usually applied for chemisorption kinetics sorption of liquid solutions [25], the model is in equation 4 and its linear form is as in equation 5:

$$\frac{dq_t}{dt} = k\,(q_e - q_t)^2 \tag{4}$$

$$\frac{t}{q} = \frac{1}{k^2 q_e^2} + \frac{1}{q_e} t \tag{5}$$

The plot of t/q against t for PSO model as in equation 5, didn't yield straight line for the whole experimental data or even for any of its portions on contrary to the straight line of plot ln (q_e-q_t) against t for PFO model, which covers the whole experimental data and suggesting that the adsorption rate here is following PFO model which would be applied to calculate adsorption rate constant (k_1).

ii. *Verification the Rate-Determining Step of the MEA-Impregnated AC Adsorption Bed*

Equation 6 is the intraparticle diffusion equation [26],

$$q_t = k_p t^{\frac{1}{2}} + c \tag{6}$$

Where:

q_t: Amount of adsorbate absorbed at any time, mg g^{-1}.
k_p: Intraparticle diffusion rate constant, mg g^{-1} $min^{-1/2}$.
t: Time, min.
c: Intercept, mg g^{-1}

The multilinearity displayed in Figure 2, the plot of the amount of CO_2 adsorbed (q_t) against the square root of time ($t^{1/2}$) is suggesting that more than one step is taking place. The straight line fitting the curve is not passing through the origin, indicating that the intraparticle diffusion is not the adsorption rate restrictive step [27]. The curve is divided into three zones where the slope of the linear part indicating the rate of adsorption and the rate controlling step is represented by the linear section with lowest slope value [28]. The first zone is the initial zone where the external diffusion of CO_2 molecules through the bulk gas phase is taking place and the slope which is representing the adsorption rate is low. The second zone is the film diffusion where the mass transfer of CO_2 molecules is continuing through the CO_2 film surrounding the AC particles. The slope of the straight line of the second zone is higher than that of the initial zone but lower than that of the third zone due to the resistance exerted by CO_2 gas film, which is indicating that this step combining with the initial zone step are slow and the overall adsorption rate is controlled by mass transfer and film resistances respectively. In the third zone, where the amount of CO_2 molecules adsorbed (q_t)

versus $t^{1/2}$ is displaying a straight line with high slope value indicating that CO_2 molecules intraparticle diffusion step is fast, where CO_2 molecules adsorption is enhanced by the fast CO_2-MEA reaction. The intercept (c) is an indicator of the thickness of the boundary layer surrounding the MEA-impregnated AC particles. Higher values of intercept suggest that the boundary layer is building up as the value of the c in the initial zone is less than that of zone 1, which is in turn less than that of zone 2 deducing that diffusion through the gas film may be considered as the controlling step [29]. CO_2 adsorption in zone 2 is approaching its final stage and the active sites on MEA-impregnated AC particles are not able to adsorb more CO_2 molecules.

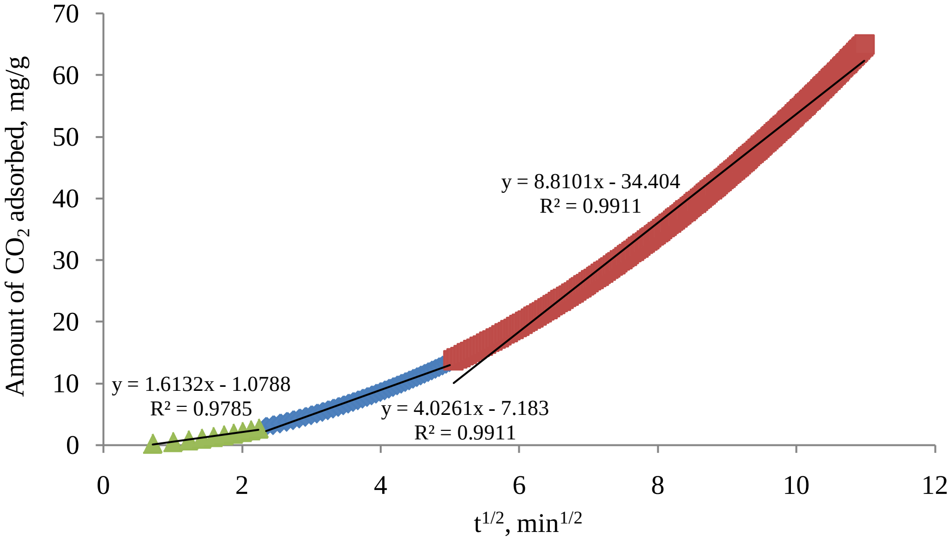

Figure 2: CO_2 Amount adsorbed, mg/g against square root of time, $min^{1/2}$

iii. *Gas Film Diffusion Model*

The transportation of CO_2 molecules from the gas stream bulk to the surface of the AC particles is playing a major role as the analysis of the intraparticle model showed that the mass transfer of CO_2 molecules through the gas film is the limiting step of CO_2 adsorption. To further inspect that gas film is the limiting step in CO_2 molecules adsorption, gas film diffusion model was applied [30], [31] and [32]:

$$\frac{q_t}{q_e} = 1 - e^{k_{fd} t} \tag{7}$$

The linearized form of equation 7 is as in equation 8:

$$\ln(1 - F) = -k_{fd} t \tag{8}$$

Where,

F: Fractional adsorption equilibrium ($F = q_t/q_e$).

k_{fd}: Film diffusion coefficient, min^{-1}.

A plot as in Figure 3 of $-\ln(1 - F)$ vs t with intercept equal to zero and R^2 equal to 0.99 is suggesting that adsorption kinetics is controlled by diffusion through the CO_2 gas film surrounding the AC particles.

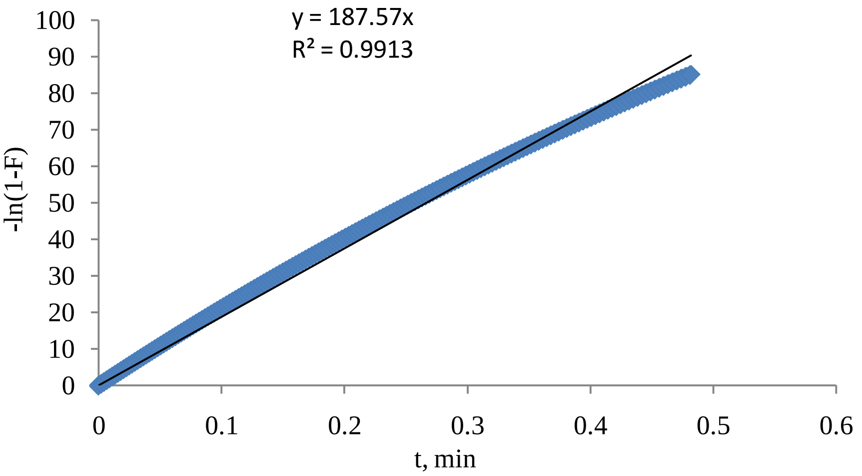

Figure 3: Plot of -ln (F-1) against time

iv. *Avrami (JMAK) Model*

Johnson-Mehl-Avrami-Kolmogorov (JMKA) model, which is called Avrami model too, is expressed inequation 9, [33] and [34]. Avrami equation describes the growth of crystallites with respect to time. In this work Avrami equation is describing the increasing numbers of CO_2 molecules by adsorption inside the AC pores.

$$\alpha = 1 - \exp\left(-k_{Av}\,(t)^n\right) \tag{9}$$

Where, α is adsorption fraction at time t, k_{Av} is the Avrami kinetic constant, and n is a constant which represents the mechanism of particles adsorption (growth).

The linearized form is as in equation 10:

$$\ln(-\ln(1-\alpha)) = nlnk_{Av} + nlnt \tag{10}$$

Plotting ln (-ln(1-α)) against ln t as in Figure 4 producing straight line (R^2=0.9991) with intercept equal to nlnk_{Av} and slope equal to n. If Avrami constant n equal to 1. Furthermore the value of Avrami exponent n, which is $1 \le n \le 2$ suggesting one dimensional growth of crystallites and that the growth is homogenous [35], which is agreeing with exponent n in micropore filling method of Dubinin-Astakhov (D-A), equation 11 and its linearized form equation 13. D-A equation is applicable for homogeneous carbonaceous adsorbents with micropore structures [36]. It was found in other study [37] that the value of D-A exponent n for MEA-impregnated beds is showing less heterogeneity and more homogeneity with their exponent n value equal to 2, where the value of exponent n in AC is 3 - 1.5. Moving from 3 to 1.5 the microporous system would be getting more heterogeneous [38] and [39].

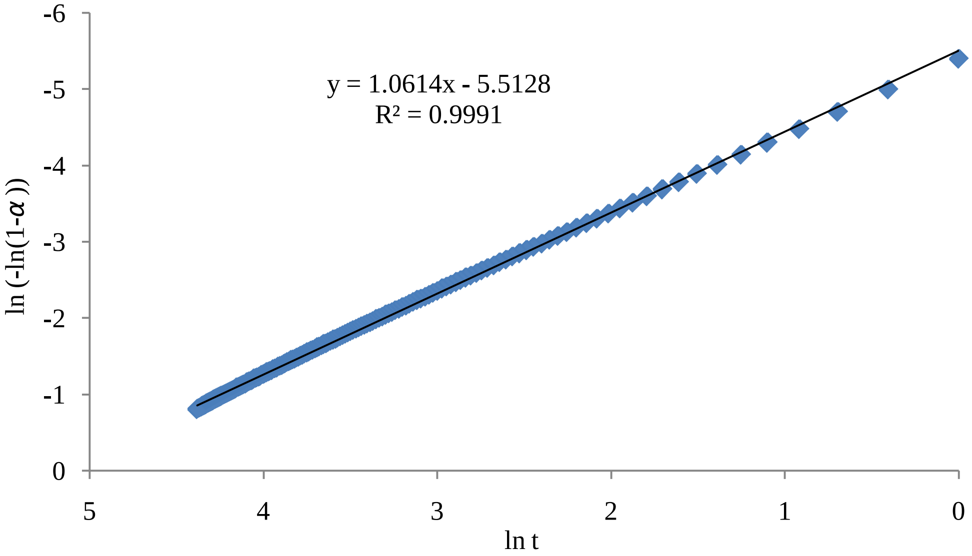

Figure 4: Plot of ln (-ln (1-α)) against ln (t)

c) *Mass Balance Mathematical Modeling*

Adsorption of CO_2 molecules from feed gas stream containing 15% CO_2 and 85% N_2 was performed in fixed bed packed column of non-impregnated and MEA-impregnated AC beds. Breakthrough time was employed as real time tool to evaluate the efficiency of the adsorption beds. CO_2 monitor was used to display the concentration (%) of the gas stream exiting the adsorption column. Graphs of CO_2 molecules concentration leaving the adsorption column plotted against time were obtained from the data acquisition logger connected to the outlet of the adsorption column.

i. *Mathematical Modeling of MEA-Impregnated 500 µm Adsorption Bed*

To formulate a general mathematical model corresponding to the mainly micropore adsorption mechanism and to cover the two stages mentioned earlier, the following assumptions were made:

1. The system operates under isothermal, isobaric and diabatic conditions.
2. The porosity of the adsorption bed was uniform and constant.
3. The equilibrium of adsorption is a nonlinear isotherm.
4. The velocity distribution is constant across the column diameter.
5. The volumetric flow rate is constant along the column.

Summarizes of the experimental parameters and simulation boundary conditions for the mathematical model validation are in Table 1:

Table 1: Experimental data and simulation boundary conditions

Operating conditions		
Pressure	1 atm	
Temperature	25°C	
Inlet concentration	6.05118E10^{-6} mol/ml	
Inlet volumetric flow rate	10 ml/min	
Adsorption column		
Material	Glass	
Inside diameter	1 cm	
Bed height	9 cm	
Bed weight	5 g	
Bed Volume	7.23 cm^3	
Adsorbent properties		
Bed type	Non-impregnated AC	MEA-impregnated AC
Particles size	500 μm	500 μm
Micropore surface area	675 m^2/g	65 m^2/g
Micropore particle porosity	0.0956 cm^3/g	0.020 cm^3/g
Porosity	0.684	0.620
Bulk density	1.6387 cm^3/g	1.6228 cm^3/g
Bed Volume	7.2285 cm^3	6.2857 cm^3
Pseudo 1st order reaction constant (k)	-	0.004836 1/min

ii. *Mathematical Model of MEA-Impregnated AC Bed*

The mathematical model was based on the CO_2 molecules breaking through the adsorption bed.

The adsorption of CO_2 molecules was declining and more CO_2 molecules were exiting the bed.

The general equation of mass balance with first order chemical reaction for CO_2 in the feed gas:

Accumulation = Input – Output + Generation

As the mass balance would be conducted on CO_2 molecules exiting the adsorption bed, the mass balance equation would be:

Output=Input– Accumulation +Generation

$$v\frac{dc_o}{dt} = qc_i - qc_{acc} + vk_1c \tag{14}$$

Where:

K_1: Pseudo first order reaction constant, 1/min.

C_i: Concentration of CO_2 entering the AC bed, mol/ml.

C_o: Concentration of CO_2 exiting the AC bed, mol/ml.

C_{acc}: Concentration of CO_2accumulated in the AC bed, mol/ml.

Equation 14 is an ordinary first order linear differential equation and the final solution would be as in Equation 15.

$$C = C_i + n\, e^{(-(q / v - k_1)t)} \tag{15}$$

Initial boundary condition:

At t = 0, C = 0

$n = -C_i$

Then equation 15 would be:

$$C = C_i - C_i\, e^{(-(q / v - k_1)t)} \tag{16}$$

Rearranging equation 16:

$$C = C_i\left(\frac{q/v}{(q/v) - k_1}\right)\left(1 - e^{-((q/v)-k_1)t}\right) \tag{17}$$

The simulated results were validated by using the experimental results of the MEA-impregnated activated carbon bed. The simulated results were compared with the experimental data. The simulated data demonstrated a reasonable agreement with the experimental data, as the root mean square error (RMSE) calculated was 6.75915E-06. The simulated and experimental data of MEA-impregnated AC beds were plotted in Figure 5.

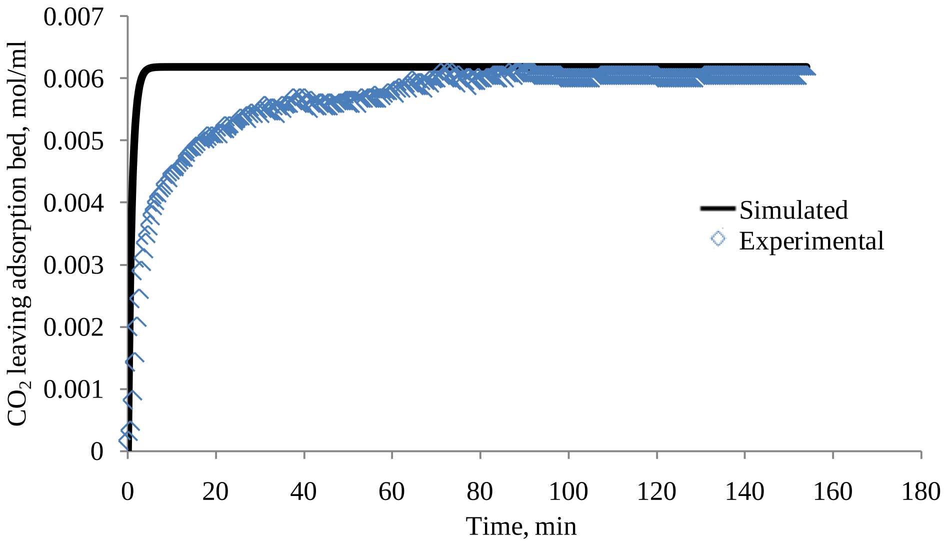

Figure 5: Comparison of CO_2 experimental and simulated breakthrough curves for MEA-impregnated AC bed (Sampled at column outlet)

IV. Conclusions

MEA-impregnated AC particles were used to adsorb CO_2 from gas mixture. Results are showing that AC particles impregnated with MEA adsorb CO_2 molecules in a pseudo first order reaction manner and that the controlling step in this reaction is the mass transfer of CO_2 molecules from through the CO_2 gas film and not the intraparticle diffusion of CO_2 molecules inside the pores of MEA-impregnated AC particles. Due to the homogeneity of the MEA-impregnated activated carbon particles the adsorption of CO_2 molecules follows the Avrami model of homogenous crystallites growth. The mass balance mathematical model showed that the experimental and simulated breakthrough curves have good agreement, as the root mean square error (RMSE) was 5.7678E-09 and 3.88532E-09 for non-impregnated and MEA-impregnated beds respectively, which also proved that the adsorption mechanism of both beds is the same.

Acknowledgment

The authors would like to thank University of Malay for offering the necessary fund for this research through the, University of Malaya Research grant UMRG RP15/2012A.

References Références Referencias

1. Rufforda T. E., Smartb S., Watsona G.C.Y., Grahama B. F., Boxalla J., Diniz da Costab J. C., Maya E. F. The removal of CO_2 and N_2 from natural gas: A review of conventional and emerging process technologies. Journal of Petroleum Science and Engineering 2012;94–95:123–54.
2. de_Richtera R. K., Mingb T., Caillola S. Fighting global warming by photocatalytic reduction of CO_2 using giant photocatalytic reactors. Renewable and Sustainable Energy Reviews 2013;19:82–106.
3. Youssef B., Serna-Guerrero R., Sayari A., Adsorption of CO_2 from dry gases on MCM-41 silica at ambient temperature and high pressure. 1: Pure CO_2 adsorption. Chemical Engineering Science 2009;64(17): 3721–28.
4. Li J-R, Ma Y., M. McCarthy C., Sculley J., Yu J., Jeong H-K., Balbuena P. B., Zhou H-C.,. Carbon dioxide capture-related gas adsorption and separation in metal-organic frameworks. Coordination Chemistry Reviews 2011;255(15–16),:1791–823.
5. Knaeble, K. S. Adsorbent selection. Adsorption research Inc., Dublin, Ohio; 2002.
6. Crini G. Recent developments in polysaccharide-based materials used as adsorbents in wastewater treatment. Prog. Polym. Sci 2005;30:38–70.
7. Labus K., Gryglewicz S., Machnikowski J. Granular KOH-activated carbons from coal-based cokes and their CO_2 adsorption capacity. Fuel 2014; 118:9–15.
8. Ozdemira I., Şahina M., Orhanb R., Erdema M., Preparation and characterization of activated carbon from grape stalk by zinc chloride activation. Fuel Processing Technology 2014;123:200-6.
9. Yan W., Tang J., Bian Z., Hu J. and Liu H. Carbon Dioxide Capture by Amine-Impregnated Mesocellular-Foam-Containing Template. Ind. Eng. Chem. Res., 2012;51 (9):3653–62.
10. Ramachandran N., Aboudheir A., Idem R., Tontiwachwuthikul P. Kinetics of the absorption of CO_2 into mixed aqueous loaded solutions of monoethanolamine and methyldiethanolamine. Ind. Eng. Chem. Res. 2006;45:2608-16.
11. Aroua M. K., Daud W.M.A.W., Yin C. Y., Adinata D. Adsorption capacities of carbon dioxide, oxygen, nitrogen and methane on carbon molecular basket

derived from polyethyleneimine impregnation on microporous palm shell activated carbon. Separation and Purification Technology 2008; 62(3):609–13.

12. Yu C-H., Huang C-H., Tan C-S. A Review of CO_2 Capture by Absorption and Adsorption 2012;12: 745–769.
13. Liu Y., Zhang L., Watanasiri S. Representing Vapor-Liquid Equilibrium for an Aqueous MEA-CO_2 System Using the Electrolyte Nonrandom-Two-Liquid Model. Ind. Eng. Chem. Res 1999;38:2080-90.
14. Ma'mun S., Nilsen R., Svendsen H. F., Solubility of Carbon Dioxide in 30 mass % Monoethanolamine and 50 mass % Methyldiethanolamine Solutions. J. Chem. Eng. Data 2005;50 (2):630–634.
15. Sayari, A., Belmabkhout, Y., and Serna-Guerrero, R.. Flue gas treatment via CO2 adsorption. Chemical Engineering Journal 2011;171 (3):760-74.
16. H. Qiu, L. Lv, B-c Pan, Q-j Zhang, Zhang W-M, Zhang Q-X. Critical review in adsorption kinetic models. Journal of Zhejiang University Science A 2009;10:716-24.
17. Sravanthi Loganathan, Mayur Tikmani, Satyannarayana Edubilli, Aakanksha Mishra, Aloke Kumar Ghoshal. CO2 adsorption kinetics on mesoporous silica under wide range of pressure and temperature. Chemical Engineering Journal Volume 256, 15 November 2014, Pages 1–8.
18. Khalil S. H., Aroua M. K., Daud W.M.A.W. Impregnation of commercial palm shell activated carbon with monoethanolamine for adsorbing CO2 from gas mixture. International Conference on Biology, Environment and Chemistry (IPCBEE) 2011;24. IACSIT Press, Singapore.
19. Mondal M. K., Balsora H. K., Varshney P., Progress and trends in CO_2 capture/separation technologies: A review, Energy 2012;46:431–41.
20. Caplow M. Kinetics of carbamate formation and breakdown, J. Am. chem. Soc. 1968;90: 6795-803.
21. Littel R. J., Versteeg G. F., van Swaaij W.P.M, Kinetics of CO_2 with primary and secondary amines in aqueous solutions-1. Zwitterion deprotonation kinetics for DEA and DIPA in aqueous blends of Alkanolamines. Chemical Engineering Science 1992;47:2027-35.
22. Lagergren S. About the theory of so-called adsorption of soluble substance. Kungliga Svenska etenskapakademiens. Handlinger 1898;24:1-39.
23. Loganathan S., Tikmani M., Edubilli S., Mishra A., Ghoshal A. K. CO_2 adsorption kinetics on mesoporous silica under wide range of pressure and temperature. Chemical Engineering Journal 2014;256:1–8.
24. Zhang Z., Zhang W., Chen X., Xia Q., Li Z. Adsorption of CO_2 on zeolite 13X and activated carbon with higher surface area. Sep. Sci. Technol. 2010;45: 710–19.
25. Ho Y. S., McKay G. Sorption of dye from aqueous solution by peat Chem. Eng. J. 1998;70:115–24.
26. Weber Jr W. J., Morris J. C. Kinetics of adsorption on carbon from solution. J. Sanit. Eng. ASCE 1963; 89: 31–59.
27. Cheunga W. H., Szetob Y. S., McKaya G, Intraparticle diffusion processes during acid dye adsorption onto chitosan. Bioresource Technology 2007;98:2897–2904.
28. Cheunga W. H., Szetob Y. S., McKaya G. Intraparticle diffusion processes during acid dye adsorption onto chitosan. Bioresource Technology 2007;98: 2897–2904.
29. Boparai H. K., Joseph M., O'Carroll D. M. Kinetics and thermodynamics of cadmium ion removal by adsorption onto nanozerovalent iron particles. Journal of Hazardous Materials 2011;186:458–65.
30. Boyd G. E., Adamson A. M., Myers L. S. Jr. J Am Chem Soc The exchange adsorption of ions from aqueous solutions by organic zeolites; kinetics 1947;69:2836-48.
31. Gupta S. S., and Bhattacharyya K. G. Adsorption of Ni (II) on clays. Journal of Colloid and Interface Science 2006;295:21–32.
32. Aroua M. K., Leonga S.P.P., Teoa L. Y., Yin C. Y. Wan Mohd Ashri Wan Dauda. Real-time determination of kinetics of adsorption of lead(II) onto palm shell-based activated carbon using ion selective electrode Bioresource Technology 99;2008:5786–92.
33. Avrami M. Kinetics of Phase Change. I. General Theory. Journal of Chemical Physics 1939;7:1103–12.
34. Elaine C. N. Lopes, Fernanda S. C. dos Anjos, Eunice F. S. Vieira, Antonio R. Cestari. An alternative Avrami equation to evaluate kinetic parameters of the interaction of Hg (II) with thin chitosan membranes. Journal of Colloid and Interface Science 2003;263:542–47.
35. Christian W. The Theory of Phase Transformation in Metals and Alloys. Pergamon Press, Oxford. 1975:20-21.
36. Dubinin M. M. Fundamentals of the theory of adsorption in micropores of carbon adsorbents: characteristics of their adsorption properties and microporous structures. Pure & Appl. Chern. 1989; 61::1841-43.
37. Khalil S. H. Effects on Surface Area, Intake Capacity and Regeneration of Impregnated Palm-Shell Activated Carbon with Monoethanolamide and 2-Amino-2-Methyl1-Propanol Equipped for CO_2 Adsorption. Journal of Earth Science & Climatic Change, 2018, 9:7 DOI: 10.4172/2157-7617.1000484.
38. Dubinin, M. M. and Stoeckli, H. F. Homogeneous and heterogeneous micropore structures in

carbonaceous adsorbents. J. Colloid Interface Sci. 1980;75: 34-42.

39. Puziy, A. M. Heterogeneity of Synthetic Active Carbons. Langmuir 1995;11:543-44.

This page is intentionally left blank

Global Journal of Researches in Engineering: C
Chemical Engineering
Volume 23 Issue 1 Version 1.0 Year 2023
Type: Double Blind Peer Reviewed International Research Journal
Publisher: Global Journals
Online ISSN: 2249-4596 & Print ISSN: 0975-5861

Moisture-dependent Physical Properties and Hydration Kinetics of Peanut Kernel

By Shubhra Shekhar, Manoj Singh & Kamlesh Prasad

Abstract- The physical properties of agricultural objects affected by moisture are essential for effective postharvest unit operations. Raw peanut in India is used in a wide variety of forms, and the process involved often soaking in water before being used as an ingredient in the preparation of different delicacies. Soaking and grinding in preparation of seasonings are commonly used to garnish the most traditional fermented foods such as *idly, dosa, vada,* and *uttapam* with several other breakfast items in the Indian subcontinent. The effect of moisture content (6.57 to 35.07%) on physical properties and the temperature (5 to 35^{0}C) dependent soaking behavior of peanut kernel of GG-20 genotype were assessed. The increase in moisture content of peanuts has affected the dimensional characteristics linearly, whereas most of the gravimetric and frictional properties followed a nonlinear trend. The feasibility of different models describing the hydration behavior was assessed for the peanut kernel. The adequacy of fitted models was determined using the coefficient of determination (R^2), chi-square (χ^2), and root mean square error (RMSE). The values of these parameters as higher R^2 ($\geq$0.96) and lower χ^2 ($\leq$0.005) and RMSE ($\leq$0.020) reflect the applicability of models in describing the soaking behavior of the peanut kernel.

Keywords: peanut, physical properties, soaking, diffusion, models, hydration.

GJRE-C Classification: DDC Code: 551.571 LCC Code: QC915

MOISTUREDEPENDENTPHYSICALPROPERTIESANDHYDRATIONKINETICSOFPEANUTKERNEL

Strictly as per the compliance and regulations of:

Moisture-dependent Physical Properties and Hydration Kinetics of Peanut Kernel

Shubhra Shekhar α, Manoj Singh σ & Kamlesh Prasad ρ

Abstract- The physical properties of agricultural objects affected by moisture are essential for effective postharvest unit operations. Raw peanut in India is used in a wide variety of forms, and the process involved often soaking in water before being used as an ingredient in the preparation of different delicacies. Soaking and grinding in preparation of seasonings are commonly used to garnish the most traditional fermented foods such as *idly, dosa,* v*ada,* and *uttapam* with several other breakfast items in the Indian subcontinent. The effect of moisture content (6.57 to 35.07%) on physical properties and the temperature (5 to 35^{0}C) dependent soaking behavior of peanut kernel of GG-20 genotype were assessed. The increase in moisture content of peanuts has affected the dimensional characteristics linearly, whereas most of the gravimetric and frictional properties followed a nonlinear trend. The feasibility of different models describing the hydration behavior was assessed for the peanut kernel. The adequacy of fitted models was determined using the coefficient of determination (R^2), chi-square (χ^2), and root mean square error (RMSE). The values of these parameters as higher R^2 ($\geq$0.96) and lower χ^2 ($\leq$0.005) and RMSE ($\leq$0.020) reflect the applicability of models in describing the soaking behavior of the peanut kernel. The rate of moisture uptake at different temperatures during hydration depicts the process as diffusion-controlled in the primary phase, with a higher absorption rate followed by a slower absorption rate during the secondary phase of hydration. Effective diffusivity in the endothermic process of moisture absorption varied from 2.905×10^{-10} to 10.754×10^{-10} (m^2/sec.) over the studied temperature range with the activation energy of 32.175 KJ/mol.

Keywords: peanut, physical properties, soaking, diffusion, models, hydration.

I. INTRODUCTION

Peanut (*Arachis hypogaea*) is the 3rd most crucial oilseed crop after soybean and cotton. Being a legume crop, it is rich in protein. This tropical cash crop is often referred to as "The king of oilseeds," groundnut, earth nut, wonder nut, or poor men's cashew nut. India is the pioneer producer of peanuts with a production of 6.48 MMT and contributed more than 18% of world production for 2020 (FAOSTAT 2022)[1]. The chief peanut-producing states in India are Gujarat, Rajasthan, Andhra Pradesh, Tamil Nadu, and Madhya Pradesh. These five states account for around 90% of the total area under peanut cultivation, mainly as the *Kharif* season crop (June - September). As a leguminous crop, it is grown in crop rotation mainly to maintain soil health and reduce soil erosion.

Eighty percent of the total peanut produced in India undergoes processing for oil extraction through either mechanical or solvent extraction in a batch or continuous process. The high temperature in most efficient mechanical extractors damages the edible quality of obtained defatted materials and is unsuitable for human consumption (BADWAIK, PRASAD, DEKA 2012)[2]. Residual solvent associated with solvent-extracted defatted peanut meal creates problems in its utilization for various value-added products (BADWAIK, PRASAD, SETH 2014)[3], therefore affecting the loss of valuable resources.

Peanut may be considered a functional food, as it contains numerous functional and health-promoting compounds, including arginine, mono, and polyunsaturated fatty acids, dietary fiber, folate, niacin, vitamin E, and most of the vital minerals (GOPALAN, RAMA SASTRI, BALASUBRAMANIAN 1971)[4] beneficial for human health. The presence of bioactive phenolic compounds provides this valuable biomaterial with a rich source of antioxidants (FRANCISCO, RESURRECCION 2008)[5]. Raw peanut in India is used in a wide variety of forms. The process involved often soaking in water before being used as an ingredient in the preparation of different delicacies. Soaking and grinding in preparation of seasonings are commonly used to garnish the most traditional fermented foods such as *idly, dosa, vada,* and *uttapam* with several other breakfast items in the Indian subcontinent (ACHAYA 1984)[6].

The physical properties of peanut kernels, like those of other seeds, become helpful in designing equipment, especially for handling, processing, and storing. The moisture content of grain affects the efficiency of cleaning, grading, and separation processes (YALÇıN, ÖZARSLAN, AKBAŞ 2007)[7]. The author has made investigations the determination of the physical properties of various leguminous splits, such as chickpeas, lentils, black gram, and green gram (BHATIA, SHARMA, PRASAD, PRASAD 2009)[8; PRASAD, VAIRAGAR, BERA 2010)[9; KAUR, SHEKHAR, KUMAR, PRASAD 2021)[10; KAUR, PRASAD 2022)[11; KAUR, PRASAD 2022)[12; KAUR, PRASAD 2021)[13].

Author α: Department of Food Process Engineering, National Institute of Technology, Rourkela, Odisha, India.
e-mail: scholarshekhar@gmail.com
Author σ: Department of Food Engineering and Technology, SLIET, Longowal, Punjab, India. e-mail: manojsingh85@gmail.com
Author ρ: Department of Food Engineering and Technology, SLIET, Longowal, Punjab, India. e-mail: profkprasad@gmail.com

Limited studies on water absorption kinetics for peanuts were carried out. The present study aims to investigate the moisture-dependent physical properties of temperature-dependent water absorption kinetics to assess the adequacy of mathematical models in describing the process of water absorption kinetics.

II. Materials and Methods

a) Sample Preparation

The dried whole peanut pods of genotype GG-20 were procured from the Central Institute of Postharvest Engineering and Technology (CIPHET), Punjab Agricultural University Campus (PAU), Ludhiana (Punjab). The whole peanut pods were cleaned and dehulled. The kernels were manually sorted to separate damaged and shrunk kernels. The sorted sound kernels (Fig. 1) were stored in air-tight glass containers and under refrigerated conditions. The samples were taken out as per the experimental requirements. The initial moisture contents of the kernels were determined using the hot air oven method (GUPTA, DAS 2000)[14]. The predetermined weight of moisture was impregnated to obtain the four levels of moisture content for the peanut kernels as 5.57±0.56%, 15.09±0.65%, 24.98±0.51%, and 35.07±0.61% (wet basis), conditioned and stored at 5±1°C. The samples for the study were taken out and kept in the ambient environmental condition in sealed pouches to equilibrate quickly and without any change of moisture content.

b) Determination of Physical Properties

The geometrical shape consisting of a cylinder and two hemispheres at the ends has been found to be quantitative appropriateness for peanuts (AKCALI, INCE, GUZEL 2006)[15]. The physical dimensions were determined randomly measured for three major perpendicular dimensions, length (L), width (W), and thickness (T), of 100 seeds of each variety using a digital vernier caliper (Mitutoyo Corporation, Japan) having the precision of 0.01mm. The geometric mean dimension (D_g) of peanut kernels was found using the relationship as given (MOHSENIN 2020)[16]:

$$D_g = \sqrt[3]{LWT} \qquad (1)$$

The criteria used to describe the shape of the seed are sphericity. Thus, the sphericity (ϕ) was accordingly computed (MOHSENIN 2020)[16] as:

$$\phi = \left[\frac{D_g}{L}\right]100 \qquad (2)$$

The surface area (S_a) was calculated (Eqn. 3) considering the geometrical properties of the kernel as:

$$S_a = \pi \times \mathrm{L} \times \mathrm{T} \qquad (3)$$

Electronic balance (Ishida Co. Ltd., Japan) was used to measure the weight of the sample to an accuracy of 0.001 g. The true density of a peanut kernel is defined as the ratio of the mass of the seed to the solid volume occupied (DESHPANDE, BAL, OJHA 1993)[17]. The liquid displacement technique determined the seed volume and its true density. The immersion time was maintained below 10 sec, which was considered too small to absorb water. The amount of displaced water was recorded from the graduated scale of the measuring cylinder (AMIN, HOSSAIN, ROY 2004)[18]. The porosity (ε) of bulk seed was computed from the values of true density (ρ_t) and bulk density (ρ_b) using the relationship (Eqn. 4) given (MOHSENIN 2020)[16]:

$$\varepsilon = \left[1 - \left(\frac{\rho_b}{\rho_t}\right)\right]100 \qquad (4)$$

To determine the angle of repose (φ), a cylinder of 50 mm diameter was used. The height and diameter of the formed heap of peanut kernels were measured to determine the angle of repose (φ) using the relationship:

$$\varphi = \arctan\frac{(2\mathrm{H})}{\mathrm{D}} \qquad (5)$$

Where H is the height of the heap (mm), and D is the diameter of the heap (mm) at its base.

The static coefficient of friction (μ) was determined for three structural surfaces, namely galvanized steel sheets, glass, and plywood. A plastic cylinder of 50 mm diameter and 60 mm height was placed on an adjustable tilting flat plate faced with the test surface and filled with a sample of about 100 g. The cylinder was raised slightly to ensure complete contact with the peanut kernel and the experimenting surface and to avoid any error being induced by the test cylinder. The setup was then inclined gradually until the cylinder started sliding down. The angle of tilt was noted from a graduated scale (DUTTA, NEMA, BHARDWAJ 1988)[19; SHEPHERD, BHARDWAJ 1986)[20].

$$\tan\alpha = \mu \qquad (6)$$

All the experiments were replicated at least ten times, and average values were reported.

c) Water Absorption during Soaking

The hydration behavior of peanut kernel was determined by soaking a 50g sample in cylindrical glass containers containing 250 ml of distilled water (1:5 w/v) (ABD EL-HADY, HABIBA 2003)[21]. Soaking water temperatures were 5, 15, 25, and 35°C. Before each experiment, the sample, containers, and distilled water were kept at the desired temperature for a few hours. Hydration behavior was precisely observed for up to 24 hours using an electronically controlled water bath to an accuracy of ±0.2°C (RESIO, AGUERRE, SUAREZ 2005)[22]. The moisture content of the sample during hydration was determined based on the sample's weight increase. Soaked kernels were immediately blotted with the muslin cloth to remove any chance of the presence of surface water before taking the reading (VERMA, PRASAD 1999)[23].

d) Modeling of Water Absorption of Peanut Kernels

The kinetics of hydration of peanut kernels was assessed using selected models presented in Table 1. Analysis of absorption behavior through selected models, the time-dependent data of moisture content, and moisture ratio (MR) of peanut kernels is essential. The moisture ratio was calculated as follows:

$$\mathrm{MR} = \frac{\mathrm{M_t - M_e}}{\mathrm{M_0 - M_e}} \tag{7}$$

Where M_o, M_e, and M_t are the initial equilibrium, and moisture at any time t, respectively. The moisture ratio data were then fitted to the different models (exponential model and Weibull model). The parameters in each model were estimated by using the nonlinear regression analysis. Adequacy of the fitted model was assessed in terms of coefficient of multiple determination (R^2), Chi-square (χ^2), and root mean square error (RMSE) to ascertain the quality fit with a condition of higher R^2 value and lower χ^2 and RMSE values (KASHANINEJAD, MAGHSOUDLOU, RAFIEE, KHOMEIRI 2007)[24].

These parameters can be calculated as follows:

$$R^2 = \frac{\left[\sum_{i=1}^{N}(MR_{exp\ .i} MR_{pre\ ,i}) - \left(\frac{(\sum_{i=1}^{N} MR_{exp\ .i})(\sum_{i=1}^{N} MR_{pre\ .i})}{N}\right)\right]^2}{\left[\left(\sum_{i=1}^{N} MR_{exp\ .i}^2 - \frac{(\sum_{i=1}^{N} MR_{exp\ .i})^2}{N}\right)\left((\sum_{i=1}^{N} MR_{pre\ .i}^2) - \frac{(\sum_{i=1}^{N} MR_{pre\ .i})^2}{N}\right)\right]} \tag{8}$$

$$\chi^2 = \frac{1}{\mathrm{N-n}} \sum_{\mathrm{i=1}}^{\mathrm{N}} (\mathrm{MR_{exp\ ,i}} - \mathrm{MR_{pre\ ,i}})^2 \tag{9}$$

$$\mathrm{RMSE} = \sqrt{\frac{1}{\mathrm{N}} \sum_{\mathrm{i=1}}^{\mathrm{N}} (\mathrm{MR_{pre\ ,i}} - \mathrm{MR_{exp\ ,i}})^2} \tag{10}$$

where $MR_{exp,i}$ is the ith experimentally observed moisture ratio, $MR_{pre,i}$ the ith predicted moisture ratio, N is the number of observations, and n is the number of constants in the model (YALÇıN, ÖZARSLAN, AKBAŞ 2007)[7; TOĞRUL, PEHLIVAN 2003)[25].

III. RESULTS AND DISCUSSION

a) Physical Properties

An increase in moisture content from 5 to 35% has shown a linear change in length (L), width (W), thickness (T), and geometric mean diameter (GMD) of peanut kernels (Fig. 2) from 14.52 to 16.37 mm, 8.40 to 9.61 mm, 7.41 to 8.79 mm, and 9.67 to 11.14 mm, respectively (Table 2). A linear dimensional increase in peanut kernels with an increase in moisture content was mainly due to the absorption of moisture that resulted in the swelling of peanut cells and thus affected kernel's dimensional properties. The linear increase in width and thickness has also been reported for popcorn kernel (KARABABA 2006)[26] and pistachio nut (KASHANINEJAD, MORTAZAVI, SAFEKORDI, TABIL 2006)[27]. A minor initial decrease in the sphericity (ϕ) of peanut kernel with further increase as the increase in moisture content is evident (Fig 2). The initial decrease in sphericity may be attributed to the initial higher rate of lateral expansion in comparison to the change in the width and thickness. However, at later stages of moisture gain, the rate of expansion in width and thickness increased more and caused to increase in sphericity. The high sphericity value suggests that the kernel tends towards a spherical shape (OMOBUWAJO, SANNI, OLAJIDE 2000)[28], being cylindrical. The surface area (S_a) of peanut kernels increased linearly from 3.38 to 4.52 cm^2 with increased moisture content. It was of overall 33.73% increase (Fig. 2). A surface area is a relevant tool in determining the shape of the kernel and indicating the material behavior on oscillating surfaces during processing (ALONGE, ADIGUN 1999)[29].

The unit mass (UM) of peanut kernel was found to be increased from 0.462 to 0.724 gm with an increase in moisture content (Table 2). Differential sphericity, surface area, and unit mass of materials serve in designing aerodynamic cleaning systems. Bulk density (ρ_B) decreased from 560 to 496 kg/m^3 with an increase in moisture (Fig. 3). This decrease in the bulk density on change of moisture content is probably due to higher volume expansion in kernel in comparison to weight change on change in moisture content (Fig. 3). A decrease in bulk density was found for chickpea seeds from 800 to 741.4 kg/m^3 with an increase in moisture content from 4.9 to 14.1% (AMIN, HOSSAIN, ROY 2004)[18]. A similar relation between moisture content and bulk density was reported for Soybean (DESHPANDE, BAL, OJHA 1993)[17], sunflower seed (GUPTA, DAS 1997)[30], and popcorn kernel (KARABABA 2006)[26]. Porosity increased linearly from 39.58 to 46.77% with an increase in moisture content, and similar trends were reported for gram (DUTTA, NEMA, BHARDWAJ 1988)[31], sunflower kernel (GUPTA, DAS 1997)[30], green gram (NIMKAR, CHATTOPADHYAY 2001)[32], chickpea seed (KONAK, CARMAN, AYDIN 2002)[33], and popcorn kernel(KARABABA 2006)[26].

The angle of repose and coefficient of friction as frictional properties are essential in designing equipment for solid flow and storage structures. The coefficient of friction between the seed and wall is an essential parameter in predicting seed pressure on walls (GUMBE, MAINA 1990)[34]. The angle of repose of peanut kernels increased from 39.01 to 50.48° with an increase in moisture content in the range of 5 to 35% (Table 2). The static coefficient of friction at various moisture levels reflects the increase in moisture content for all the analyzed surfaces (Fig. 4). This is due to the increased adhesion properties between the seed and the material surfaces at higher moisture levels.

b) Soaking Kinetics

The behavior of moisture uptake during time-dependent soaking by peanut kernel at temperatures 5, 15, 25, and 35°C is shown in Fig. 5. An early rapid hydration rate in the primary phase with a slower hydration rate in the second phase was observed (Fig. 5). The time needed for the transition of phase was found by applying the creep deformation properties in the water absorption process, observed to be temperature-dependent, and were 2.80, 2.56, 1.89, and 1.24 hrs at 5, 15, 25, and 35°C, respectively. The diffusion process governs the rapid initial water uptake in the primary phase was probably due to the filling of capillaries on the surface of the seed coats. A decrease in water absorption rate further in the relaxation phase may be attributed to the reason that water filling decreased the driving force. At any time, the moisture content of the kernels increased with temperature, indicating that the amount of water absorbed during hydration was a function of both soaking time and temperature (Fig. 5). Similar results were found in the case of rice (KASHANINEJAD, MAGHSOUDLOU, RAFIEE, KHOMEIRI 2007)[24]. The water gain increases with the temperature increase of soaking water (Fig. 5). This increase is due to changes in diffusion resistance. Higher temperatures are known to expand and soften the material, which has affected the intactness and lowered the diffusion resistance to water transfer. Due to this, water gain cannot follow the pace of increased temperature. Temperature-induced softening has been reported for soybean (SINGH, KULSHRESTHA 1987)[35], chickpea(SAYAR, TURHAN, GUNASEKARAN 2001)[36], and kidney bean (ABU-GHANNAM, MCKENNA 1997)[37].

c) Fitting of the Model Equation

i. *Empirical Models*

Table 3 presents the fitted Peleg, Exponential, and Weibull models as nonlinear regression models to describe the water absorption characteristic of peanut kernels at hydration temperatures of 5 to 35°C. All selected models accurately described peanut kernel's water absorption at the hydration temperatures from 5 to 35°C. The selected models gave accurate predictions and satisfactorily described soaking characteristics as R^2 values were equal to or higher than 96.36%, RMSE values were lower than 0.005 with χ^2 valued lower than 0.005 (Table 3).

Appraisal of the Peleg rate constant (K_1) reflects a linear decrease in its value from 0.065 to 0.017 hr/%mc (db) with the increasing temperature from 5 to 35°C (Table 3). The term "inverse of K_1" is called the initial rate of absorption; thus, at a given temperature, as K_1 decreases, the amount of water absorbed becomes greater (PRASAD, VAIRAGAR, BERA 2010)[9]. This resulted in a lower K_1 at 35°C compared to a lower temperatures depicting a higher initial water absorption rate for peanut kernel. Further, the water absorption process proceeded at a slower pace and ceased attaining the equilibrium water content. The Peleg capacity constant, $K_{2,}$ as *the* absorption ability of foods showed a marginal increase with temperature (Table 3), reflecting the property of peanut kernel towards water absorption capacity.

The probabilistic Weibull model describes a system's behavior with some degree of variability (CUNHA, OLIVEIRA, OLIVEIRA 1998)[38]. Weibull shape parameter (α) is a behavior index that depends on the process mechanism, and the higher its value, the slower the process in the initial phase of absorption (CUNHA, OLIVEIRA, OLIVEIRA 1998)[38; MACHADO, OLIVEIRA, GEKAS, SINGH 1998)[39]. Thus, the inverse of the Weibull shape parameter was thus considered an indicator of the initial rate of the hydration process. An increase in the temperature of soaking thus reduced the value of α from 5.609 to 1.546, further justifying the obtained temperature-dependent soaking behavior for peanut kernel (Table 3).

Weibull scale parameter (β) represents the time needed to accomplish approximately 63% of total absorbed water (CUNNINGHAM, MCMINN, MAGEE, RICHARDSON 2007)[40]. Table 3 shows the effect of temperature change on relative rates of moisture diffusion and thus affecting the overall absorption process. This implies that with an increase in temperature from 5 to 35°C, the absorption rate in the primary phase of soaking was accelerated significantly (Fig. 5).

Fitting the exponential model to the experimental data at four different temperatures for the hydration process (Fig. 6) depicts an increasing trend of hydration rate constant (K) with the soaking temperature (Table 3). The high observed value of the coefficient of determination (R^2) confirmed the applicability in the prediction of the soaking process of the peanut kernel.

A large amount of absorbed water is present in the first phase of the process and further reaches equilibrium in the relaxation phase of soaking. However, at lower temperatures, the absorbed water in the primary soaking phase is less, and the absorption continues in the second phase. The values for the parameters K_1, K_2; K, and α & β in Peleg, Exponential, and Weibull models, respectively, supported the findings.

ii. *Diffusivity Model and Activation Energy*

To predict moisture diffusivity during the soaking of peanut kernels, the second Fick's law solution for diffusion out of an infinite cylinder being length of more than twice the width was used. For this purpose, the assumptions considered were (i) the effective diffusion coefficient is independent of moisture concentration, (ii) the volume of the kernel does not change during water absorption, and (iii) the surface of the kernel reaches the equilibrium moisture content instantaneously upon immersion in absorption media. The general series solution of Fick's second law in the infinite cylinder is given below (CRANK 1975)[41]:

$$\mathrm{MR} = \sum_{n=1}^{\infty} \frac{4}{\beta_n^2} exp\left[-\frac{\beta_n^2}{R^2} \times D_e t\right] \qquad (11)$$

D_e is the effective diffusivity (m^2/sec.) and R is the characteristics radius of the cylinder. Eqn calculated the effective diffusion coefficient. (11) using slopes derived from the linear regression of ln (MR) against time data. The effective diffusion coefficient during the soaking of peanut kernels varied from 2.9053×10-10 to 10.753×10-10 (m^2/sec.) over the temperature range studied 5-35^{0}C (Table 4).

A similar result was also obtained with other agricultural seeds. The effectiveness of diffusivity during soaking of rice varied from 5.58× 10^{-11} to 3.57 × 10^{-11} (m^2/sec.) in the temperature range from 25 to 70^{0}C (KASHANINEJAD, MAGHSOUDLOU, RAFIEE, KHOMEIRI 2007)[24], in case of soybean, varied from 1.08 × 10-10 to 2.00 × 10-10 m^2/sec. in the temperature range from 40 to 60^{0}C (HSU 1983)[42], and 1.632× 10^{-9} to 3.237× 10^{-9} (m^2/sec.) in case of splits chickpea at the hydration temperature range of 40 to 60^{0}C (PRASAD, VAIRAGAR, BERA 2010)[9].

The effect of temperature on effective diffusivity is generally described using the Arrhenius- type relationship to obtain a better agreement of the predicted curve with experimental data:

$$D_{\mathrm{e}} = D_0 \exp\left(-\frac{E_a}{RT_a}\right) \qquad (12)$$

D_0 is a diffusivity-constant equivalent to the diffusivity at infinitely high temperatures, Ea is the activation energy (K J/mol), R is the universal gas constant (8.314 J/mol. K), and Ta is the absolute temperature. The logarithm of D_e as a function of the reciprocal of absolute temperature (T_a) is plotted in Fig.7. The results show a linear relationship between (log D_e) and (1/T_a) or an Arrhenius-type relationship (Eqn. 12). The diffusivity constant (D_0) and activation energy (E_a) calculated from the linear regression is 8.010 (m^2/sec.) and 32.175 (KJ/mol), respectively. This value is comparable to those reported in the literature for water absorption in some legumes. This activation energy is in reasonable agreement with the data presented by several author's for other grains. Activation energy (Ea) value of 30.0 KJ/mol in the case of whole rice grains (BELLO, TOLABA, SUAREZ 2004)[43] and 22.49 to 22.70 KJ/mol in the case of hydration of chickpea splits of different shapes (PRASAD, VAIRAGAR, BERA 2010)[9].

IV. Conclusions

The hydration kinetics of peanut kernel (GG-20) in plain water at different temperatures was examined. The soaking process exhibited an initial faster rate of water absorption followed by a slower pace during the secondary absorption phase. The transition from primary absorption phases occurred approximately between 1.23 to 2.80 hrs, depending on the soak water temperature, which may be used as the deciding time for soaking of peanut. The moisture absorption was an endothermic process with heat absorption of 32.175 KJ/mol.

References Références Referencias

1. FAOSTAT *FAOSTAT statistics database*. Edtion ed. Rome: FAO, 2022.
2. BADWAIK, L., PRASAD, K. DEKA, S. Optimization of extraction conditions by response surface methodology for preparing partially defatted peanut. International Food Research Journal, 2012, 19(1), 341.
3. BADWAIK, L. S., PRASAD, K. SETH, D. Optimization of ingredient levels for the development of peanut based fiber rich pasta. Journal of Food Science and technology, 2014, 51(10), 2713-2719.
4. GOPALAN, C., RAMA SASTRI, B. BALASUBRAMANIAN, S. Nutritive value of Indian foods 1971.
5. FRANCISCO, M. L. D. RESURRECCION, A. Functional components in peanuts. Critical reviews in food science and nutrition, 2008, 48(8), 715-746.
6. ACHAYA, K. T. Everyday Indian processed foods 1984.
7. YALÇıN, İ., ÖZARSLAN, C. AKBAŞ, T. Physical properties of pea (Pisum sativum) seed. Journal of Food Engineering, 2007, 79(2), 731-735.
8. BHATIA, T., SHARMA, R., PRASAD, K. PRASAD, K. Studies on some physical properties of protein-rich legume (Lens esculantus) splits. Asian Journal of Chemistry, 2009, 21(10), S103-107.
9. PRASAD, K., VAIRAGAR, P. BERA, M. Temperature dependent hydration kinetics of Cicer arietinum splits. Food Research International, 2010, 43(2), 483-488.
10. KAUR, R., SHEKHAR, S., KUMAR, P. PRASAD, K. Image Analysis as a Non-Destructive Approach in Selective Characterization of Promising Indian Chickpea Cultivars. In *Biology and Life Sciences Forum*. 2021, vol. 6, p. 112.
11. KAUR, R. PRASAD, K. Characterization and classification of selective Indian Chickpea cultivars based on physical and hydration properties, using

Image and Multivariate analysis. Legume Science, 2022, 4(3), e168.
12. KAUR, R. PRASAD, K. Elucidation of chickpea hydration, effect of soaking temperature, and extent of germination on characteristics of malted flour. Journal of Food Science, 2022, 87(5), 2197-2210.
13. KAUR, R. PRASAD, K. Effect of hydrothermal exposure on physical properties of Cicer Arietinum seeds. AIP Conference Proceedings, 2021, 2352, 1-8.
14. GUPTA, R. DAS, S. Fracture resistance of sunflower seed and kernel to compressive loading. Journal of Food Engineering, 2000, 46(1), 1-8.
15. AKCALI, I., INCE, A. GUZEL, E. Selected physical properties of peanuts. International Journal of Food Properties, 2006, 9(1), 25-37.
16. MOHSENIN, N. N. *Physical properties of plant and animal materials: v. 1: physical characteristics and mechanical properties.* Edtion ed.: Routledge, 2020. ISBN 1000122638.
17. DESHPANDE, S., BAL, S. OJHA, T. Physical properties of soybean. Journal of Agricultural Engineering Research, 1993, 56(2), 89-98.
18. AMIN, M., HOSSAIN, M. ROY, K. Effects of moisture content on some physical properties of lentil seeds. Journal of Food Engineering, 2004, 65(1), 83-87.
19. DUTTA, S., NEMA, V. K. BHARDWAJ, R. Physical properties of gram. Journal of Agricultural Engineering Research, 1988, 39(4), 259-268.
20. SHEPHERD, H. BHARDWAJ, R. Moisture-dependent physical properties of pigeon pea. Journal of Agricultural Engineering Research, 1986, 35(4), 227-234.
21. ABD EL-HADY, E. HABIBA, R. Effect of soaking and extrusion conditions on antinutrients and protein digestibility of legume seeds. LWT-Food Science and Technology, 2003, 36(3), 285-293.
22. RESIO, A. N. C., AGUERRE, R. J. SUAREZ, C. Analysis of simultaneous water absorption and water–starch reaction during soaking of amaranth grain. Journal of Food Engineering, 2005, 68(2), 265-270.
23. VERMA, R. PRASAD, S. Kinetics of absorption of water by maize grains. Journal of Food Engineering, 1999, 39(4), 395-400.
24. KASHANINEJAD, M., MAGHSOUDLOU, Y., RAFIEE, S. KHOMEIRI, M. Study of hydration kinetics and density changes of rice (Tarom Mahali) during hydrothermal processing. Journal of Food Engineering, 2007, 79(4), 1383-1390.
25. TOĞRUL, İ. T. PEHLIVAN, D. Modelling of drying kinetics of single apricot. Journal of Food Engineering, 2003, 58(1), 23-32.
26. KARABABA, E. Physical properties of popcorn kernels. Journal of Food Engineering, 2006, 72(1), 100-107.
27. KASHANINEJAD, M., MORTAZAVI, A., SAFEKORDI, A. TABIL, L. Some physical properties of Pistachio (Pistacia vera L.) nut and its kernel. Journal of Food Engineering, 2006, 72(1), 30-38.
28. OMOBUWAJO, T., SANNI, L. OLAJIDE, J. Physical properties of ackee apple (Blighia sapida) seeds. Journal of Food Engineering, 2000, 45(1), 43-48.
29. ALONGE, A. ADIGUN, Y. Some physical and aerodynamic properties of sorghum as related to cleaning. In *21st annual conference of the Nigerian society of agricultural engineers (NSAE). Federal Polytechnic Bauchi, Nigeria.* 1999.
30. GUPTA, R. DAS, S. Physical properties of sunflower seeds. Journal of Agricultural Engineering Research, 1997, 66(1), 1-8.
31. DUTTA, S., NEMA, V. BHARDWAJ, R. Thermal properties of gram. Journal of Agricultural Engineering Research, 1988, 39(4), 269-275.
32. NIMKAR, P. CHATTOPADHYAY, P. PH—Postharvest Technology: some physical properties of green gram. Journal of Agricultural Engineering Research, 2001, 80(2), 183-189.
33. KONAK, M., CARMAN, K. AYDIN, C. PH—Postharvest Technology: Physical properties of chick pea seeds. Biosystems engineering, 2002, 82(1), 73-78.
34. GUMBE, L. MAINA, C. Friction coefficient of cereal grains on various surfaces. AMA, Agricultural Mechanization in Asia, Africa and Latin America, 1990, 21(4), 61-64.
35. SINGH, B. KULSHRESTHA, S. Kinetics of water sorption by soybean and pigeonpea grains. Journal of Food Science, 1987, 52(6), 1538-1541.
36. SAYAR, S., TURHAN, M. GUNASEKARAN, S. Analysis of chickpea soaking by simultaneous water transfer and water–starch reaction. Journal of Food Engineering, 2001, 50(2), 91-98.
37. ABU-GHANNAM, N. MCKENNA, B. Hydration kinetics of red kidney beans (Phaseolus vulgaris L.). Journal of Food Science, 1997, 62(3), 520-523.
38. CUNHA, L. M., OLIVEIRA, F. A. OLIVEIRA, J. C. Optimal experimental design for estimating the kinetic parameters of processes described by the Weibull probability distribution function. Journal of Food Engineering, 1998, 37(2), 175-191.
39. MACHADO, M. D. F. T., OLIVEIRA, F. A., GEKAS, V. SINGH, R. P. Kinetics of moisture uptake and soluble-solids loss by puffed breakfast cereals immersed in water. International Journal of Food Science & Technology, 1998, 33(3), 225-237.
40. CUNNINGHAM, S., MCMINN, W., MAGEE, T. RICHARDSON, P. Modelling water absorption of pasta during soaking. Journal of Food Engineering, 2007, 82(4), 600-607.
41. CRANK, J. *The Mathematics of Diffusion.* Edtion ed.: Oxford University Press, New York, 1975.

42. HSU, K. H. Effect of temperature on water diffusion in soybean. Journal of Food Science, 1983, 48(4), 1364-1365.

43. BELLO, M., TOLABA, M. P. SUAREZ, C. Factors affecting water uptake of rice grain during soaking. LWT-Food Science and Technology, 2004, 37(8), 811-816.

Fig. 1: Charged coupled device snapshot showing shelled peanut kernels of GG-20 variety

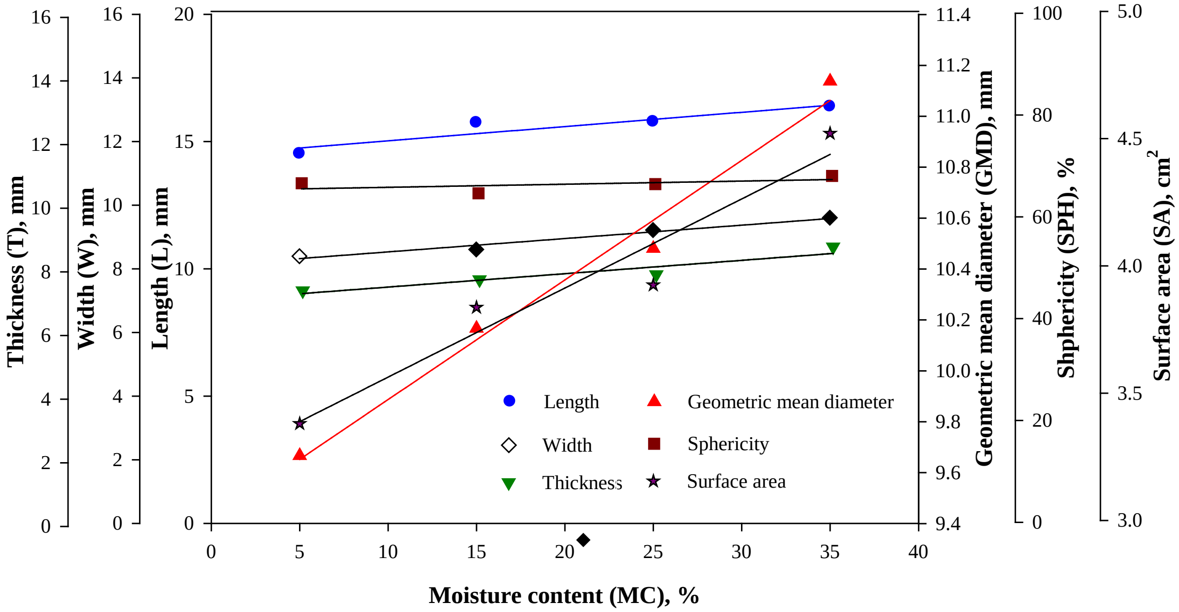

Fig. 2: Moisture dependent dimensional characteristics of peanut kernels

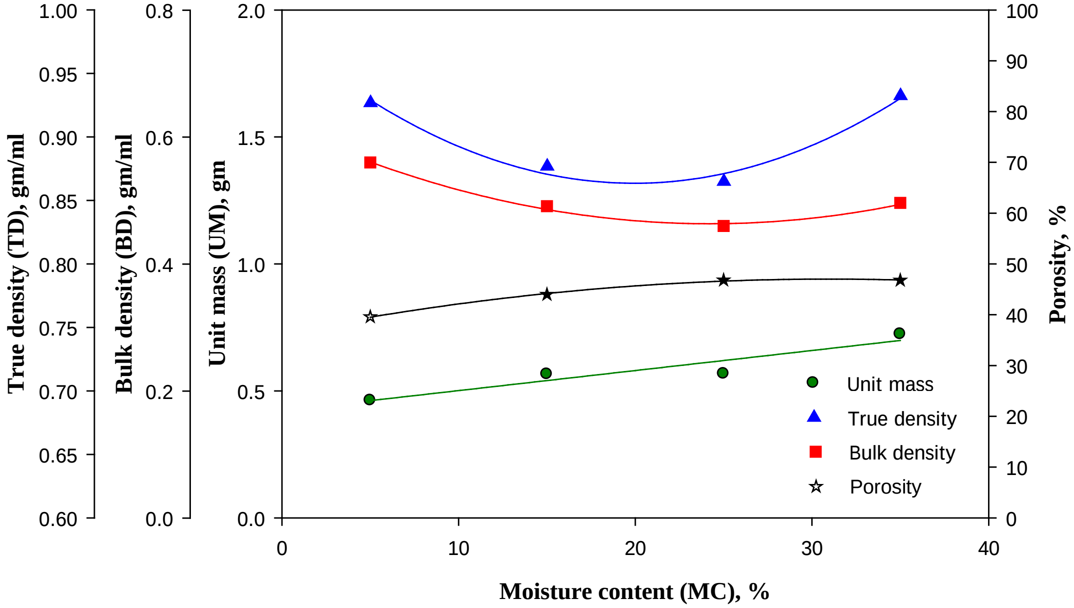

Fig. 3: Moisture dependent gravimetric characteristics of peanut kernels

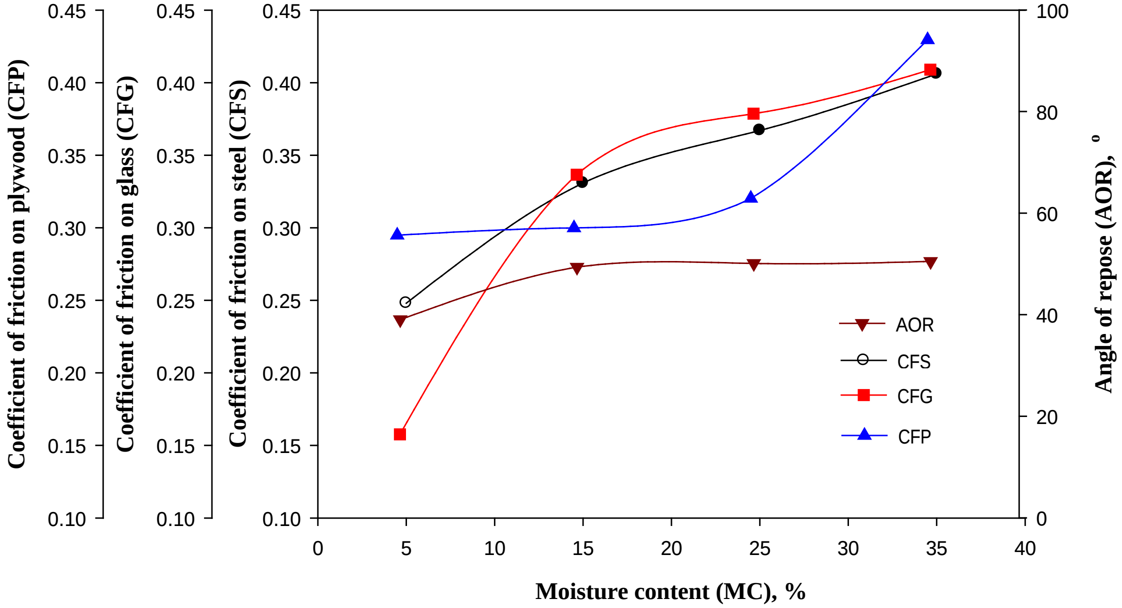

Fig. 4: Moisture dependent frictional characteristics of peanut kernels

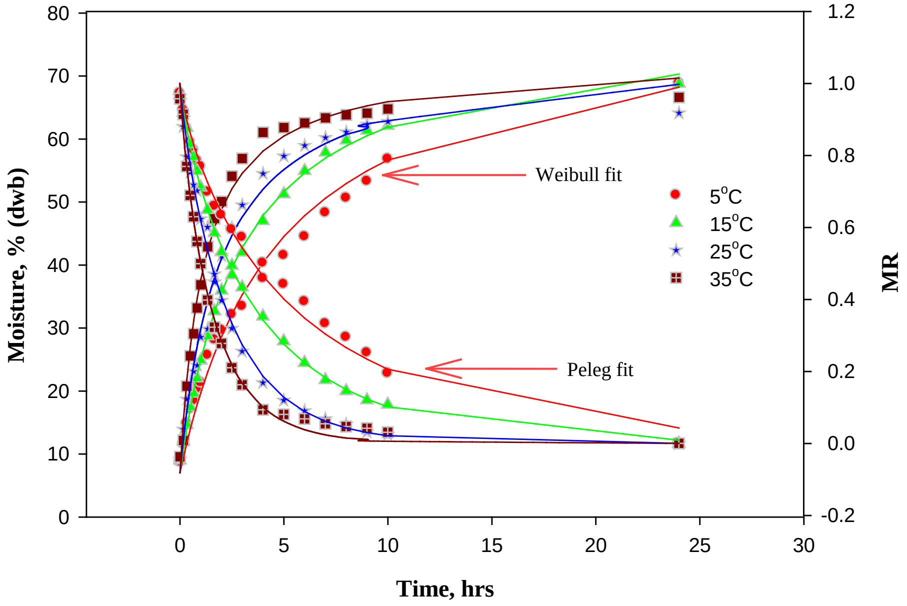

Fig. 5: Temperature dependent hydration characteristics of peanut kernel (Peleg and Weibull fit)

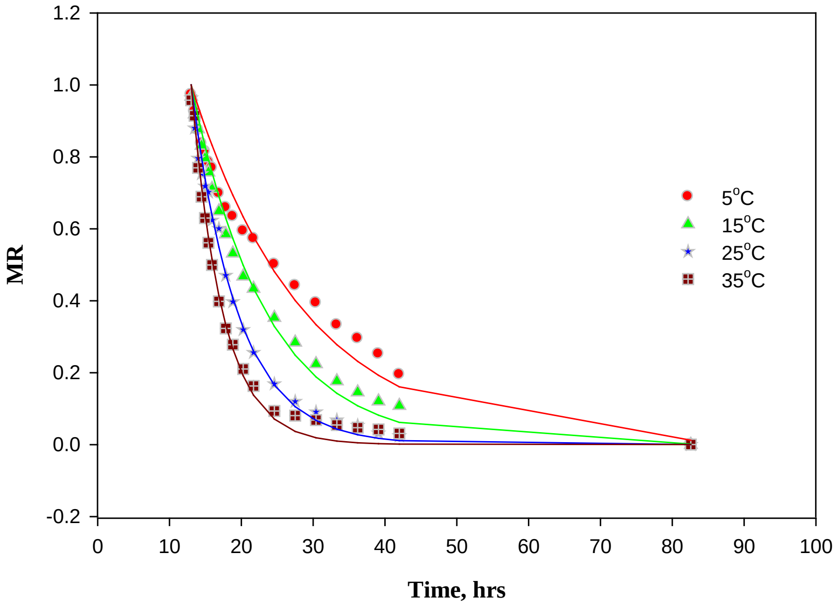

Fig. 6: Temperature dependent hydration characteristics of peanut kernel (Exponential fit)

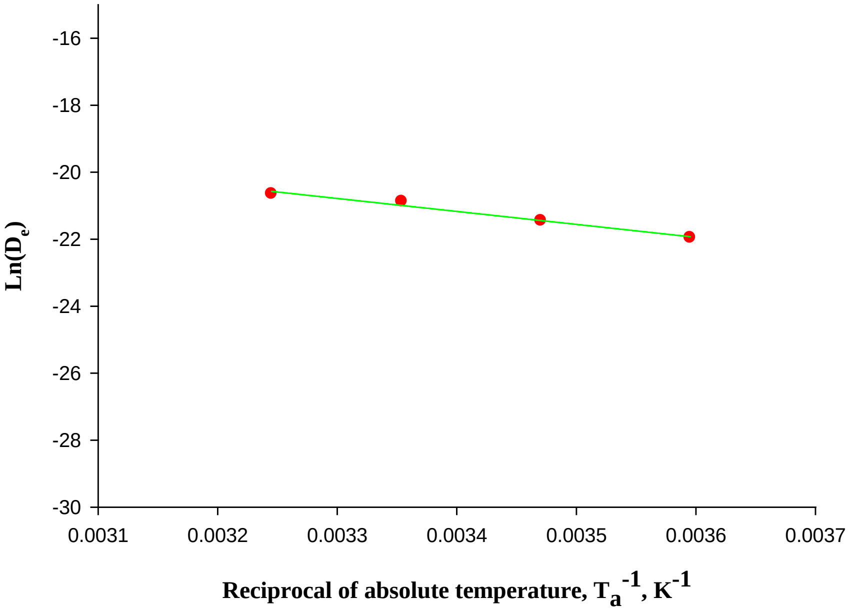

Fig. 7: Arrhenius plot of effective diffusivity of peanut kernels

Table 1: Models used for describing the peanut kernel hydration data

Model Name	Equation
Peleg	$M = M_0 + \frac{t}{(K_1 + K_2 t)}$
Exponential	$MR = exp(-kt)$
Weibull	$MR = Exp\,(-({}^{t}/_{\propto})^{\beta})$

Table 2: Moisture dependent physical properties of peanut kernel (GG-20)

Parameters	Moisture Levels of shelled peanut (%, wwb)			
	6.57±0.44%	15.74±0.01%	25.21±0.03%	35.07of ±0.09%
Length, mm	14.52±1.48	15.74±1.41	15.78±1.52	16.37±1.20
Width, mm	8.40±0.72	8.61±0.44	9.22±0.49	9.61±0.47
Thickness, mm	7.41±0.43	7.76±0.58	7.92±0.65	8.79±0.70
GMD, mm	9.67±0.66	10.17±0.56	10.48±0.54	11.14±0.50
Sphericity, %	66.60±4.20	64.61±3.66	66.44±4.97	68.03±4.56
Surface Area, cm^2	3.38±0.45	3.84±0.50	3.93±0.47	4.52±0.43
Unit Mass, gm	0.462±0.161	0.565±0.127	0.567±0.139	0.724±0.143
Bulk Density, kg/m^3	560.0±10	491.0±7.0	460.0±12.0	496.0±17.0
True Density, gm/ml	0.927±0.010	0.877±0.016	0.865±0.019	0.932±0.026
Porosity, %	39.58±0.95	43.98±1.63	46.81±1.09	46.77±0.97
Angle of Repose, degree	39.01±1.87	49.35±1.55	50.09±1.06	50.48±0.68
CSF (Steel)	0.248±0.004	0.331±0.014	0.367±0.008	0.406±0.006
CSF (Glass)	0.158±0.007	0.337±0.020	0.379±0.010	0.409±0.006
CSF (Plywood)	0.295±0.004	0.300±0.008	0.320±0.013	0.430±0.028

Table 3: Estimation of the parameters and goodness of fit for Peleg, Exponential and Weibull models

Temperature (°C)	Peleg Model					Exponential Model				Weibull Model				
	K_1	K_2	R^2	χ^2	RMSE	K	R^2	χ^2	RMSE	α	β	R^2	χ^2	RMSE
5	0.065	0.014	0.9804	0.0007	0.0115	0.183	0.9636	0.0031	0.0546	5.609	0.789	0.9854	0.0013	0.0346
15	0.042	0.014	0.9984	0.0001	0.0077	0.278	0.9863	0.0046	0.0363	3.683	0.826	0.9989	0.0001	0.0105
25	0.029	0.015	0.9874	0.0005	0.0204	0.450	0.9921	0.0008	0.0284	2.256	0.905	0.9946	0.0006	0.0234
35	0.017	0.015	0.9905	0.0004	0.0179	0.662	0.9909	0.0009	0.0294	1.546	0.873	0.9947	0.0006	0.0224

Table 4: Temperature dependent effective diffusion coefficient of peanut kernel

Temperature (°C)	Effective diffusivity (m^2/sec)
5	2.905×10^{-10}
15	4.833×10^{-10}
25	8.581×10^{-10}
35	10.753×10^{-10}

This page is intentionally left blank

Global Journal of Researches in Engineering: C
Chemical Engineering
Volume 23 Issue 1 Version 1.0 Year 2023
Type: Double Blind Peer Reviewed International Research Journal
Publisher: Global Journals
Online ISSN: 2249-4596 & Print ISSN: 0975-5861

Modeling of CO Oxidation by Diffusion of Oxygen Atoms in Ceria-Zirconia Particulates in a Three-Way Catalyst Particle Membrane Filter

By Phyozin Koko & Katsunori Hanamura

Abstract- In order to design a microporous membrane filter comprising Three-way Catalyst (TWC) particles with a size distribution of 1 to 2 microns, isothermal CO oxidation experiments and numerical simulations were conducted to investigate the transport of oxygen atoms within primary Ceria-Zirconia (CZ) particulates. These spherical TWC particles were fabricated through the agglomeration of primary CZ and alumina particulates, incorporating Pd and Rh catalysts. By comparing experimental CO_2 emissions with simulation results over time, a temperature-dependent diffusion coefficient was determined. The simulation results reveal that the effective distance of oxygen atom transport within CZ particulates, heterogeneously distributed in the spherical TWC particle, is limited to approximately 100 nm from the surface of agglomerated spherical TWC particles within a temperature range of 175 to 225°C.

Keywords: modeling, diffusion, three-way-catalyst, membrane particulate filter.

GJRE-C Classification: LCC Code: TJ807-83

MODELINGOFCOOXIDATIONBYDIFFUSIONOFOXYGENATOMSINCERIAZIRCONIAPARTICULATESINATHREEWAYCATALYSTPARTICLEMEMBRANEFILTER

Strictly as per the compliance and regulations of:

Modeling of CO Oxidation by Diffusion of Oxygen Atoms in Ceria-Zirconia Particulates in a Three-Way Catalyst Particle Membrane Filter

Phyozin Koko [α] & Katsunori Hanamura [σ]

Abstract- In order to design a microporous membrane filter comprising Three-way Catalyst (TWC) particles with a size distribution of 1 to 2 microns, isothermal CO oxidation experiments and numerical simulations were conducted to investigate the transport of oxygen atoms within primary Ceria-Zirconia (CZ) particulates. These spherical TWC particles were fabricated through the agglomeration of primary CZ and alumina particulates, incorporating Pd and Rh catalysts. By comparing experimental CO_2 emissions with simulation results over time, a temperature-dependent diffusion coefficient was determined. The simulation results reveal that the effective distance of oxygen atom transport within CZ particulates, heterogeneously distributed in the spherical TWC particle, is limited to approximately 100 nm from the surface of agglomerated spherical TWC particles within a temperature range of 175 to 225°C.

Keywords: modeling, diffusion, three-way-catalyst, membrane particulate filter.

I. Introduction

It is essential to implement an efficient after treatment system for internal combustion engines during the transitional period until the full adoption of cleaner technologies is accomplished. To attain net-zero emission by 2050, exhaust gases from automobile engines have emerged as a significant contributor to air pollution, which is 25% of total CO_2 emission, currently ranked as a second largest source, leading to a global concern for their adverse effects on public health [1-3]. Therefore, an efficient and effective exhaust gas aftertreatment system plays an important role to reduce the solid and gaseous pollutant emissions from internal combustion engines. In conventional exhaust gas aftertreatment systems of gasoline-fueled engines, a gasoline particulate filter (GPF) is installed for filtration of solid particulate matters. Besides, a three-way catalytic converter (TWC) is used to simultaneously reduce harmful gaseous pollutants such as carbon monoxide (CO), nitrogen oxides (NO_x), and hydrocarbons (HCs) [4]. The literature has extensively been reported on the purification performance of combined TWC and GPF using wash-coating technology, commonly known as a catalyzed gasoline particulate filter (cGPF). Through application of catalyst materials deposited on the cGPF filter substrate, an integrated catalytic filter can offer a distinct advantage of not only trapping soot, but also facilitating the purification of gaseous pollutants in a single unit [5, 6]. However, the pressure-drop between the inlet and outlet of the integrated filter increases drastically because some pores are blocked by the coated TWC-paste.

Cerium oxides are well-established oxygen storage materials that have been widely used in various catalytic applications. They are particularly important as a catalytic component in TWCs installed in the exhaust gas aftertreatment systems of gasoline engines [7, 8]. The primary function of a TWC that includes cerium oxides is to simultaneously reduce three major gaseous pollutants, NO_x, CO, and HCs, through oxidation and reduction reactions. Maximal conversion yields can be achieved with an air-fuel ratio around the stoichiometric point for gasoline engines. If there are fluctuations in the oxygen concentration in the positive (fuel-lean) or negative (fuel-rich) direction around the stoichiometric point, excess oxygen can be stored by cerium oxides under a fuel-lean condition, while additional oxygen atoms can be supplied by cerium oxides under the fuel-rich conditions. The range of the air-fuel ratio for simultaneous reduction becomes slightly wider around the stoichiometric point as a well-known window [9, 10]. Ceria-zirconia (CZ) catalysts are commonly utilized to increase the oxygen storage capacity thereby enhancing the high-redox catalytic performance of ceria in TWCs. Since the exhaust gas temperature in gasoline-fueled engines typically reaches approximately 900°C, CZ is composited with alumina (Al_2O_3) to prevent the sintering effect or thermal degradation [11].

Recently, particle membrane filters have been manufactured by the authors using various catalyst components with the aim of improving soot oxidation kinetics and mitigating exhaust gas pollutants [12–14]. In contrast to wash-coated catalyzed particulate filters as mentioned above, catalyst particles were percolated as a membrane on the surface of a GPF substrate, which results in almost 100% filtration efficiency from the beginning of soot trapping and a low pressure-drop filter compared with the conventional filters [15]. By fabricating a particle membrane filter composed of three-way catalyst particles, in addition to a 100% initial

---

Author α σ: Department of Mechanical Engineering, School of Engineering, Tokyo Institute of Technology, Japan.
e-mail: koko.p.aa@m.titech.ac.jp

soot filtration efficiency, a simultaneous reduction of gaseous pollutants were achieved in a single unit [16]. Based on the findings from our previous parametric study on the fabrication of TWC particles membrane filters, the porosity of the TWC particle membrane reaches 64% under the condition of a mean particle size of 1.2 um and a superficial velocity of 5 mm/s [17]. The high porosity membrane filter contributes to low pressure-drop filtration of soot.

For the conventional TWC wash-coated filters [18, 19] and the conventional catalytic converters [20, 21], the macroscopic reaction kinetics modelling has been extensively developed and the microscopic transport of oxygen atoms in ceria has been reported [22 – 25] under the condition of the practical temperature above 700°C. However, if the thermal efficiency of engines for passenger's vehicles can be increased up to more than 50% (already reached up to 52.63%) to reduce emission of CO_2, the exhaust gas temperature at the engine out will be decreased around 300°C to 400°C [26]. By utilizing the TWC particles membrane filter proposed by the authors, it is feasible to achieve not only almost 100% initial soot filtration efficiency with low pressure-drop but also simultaneous reduction of exhaust gas pollutants as an integrated after-treatment system even under such a low temperature condition. For effective utilization of CZ particulates for chemical reaction, the transport phenomena of oxygen atom around the single primary CZ particulate should be investigated. Using the spherical agglomerated TWC particle including primary CZ particulates manufactured by the authors, the oxygen atom transport in the CZ can be analyzed by a simplified mathematical model compared with the conventional TWC wash-coated filters. In the current study, the diffusion coefficient of the oxygen atom in CZ particulate is determined through experiment and numerical simulation. Besides, the transport distance of oxygen atom in the CZ for CO oxidation is clarified under the condition of a range of temperature from 175°C to 225°C.

II. EXPERIMENTAL PROCEDURES

Figure 1 describes a miniature-sized particulate filter with a precise dimension as length x width x height (10 mm x 10 mm x 10 mm), comprised of 7x7 square channels. The miniature-sized filter substrate sample was extracted from conventional silicon carbide (Si-C) substrates of full-sized particulate filters. A high-temperature-resistant ceramic paste was utilized to seal alternating ends of the channels to create a wall-flow configuration, as illustrated in Fig. 2, in which the working gas passes through the channel walls.

Figure 3 displays a schematic diagram of the fabrication process of a three-way catalyst (TWC) particle membrane filter on a miniature filter substrate. The experimental procedure and fabrication process were discussed in detail in the previous literature [17]. The slurry used in its fabrication was comprised of 20 wt.% of primary nanometer-sized TWC particulates prepared using distilled water. These particles had an average diameter of approximately 200 nm, as shown in the TEM image in Fig. 3. The chemical composition of the primary TWC-particulates is the same as that of a commercial monolith converter, as shown in Table 1. The TWC particulate slurry was introduced into an acrylic tube to generate small droplets with a size range of 5-10 um using an ultrasonic atomizer (60 Hz frequency). Nitrogen gas was

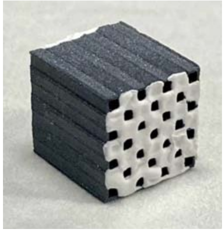

Fig. 1: Miniature particulate filter made of Si-C

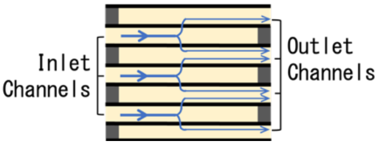

Fig. 2: Schematic of a wall-flow filter

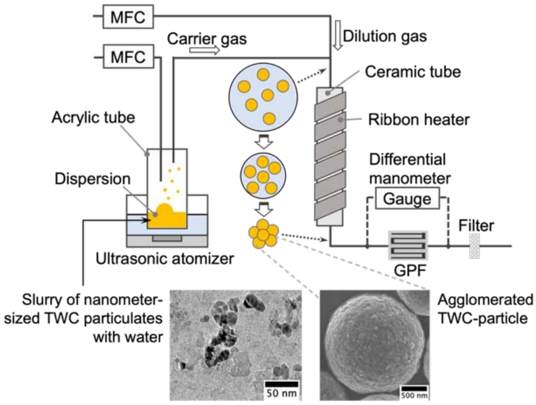

Fig. 3: Schematic diagram of the manufacturing process of TWC-particle membrane filter

Table 1: Chemical composition of TWC slurry

Chemical compounds		Composition (%)
Palladium oxide	PdO	1.45
Rhodium oxide	Rh_2O_3	0.26
Cerium dioxide	CeO_2	18.3
Zirconium dioxide	ZrO_2	26.10
Aluminum oxide	Al_2O_3	47.70
Lanthanum oxide	La_2O_3	3.28
Neodymium oxide	Nd_2O_3	2.90

introduced into the acrylic tube at a flow rate of 50 mL/min to transport the atomized water droplets, including TWC particulates from the tube. The gas-suspended droplets containing TWC particulates were then mixed with a dilution gas to achieve a superficial velocity of 5 mm/s and a humidity lower than the dew point, even at room temperature. Nitrogen gas-diluted dispersed water droplets were introduced into an evaporator, which was kept at constant temperature of 280°C using a ribbon heater. Since only water was vaporized, the primary TWC particulates agglomerated, as shown in the SEM image of Fig. 3. The agglomerated nitrogen dispersed TWC particles, ranging in size from 1 to 2 μm, were deposited as a membrane layer onto a miniaturized filter substrate. Then, as in our previous study, the fabricated membrane filter was sintered at 900°C for 4 hours to maintain the percolation structure of the TWC membrane with a minimal peeling rate [27].

A scanning electron microscopic (SEM) cross-sectional image of a TWC particle membrane filter on a substrate is presented in Fig. 4. The thickness of the membrane layer is approximately 40 microns in which the agglomerated TWC particles (arithmetic mean diameter of 1.2 um) are percolated. The porosity of the membrane was measured as approximately 64.4% [17]. The size of the agglomerated TWC particles was controlled by adjusting the weight percentage of the primary TWC particulates in the slurry. The primary TWC particulates are homogeneously dispersed throughout the entire cross-sectional area of a single agglomerated TWC particle, as shown in the SEM images of Fig. 4.

However, using a back-scattered electron mode, a non-homogeneous composition distribution was observed, as shown in Fig. 5(a). In this figure, the bright colored areas are ceria-zirconia (CZ) particulates since CZ has the highest atomic number compared to the other components of the slurry. The dark gray areas were identified as aluminum oxide particulates. The ratio of these areas was analyzed using Image-J program. The results presented in Fig. 5(b) revealed that the average CZ-particulate area occupied approximately 50% of the whole cross-sectional area of a single agglomerated TWC particle.

Figure 6 shows a schematic diagram of an isothermal CO oxidation experimental setup. A working gas consisting of CO (44 ppm) with the balance as N_2, was introduced (with no oxygen supplied in the working gas) through the TWC particle membrane at a superficial velocity of 20 mm/s and temperatures of 175, 200 and 225°C to investigate the transport of oxygen atoms in the TWC particles. Temperature was measured using a thermocouple inserted in an outflow channel of the substrate filter. It was fixed by an electric heater with a PID feedback system. The concentrations of CO and CO_2 were measured as a function of time using an infrared gas analyzer after the gas stream was passed through the membrane. The supplied CO concentration was calibrated after each measurement under each temperature condition using a by-pass line. Before the experiment, all pre-adsorbed gas molecules on the catalyst surface were removed by passing N_2 gas through the membrane.

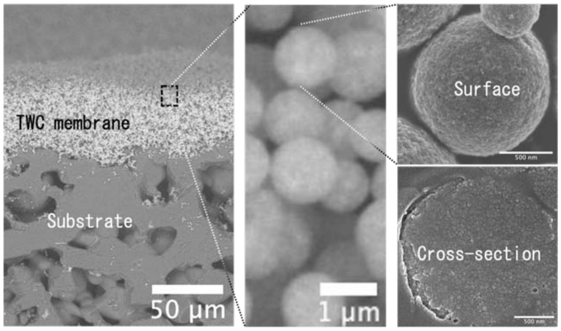

Fig. 4: Surface and cross-sectional morphology of agglomerated TWC-particles

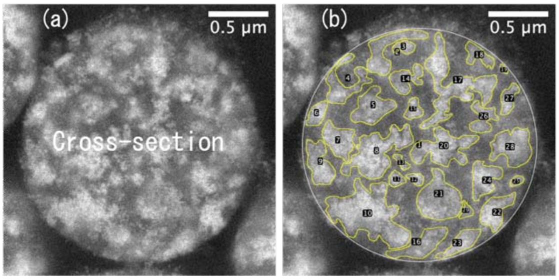

Fig. 5: Elemental analysis of the cross-section of an agglomerated TWC-particle using a back-scattered electron mode

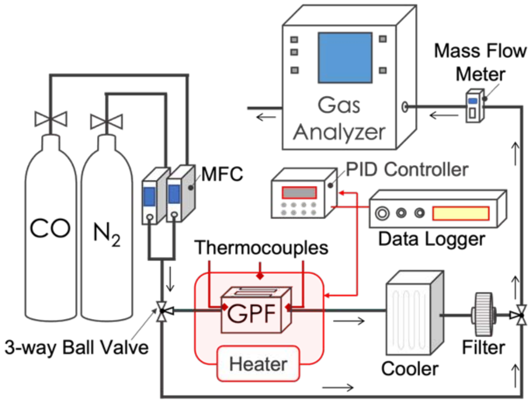

Fig. 6: Experimental setup of CO oxidation measurement through a TWC-particle membrane

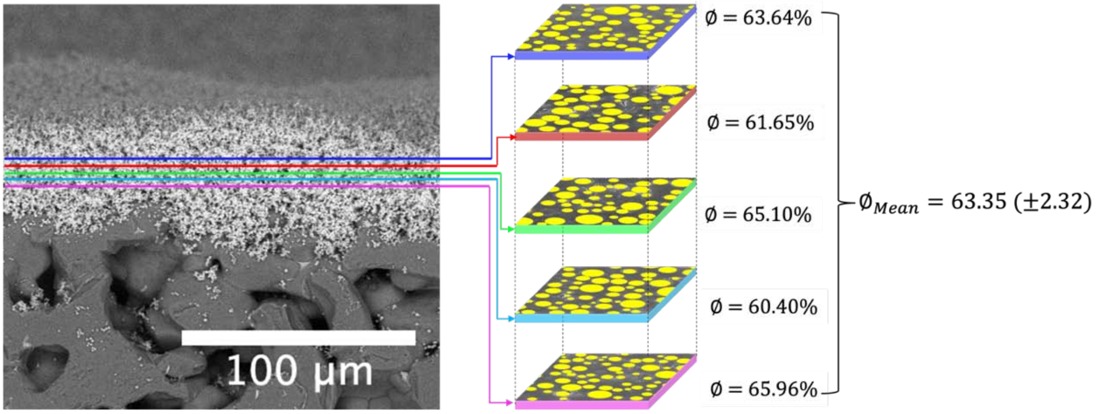

Fig. 7: Measurement of Porosity (ϕ) distribution through image processing analysis showing a homogeneous porous medium along the membrane thickness

III. NUMERICAL SIMULATION

In the numerical simulation model, the following assumptions were made:

1) The agglomerated particle sizes were assumed to be as the same as the arithmetic mean diameter, 1.2 um.
2) Diffusion of oxygen atoms from CZ-particulates was assumed to be an isotropic process, involving one-dimensional diffusion from the bulk of a particulate to the surface (in the x-direction).
3) The chemical reaction occurred at the surface of spherical agglomerated particles by reacting with diffused oxygen atoms from the bulk of CZ-particulates.
4) The temperature of working gas along the membrane thickness direction (z-direction as depicted in the Fig. 8) was uniform during the reaction. Because the generated heat by the exothermic reaction is negligibly small which cannot vary the working gas temperature.
5) The oxygen concentration of TWC-particles percolated in the same location in the discrete volume of the membrane with a uniform concentration throughout the reaction.

As described in Fig. 7, the porosity (ϕ) distribution was consistent (with a discrepancy of ±2.32%) along the membrane thickness direction (z-direction) since the percolation structure of the spherical TWC-particles membrane consists of a homogeneous porous medium [17]. In such a medium, the properties of a percolation structure, such as porosity and permeability, are constant throughout the medium. This uniformity means that the flow characteristics and the resistance to flow are the much the same in all directions. Besides, the tortuosity of the membrane was estimated as small as 1.02013. Therefore, a straight flow characteristic along the membrane thickness direction was assumed in this model. Additionally, from an order estimation of the convective, pressure drop and viscous terms of the Navier Stokes equations under the experimental conditions, the pressure drop and viscous terms are dominant. In fact, the Reynolds number along the membrane is as low as 0.027. Therefore, the working gas flow in this direction becomes the lowest pressure drop, *i.e.*, flow in the z-direction is perpendicular to the membrane layer. As a result, even if the working gas is introduced in the channel direction, from left to right in Fig. 8, the average velocity in the membrane can be assumed to be unidirectional and in the *z*-direction.

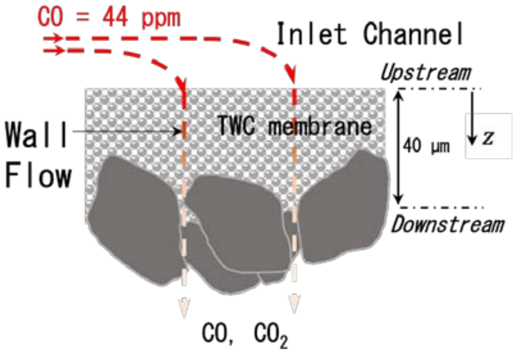

Fig. 8: Schematic of the CO concentration distribution in a three-way catalyst membrane

Figure 8 shows a schematic diagram of streamlines in the membrane filter. Here, the working gas is fed into the membrane layer through an inlet channel in a wall-flow pattern in a uniformly distributed manner. Assuming a one-dimensional, incompressible and uniform flow with a characteristic velocity (superficial velocity) at the membrane layer, only a decrease in CO concentration through oxidation should be considered along the flow direction (in the z-direction). Additionally, it was hypothesized that CO reacts with oxygen atoms diffused from the inside of the CZ material, and the reaction occurs at the TWC particle surfaces as follows.

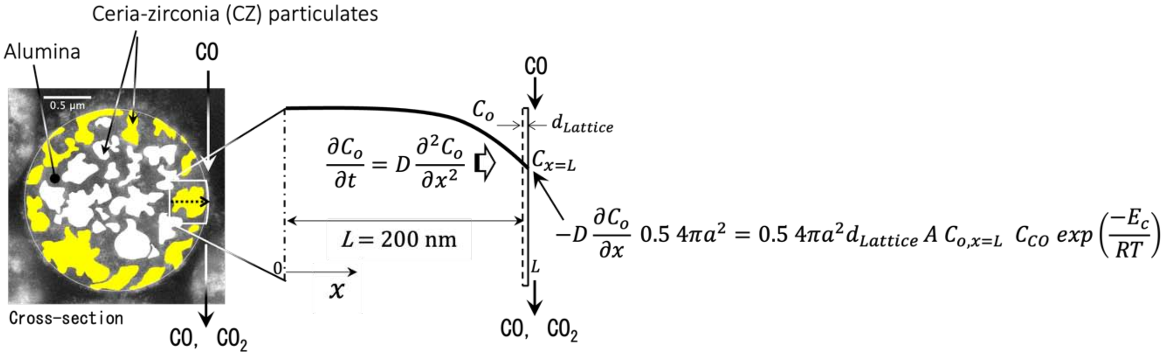

Fig. 9: Schematic image of diffusion-controlled CO oxidation in a three-way catalyst particle membrane model

$$CO + O_{diff} \rightarrow CO_2 \tag{1}$$

$$\frac{\partial C_{CO}}{\partial t} + u\frac{\partial C_{CO}}{\partial z} = 0.5\ \ n\ \ 4\pi a^2 d_{Lattice}\ \ C_{0,x=L}\ \ A\ \ C_{CO}\ exp\left(\frac{-E_c}{RT}\right) \tag{2}$$

The rate of the reaction can be expressed as an Arrhenius-type equation that is proportional to the CO concentration, the number of oxygen atoms present at the TWC particle surface, and the number density of TWC particles. Thus, the governing equation can be written as Eq. 2.

Here, the concentration of CO (C_{co}), superficial velocity (u), time (t), space axis in the flow direction (z), number of TWC particles in a unit volume (*n*), radius of the TWC particle (*a*), lattice constant of CZ material ($d_{Lattice}$), oxygen atom concentration in the CZ material ($C_{o,x=L}$), activation energy for oxidation at the surface of a TWC particle (E_c), gas constant (*R*), and absolute temperature (*T*) are all parameters in the governing equation (Eq. 2). This equation describes the reaction rate as an Arrhenius-type expression that is proportional to the CO concentration, the number of oxygen atoms at the TWC particle surface, and the number density of TWC particles. The product of $4\pi a^2$ and $d_{lattice}$ represents a thin shell volume at the TWC particle surfaces. The lattice constant of CZ material ($d_{lattice}$) was 0.5 nm, obtained from previous work [28]. The factor, 0.5, on the right-hand side of Eq. (2) represents the CZ surface area ratio, 50%, in the spherical surface area of the TWC particles, which is discussed below. Transport of oxygen atoms by diffusion in the CZ material should be simultaneously calculated to obtain the oxygen atom concentration at the TWC particle surfaces.

In the simulation, a volume averaging method was used along the membrane thickness (z-direction). The oxygen concentration of the particles varies with respect to their location in the membrane. Therefore, a discrete thickness of 4 um was considered as a control volume that contained approximately 1.28 x 10^9 particles. The total number of particles percolated in a control volume with a particular thickness can be calculated using Eq. 3.

$$S\ \ L\ \ \varepsilon = N\ \ \frac{4}{3}\ \ \pi\ \ r^3 \tag{3}$$

where *S* is the total surface area of the membrane, *L* is the thickness of the membrane, ε is the packing fraction of the membrane, *N* is the total number of particles and *r* is the particle radius.

In Fig. 9, a schematic illustration of diffusion-controlled CO oxidation is presented. The initial oxygen concentration volume was calculated according to the oxygen vacancy concentration (66.67%) and the lattice parameter (0.5 nm) of the ceria-zirconia material [11, 28]. According to back-scattered electron imagery using FESEM, the primary CZ-particulates were heterogeneously distributed in a spherical agglomerated particle as mentioned in Fig. 5. Individual CZ-particulates were separate from each other. CZ-particulates located at the surface of the single spherical agglomerated particle (yellow-colored CZ-particulates in Fig. 5) contribute to oxygen atom supply. Here, CO molecules flowing along the spherical surface react with the supplied oxygen atoms at the interfaces between the gas phase and the exposed CZ-particulate surfaces. Therefore, it can be assumed that the oxygen atoms will be transported to the surface (to the interface) from the inside of the bulk material, one-dimensionally in the *x*-direction, as shown in Fig. 9. Therefore, a one-dimensional diffusion equation for oxygen atoms in the *x*-direction can be expressed as Eq. 4.

$$\frac{\partial C_o}{\partial t} = D\frac{\partial^2 C_o}{\partial x^2} \tag{4}$$

Here, C_o represents oxygen atom concentration, *t* is time, *x* is the axis from the inside to the surface of the CZ and *D* is the diffusion coefficient of oxygen atoms in the CZ material.

$$D = D_0\ exp\left(\frac{-E_a}{RT}\right) \tag{5}$$

According to the experimental results of isothermal CO conversion, emissions of CO_2 were increased at higher temperatures, as shown in Fig. 10.

The experimental results show that the logarithmic function of the diffusion rate was proportional to the inverse of absolute temperature. From this linearity, the Arrhenius-type expression is suitable for representing the diffusion of oxygen atoms over the temperature range of the current study. The diffusion coefficient is an Arrhenius type expression described in Eq. 5, where D_o is the pre-exponential diffusivity and E_a is the activation energy for diffusion.

The boundary conditions for $x = 0$ and $x = L$ are expressed as Eq. 6 and 7, respectively. There is no diffusion at $x = 0$, while the molar flux of oxygen atoms obtained from the concentration gradient at $x = L$ in the CZ material is equal to the consumption rate of CO by oxidation at the TWC particle surfaces as follows.

$$\frac{\partial C_O}{\partial x} = 0 \qquad\qquad at\ x = 0 \qquad (6)$$

$$-D\frac{\partial C_O}{\partial x} = A\ d_{Lattice}\ \ C_{O,x=L}\ \ C_{CO}\ exp\left(\frac{-E_c}{RT}\right) \qquad at\ x = L \qquad (7)$$

The process of fitting oxygen atom flux data, obtained from both experimental and numerical simulations, was initiated at a temperature of 175°C. Since the diffusion coefficient governing the transport of oxygen atoms within the CZ particulate is an unknown value, an inverse approach was employed to estimate the diffusion coefficient, denoted as D in Eq. 4. Additionally, for CO oxidation at the agglomerated TWC particle surfaces, the pre-exponential factor A needed to be estimated by fitting the time history of the oxygen atom flux. This approach involved iteratively adjusting both the diffusion coefficient D and collision frequency A values while fitting the time history of the oxygen atom flux at the TWC particle surface. In accordance with Eq. 7, altering the D values results in a change in the slope of the curve, whereas adjustments to the A values lead to variations in the flux amount (i.e., along the y-axis in Figure 11). Once a good agreement between experimental and numerical results was achieved at 175°C, higher D values were used for the higher temperature conditions (i.e., 200°C and 225°C) while maintaining the same A values. The activation energy E_a and pre-exponential diffusivity D_o in Eq. 5 were simultaneously estimated from an Arrhenius plot. Here, a straight-line relationship in the plot was iterated multiple times by changing various D values, until the goodness of fit was achieved up to 0.998. The activation energy E_c was 9 kJ/mol, obtained from earlier literature [29, 30]. The mean radius of the TWC particle a and the mean size of the primary CZ particulate L are assumed to be 0.6 nm and 200 nm, respectively, based on SEM and TEM images obtained in the experiment.

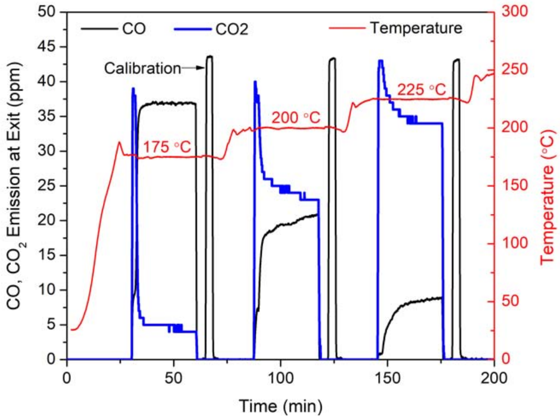

Fig. 10: Isothermal CO oxidation by a TWC membrane at 175, 200 and 225°C

Table 2: Summary of fitted diffusion parameters

Temperature (°C)	Diffusion coefficient, D (m^2 sec^{-1})	Collision Frequency, A (m^3 mol^{-1} sec^{-1})
175	2.3 x10^{-19}	1.55 x10^9
200	8.4 x10^{-19}	
225	3.1 x10^{-18}	

IV. Results and Discussion

Figure 10 presents the experimental results of isothermal CO oxidation by TWC particle membranes at different temperatures (175, 200, and 225°C). The temperature of the miniature-sized filter with the membrane is indicated in red color on the right-hand side vertical axis. It is increased using an electric heater under a nitrogen atmosphere. At the start of the experiment, CO (44 ppm) was introduced with the temperature fixed at 175°C. The black and blue lines illustrate emissions of CO and CO_2, respectively. After 30 minutes, CO and CO_2 emissions were approximately 7% and 37%, respectively. Therefore, a significant amount of CO was oxidized by the TWC particle membrane, even in the absence of supplied oxygen. However, CO_2 emissions decreased over time while CO emissions increased. The isothermal CO oxidation experiment was stopped after 30 minutes. Before proceeding with the next higher temperature experiment, the supplied CO concentration was confirmed as 44 ppm. This cycle represents an isothermal CO oxidation experiment for one temperature condition. With increased temperature, from 175 to 225°C, the initial CO emission approaches to zero, and the decrease in CO_2 emission was not significant. Furthermore, it was observed that CO_2 emission does not decrease over time when the temperature exceeds 300°C.

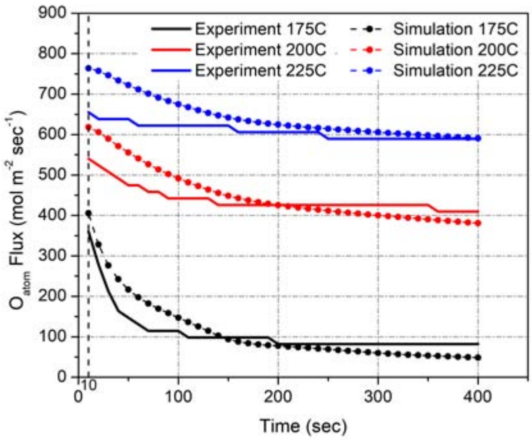

Fig. 11: Fitting of oxygen atom flux

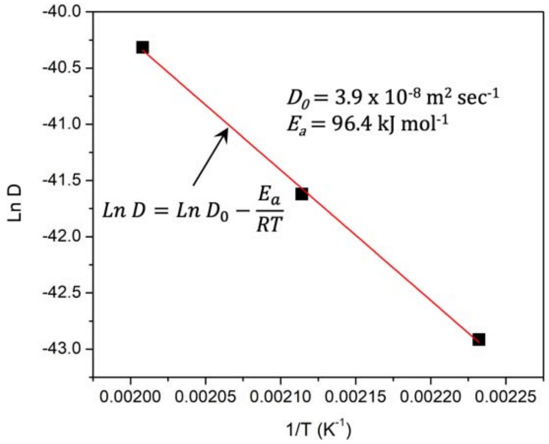

Fig. 12: Arrhenius plot for activation energy and pre-exponential factor of oxygen atom diffusion

Figure 11 shows fitting results between experimental and numerical oxygen atom fluxes at the TWC particle surfaces. Here, the oxygen atom flux in the experiment was estimated from the required number of oxygen atoms to produce one mole of CO_2, calculated from emission concentrations with respect to time. In numerical simulation, the flux was obtained from the gradient of oxygen atom concentration at the surface of the CZ material. The fitting parameter *A*, which is the pre-exponential factor for oxidation, contributes to an increase or a decrease in flux in the entire region during the elapsed time. *D* is the diffusion coefficient of oxygen atoms that contributes to a decreasing rate of flux over time. The numerical results agree well with the experimental data using a combination of fitting parameters, shown in Table 2. There were some discrepancies in the data at the beginning of oxidation, especially at higher temperatures. The concentration of introduced CO was initially stepwise in the numerical simulation, while there was a gradually increased initial condition, from 0 to 44 ppm, in the experiment. Therefore, to remove uncertainties at the initial times, the calculated oxygen atom flux from the experiment was fitted starting from 10 seconds until the end of measurement (i.e., 400 seconds), as shown in Fig. 10. Using the obtained diffusion coefficient D from the fitting, the activation energy Ea and pre-exponential factor Do were estimated as 96.4 kJ/mol and 3.904 x 10-8 m2/s from the Arrhenius plot, as shown in Fig. 12.

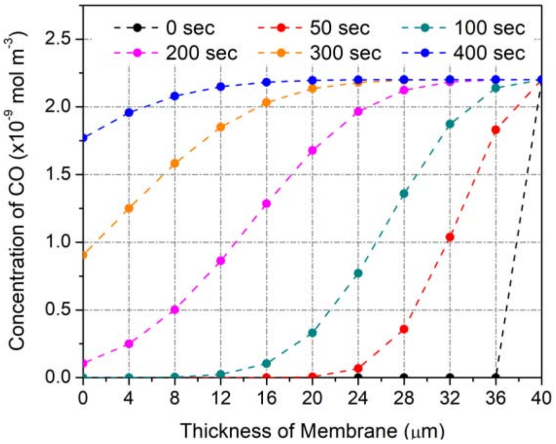

(a) 175°C

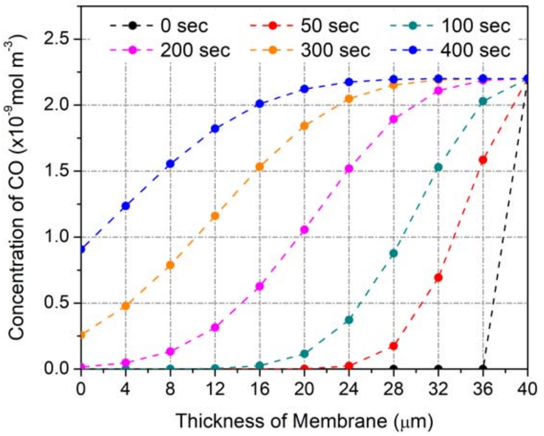

(b) 200°C

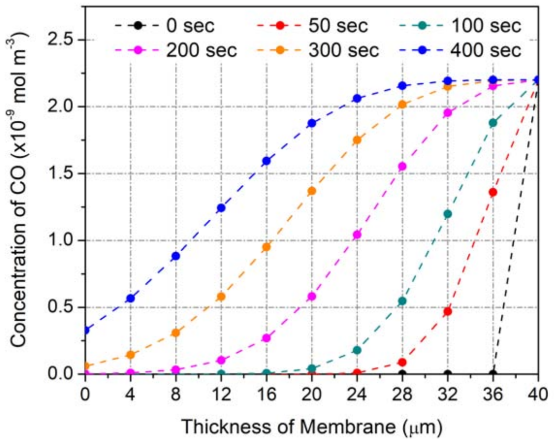

(c) 225°C

Fig. 13: Concentration distribution of CO along the membrane thickness at 175°C (a), 200°C (b) and 225°C (c)

Figure 13 shows variation of CO concentration distributions along the flow direction with respect to time from the beginning to an elapsed time of 400 seconds at 175, 200 and 225°C using the fitting parameters obtained above. Here, the working gas flows from the right to the left with a superficial velocity of 20 mm/s, and the concentration of CO at the right-hand side is fixed at 2.2 x 10^{-9} mol/m^3 (44 ppm). The concentration of introduced CO was decreased along the thickness by CO oxidation in the membrane, even at 175°C (Fig. 13(a)). There was no emission of CO for up to 100 seconds, although this doesn't agree with the experimental results. However, the CO concentration in entire region of the membrane was increased with respect to time due to a decreased oxidation rate even under an isothermal oxidation condition. Then, 400 seconds later, a high level of CO was emitted in the case of 175°C (Fig. 13(a)). With increased temperature, from 175 to 225°C, the emission at 400 seconds was less since more CO was oxidized.

Figures 14(a), 14(b) and 14(c) show variations of oxygen atom concentration distributions in the CZ material in a TWC particle located at the top surface of the membrane with respect to time at 175, 200 and 225°C, respectively. However, Figs. 15 and 16 show the same data at the middle and bottom surfaces of the membrane. The concentration gradient at the bottom surface of the membrane is smaller than that of the top and middle since the CO concentration decreases along the flow direction. Here, since at the right-hand end of each graph, oxygen reacts with CO and the oxygen concentration was decreased with respect to time. According to the CO oxidation rate at the right-hand end, oxygen is supplied by diffusion from the inside of the CZ particulate. As a result, the oxygen concentration was decreased in the *x*-direction at each time step. Moreover, with consumption of oxygen atoms, its concentration in the CZ particulate was decreased with time. With increasing temperature, from 175 (Fig. 14(a)) to 225°C (Fig. 14(c)), since the diffusion coefficient of oxygen atoms is increased as predicted by the Arrhenius expression, the concentration gradient at the surface (at the right-hand end) becomes smaller while the transport range becomes wider.

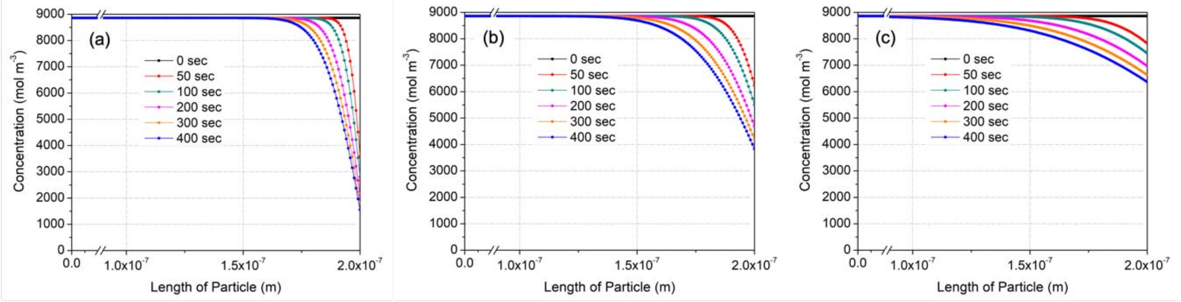

Fig. 14: Concentration profiles of CZ-particulates located at the upstream side of the membrane at 175°C (a), 200°C (b) and 225°C (c)

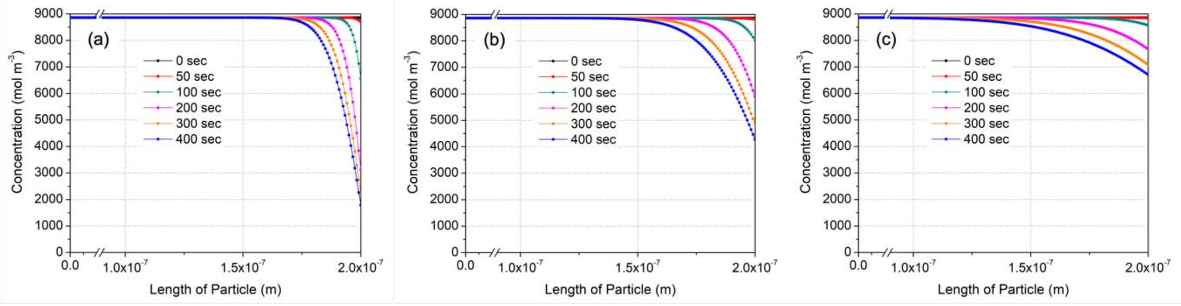

Fig. 15: Concentration profiles of CZ-particulates located at the middle of the membrane at 175°C (a), 200°C (b) and 225°C (c)

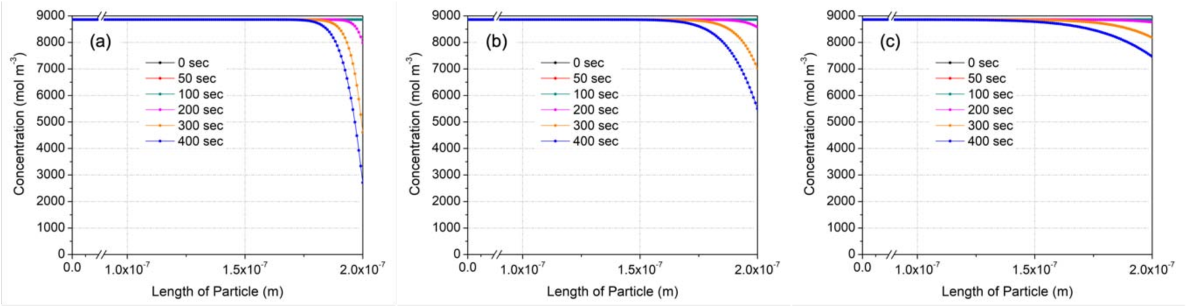

Fig. 14: Concentration profiles of CZ-particulates located at the downstream side of the membrane at 175°C (a), 200°C (b) and 225°C (c)

V. Conclusions

In this study, the diffusion-controlled oxygen transport process in ceria-zirconia (CZ) particulates located at the surface of the spherical TWC particles, which are the elements of the TWC particle membrane filter, was investigated through isothermal CO oxidation experiments and numerical modeling. Although the electron micrograph of cross-sectional view of a spherical TWC particle was exhibited as a homogeneously agglomerated structure, the primary CZ particulates were separated from each other within alumina at the spherical surface under a back-scattered electron mode. Moreover, the simulation results revealed that the oxygen atoms transport range of approximately 100 nm from the surface of the CZ particulates were mainly contributed to the reaction under a low temperature range of 175°C to 225°C. A few microns-sized TWC particles membrane wall-flow filter will become useful for a low-temperature exhaust gas due to the high specific surface area to enhance the purification reaction though the oxygen atom transport range is limited as obtained here.

Acknowledgement

This paper is obtained as a result of a grant project (JPNP21014) conducted by The Research Association of Automotive Internal Combustion Engines (AICE) with support from the New Energy and Industrial Technology Development Organization (NEDO). The author(s) would like to express their sincere gratitude to them.

References Références Referencias

1. Khalifa AA, Ibrahim AJ, Amhamed AI, El-Naas MH(2022) Accelerating the transition to a circular economy for net-zero emissions by 2050: A systematic review. Sustainability 14(18):410-430 https://doi.org/10.3390/su141811656
2. Krause J, Thiel C, Tsokolis D (2020) EU road vehicle energy consumption and CO2 emissions by 2050 – Expert-based scenarios. Energy Policy 138:134-147 https://doi.org/10.1016/j.enpol.2019.111224
3. Twigg, MV (2011) Catalytic Control of Emissions from Cars. Catalysis Today 163:33-41 https://doi.org/10.1016/j.cattod.2010.12.044
4. Joshi A, Johnson TV (2018) Gasoline particulate filters – A review. Emission control science and technology 4:219-239 https://doi.org/10.1007/s40825-018-0101-y
5. Qian Y, Li Z, Yu, Wang X, Lu X (2019) Review of the state-of-the-art of particulate matter emissions from modern gasoline fueled engines. Applied Energy 238:1269-1298 https://doi.org/10.1016/j.apenergy.2019.01.179
6. Richter J M, Klingmann R, Spiess S, Wong K (2012) Application of catalyzed gasoline particulate filters to GDI vehicles. SAE International Journal of Engines 5(3):1361-1370 https://doi.org/10.4271/2012-01-1244
7. Montini T, Melchionna M, Monai M, Fornasiero P (2016) Fundamentals and catalytic applications of CeO_2-based materials. Chemical Reviews 116(10):5987-6041 https://doi.org/10.1021/acs.chemrev.5b00603
8. Melchionna M, Fornasiero P (2014) The role of ceria-based nanostructured materials in energy applications. Materials Today 17 (7):349-357 https://://doi.org/10.1016/j.mattod.2014.05.005
9. Wang J, Chen H, Hu Z, Yao M, Li Y (2014) A review on the Pd-based three-way catalyst. Catalysis Reviews57(1):79-144 https://doi.org/10.1080/01614940.2014.977059
10. Li P, Chen X, Li Y, Schwank JW (2019) A review on oxygen storage capacity of CeO_2-based materials: Influence factors, measurement techniques, and applications in reactions related to catalytic automotive emission control. Catalysis Today 327:90-115 https://doi.org/10.1016/j.cattod.2018.05.059
11. Suzuki T, Morikawa A, Suda, A (2002) Alumina-Ceria-Zirconia composite oxide for three-way catalyst, Special Issue Oxygen Storage Materials for Automotive-Ceria-Zirconia Solid Solution, R&D Review of Toyota CRDL 37(4):28-33.
12. Suteerapongpun T, Kitagawa Y, Srilomsak M, Hanamura K (2020) Development of membrane filter

made of alumina and silver-palladium particles for high-filtration efficiency, low-pressure drop and low-soot oxidation temperature. International Journal of Automotive Engineering 11(4):51-158 https://doi.org/10.20485/jsaeijae.11.4_151

13. Hanamura K, Inaba M, Kawabe K, Mitarai K (2022) Oxidation enhancement of particulate matters deposited on catalyzed membrane filter by nitrogen oxides diffusion. Transactions of Society of Automotive Engineers of Japan 53(1):100-106 https://doi.org/10.11351/jsaeronbun.53.100
14. Karin P, Hanamura K (2010) Microscopic visualization of particulate matter trapping and oxidation behaviors in a diesel particulate catalyst-membrane filter. JSAE Annual Congress Research Paper 41(4):853-858 https://doi.org/10.11351/jsaeronbun.41.853
15. Nakajima S, Sanui R, Hanamura K (2017) Soot trapping by high-permeability porous membrane filter made of aggregates of alumina nanoparticles. International Journal of Automotive Engineering 8(3):105-111 https://doi.org/10.20485/jsaeijae.8.3_105
16. Hanamura K, Fujii S, Teerapat S (2023) A study of multi-functional membrane filters made of fine catalyst particles. SAE Technical Paper 2023-32-0125.
17. Koko P, Suteerapongpun T, Hanamura K (2023) Measurement of porosity in three-way catalyst particles membrane filter using electron microscopy image analysis. International Journal of Automotive Engineering 14(1):27-34 https://doi.org/10.20485/jsaeijae.14.1_27
18. Taibani AZ and Kalamkar V (2012) Experimental and computational analysis of behavior of three-way catalytic converter under axial and radial flow conditions. International Journal of Fluid Machinery and Systems 5(3):134:142 https://doi.org/10.5293/IJFMS.2012.5.3.134
19. Tsinglou DN, Koltsakis GC, Peyton Jones JC (2002) Oxygen storage modeling in three-way catalytic converters. Industrial and Engineering Chemistry Research 41(5):1152:1165 https://doi.org/10.1021/ie010576c
20. Yamauchi T, Kubo S, Mizukami T, Sato N, Aono N (2011) Numerical simulation for optimal design of a multifunctional three-way catalytic converter with detailed chemistry. R&D Review of Toyota CRDL 42(1):33:42.
21. Walter R, Neumann J, Hinrichsen O (2022) A model-based analysis of washcoat distribution on zoned coated gasoline particulate filters. Chemical Engineering Journal 441:135615 https://doi.org/10.1016/j.cej.2022.135615
22. Yashiro K, Onuma S, Kaimai A (2002) Mass transport properties of $Ce_{0.9}Gd_{0.1}O_{2-\delta}$ at the surface and in the bulk. Solid State Ions 152-153:469-476 https://doi.org/10.1016/S0167-2738(02)00375-2
23. Ackermann S, Scheffe JR, Steinfeld A (2014) Diffusion of oxygen in ceria at elevated temperatures and its application to H_2O/CO_2 splitting thermochemical redox cycles. The Journal of Physical Chemistry 118:5216-5225 https://doi.org/10.1021/jp500755t
24. Stan M, Zhu YT, Jiang H, Butt D (2004) Kinetics of oxygen removal from ceria. Journal of Applied Physics 95(7):3358-3361 https://doi.org/10.1063/1.1650890
25. Nagasawa T, Kobayashi A, Sato S, Kosaka H, Kim K, You HM, Hanamura K, Terada A, Mishima T (2023) Visualization of oxygen storage process in Pd/CeO_2-ZrO_2 three-way catalyst based on isotope quenching technique. Chemical Engineering Journal 453:139937 https://doi.org/10.1016/j.cej.2022.139937
26. Nagasawa T, Okura Y, Yamada R, Sato S, Kosaka H, Yokomori T, Lida N (2021) Thermal efficiency improvement of super-lean burn spark ignition engine by stratified water insulation on piston top surface. International Journal of Engine Research 22(5): 1421-1439 https://doi.org/10.1177/1468087420908164
27. Arai S, Fujii S. Koko P, Suteerapongpun T, Hanamura K (2023) Durability of three-way-catalyst-particles membrane filter for fluid-dynamic shear stress. International Journal of Automotive Engineering 54(3):141-152 https://doi.org/10.11351/jsaeronbun.54.566
28. Gul SR, Khan M, Zeng Y, Lin M, Wu B, Tsai C (2018) Electronic band structure variations in the ceria doped zirconia: A first principles study. Materials 11(7):329-341 https://doi.org/10.3390%2Fma11071238
29. Christou SY, Costa CN, Efstathiou, AM (2004) A two-step reaction mechanism of oxygen release from Pd/CeO2: Mathematical modelling based on step gas concentration experiments. Topics in Catalysis 30:325-331 https://doi.org/10.1023/B:TOCA.0000029770.40236.44
30. Christou SY, Costa CN, Efstathiou, AM (2003) Mathematical modeling of the oxygen storage capacity phenomenon studied by CO pulse transient experiments over Pd/CeO2 catalyst. Journal of Catalysis 219:259-272 https://doi.org/10.1016/S0021-9517(03)00151-9

Global Journals Guidelines Handbook 2023

www.GlobalJournals.org

MEMBERSHIPS

FELLOWS/ASSOCIATES OF ENGINEERING RESEARCH COUNCIL

FERC/AERC MEMBERSHIPS

INTRODUCTION

FERC/AERC is the most prestigious membership of Global Journals accredited by Open Association of Research Society, U.S.A (OARS). The credentials of Fellow and Associate designations signify that the researcher has gained the knowledge of the fundamental and high-level concepts, and is a subject matter expert, proficient in an expertise course covering the professional code of conduct, and follows recognized standards of practice. The credentials are designated only to the researchers, scientists, and professionals that have been selected by a rigorous process by our Editorial Board and Management Board.

> Associates of FERC/AERC are scientists and researchers from around the world are working on projects/researches that have huge potentials. Members support Global Journals' mission to advance technology for humanity and the profession.

FERC

FELLOW OF ENGINEERING RESEARCH COUNCIL

FELLOW OF ENGINEERING RESEARCH COUNCIL is the most prestigious membership of Global Journals. It is an award and membership granted to individuals that the Open Association of Research Society judges to have made a 'substantial contribution to the improvement of computer science, technology, and electronics engineering.

> The primary objective is to recognize the leaders in research and scientific fields of the current era with a global perspective and to create a channel between them and other researchers for better exposure and knowledge sharing. Members are most eminent scientists, engineers, and technologists from all across the world. Fellows are elected for life through a peer review process on the basis of excellence in the respective domain. There is no limit on the number of new nominations made in any year. Each year, the Open Association of Research Society elect up to 12 new Fellow Members.

Benefit

To the institution

Get letter of appreciation

Global Journals sends a letter of appreciation of author to the Dean or CEO of the University or Company of which author is a part, signed by editor in chief or chief author.

Exclusive Network

Get access to a closed network

A FERC member gets access to a closed network of Tier 1 researchers and scientists with direct communication channel through our website. Fellows can reach out to other members or researchers directly. They should also be open to reaching out by other.

Career Credibility Exclusive Reputation

Certificate

Certificate, LoR and Laser-Momento

Fellows receive a printed copy of a certificate signed by our Chief Author that may be used for academic purposes and a personal recommendation letter to the dean of member's university.

Career Credibility Exclusive Reputation

Designation

Get honored title of membership

Fellows can use the honored title of membership. The “FERC” is an honored title which is accorded to a person’s name viz. Dr. John E. Hall, Ph.D., FERC or William Walldroff, M.S., FERC.

Career Credibility Exclusive Reputation

Recognition on the Platform

Better visibility and citation

All the Fellow members of FERC get a badge of "Leading Member of Global Journals" on the Research Community that distinguishes them from others. Additionally, the profile is also partially maintained by our team for better visibility and citation. All fellows get a dedicated page on the website with their biography.

Career Credibility Reputation

FUTURE WORK

GET DISCOUNTS ON THE FUTURE PUBLICATIONS

Fellows receive discounts on the future publications with Global Journals up to 60%. Through our recommendation programs, members also receive discounts on publications made with OARS affiliated organizations.

Career Financial

GJ ACCOUNT

UNLIMITED FORWARD OF EMAILS

Fellows get secure and fast GJ work emails with unlimited storage of emails that they may use them as their primary email. For example, john [AT] globaljournals [DOT] org.

Career Credibility Reputation

PREMIUM TOOLS

ACCESS TO ALL THE PREMIUM TOOLS

To take future researches to the zenith, fellows receive access to all the premium tools that Global Journals have to offer along with the partnership with some of the best marketing leading tools out there.

Financial

CONFERENCES & EVENTS

ORGANIZE SEMINAR/CONFERENCE

Fellows are authorized to organize symposium/seminar/conference on behalf of Global Journal Incorporation (USA). They can also participate in the same organized by another institution as representative of Global Journal. In both the cases, it is mandatory for him to discuss with us and obtain our consent. Additionally, they get free research conferences (and others) alerts.

Career Credibility Financial

EARLY INVITATIONS

EARLY INVITATIONS TO ALL THE SYMPOSIUMS, SEMINARS, CONFERENCES

All fellows receive the early invitations to all the symposiums, seminars, conferences and webinars hosted by Global Journals in their subject.

Exclusive

Publishing Articles & Books

Earn 60% of sales proceeds

Fellows can publish articles (limited) without any fees. Also, they can earn up to 70% of sales proceeds from the sale of reference/review books/literature/publishing of research paper. The FERC member can decide its price and we can help in making the right decision.

Exclusive Financial

Reviewers

Get a remuneration of 15% of author fees

Fellow members are eligible to join as a paid peer reviewer at Global Journals Incorporation (USA) and can get a remuneration of 15% of author fees, taken from the author of a respective paper.

Financial

Access to Editorial Board

Become a member of the Editorial Board

Fellows may join as a member of the Editorial Board of Global Journals Incorporation (USA) after successful completion of three years as Fellow and as Peer Reviewer. Additionally, Fellows get a chance to nominate other members for Editorial Board.

Career Credibility Exclusive Reputation

And Much More

Get access to scientific museums and observatories across the globe

All members get access to 5 selected scientific museums and observatories across the globe. All researches published with Global Journals will be kept under deep archival facilities across regions for future protections and disaster recovery. They get 10 GB free secure cloud access for storing research files.

AERC

ASSOCIATE OF ENGINEERING RESEARCH COUNCIL

ASSOCIATE OF ENGINEERING RESEARCH COUNCIL is the membership of Global Journals awarded to individuals that the Open Association of Research Society judges to have made a 'substantial contribution to the improvement of computer science, technology, and electronics engineering.

> The primary objective is to recognize the leaders in research and scientific fields of the current era with a global perspective and to create a channel between them and other researchers for better exposure and knowledge sharing. Members are most eminent scientists, engineers, and technologists from all across the world. Associate membership can later be promoted to Fellow Membership. Associates are elected for life through a peer review process on the basis of excellence in the respective domain. There is no limit on the number of new nominations made in any year. Each year, the Open Association of Research Society elect up to 12 new Associate Members.

BENEFIT

TO THE INSTITUTION

GET LETTER OF APPRECIATION

Global Journals sends a letter of appreciation of author to the Dean or CEO of the University or Company of which author is a part, signed by editor in chief or chief author.

EXCLUSIVE NETWORK

GET ACCESS TO A CLOSED NETWORK

A AERC member gets access to a closed network of Tier 1 researchers and scientists with direct communication channel through our website. Associates can reach out to other members or researchers directly. They should also be open to reaching out by other.

Career Credibility Exclusive Reputation

CERTIFICATE

CERTIFICATE, LOR AND LASER-MOMENTO

Associates receive a printed copy of a certificate signed by our Chief Author that may be used for academic purposes and a personal recommendation letter to the dean of member's university.

Career Credibility Exclusive Reputation

DESIGNATION

GET HONORED TITLE OF MEMBERSHIP

Associates can use the honored title of membership. The “AERC” is an honored title which is accorded to a person’s name viz. Dr. John E. Hall, Ph.D., AERC or William Walldroff, M.S., AERC.

Career Credibility Exclusive Reputation

RECOGNITION ON THE PLATFORM

BETTER VISIBILITY AND CITATION

All the Associate members of AERC get a badge of "Leading Member of Global Journals" on the Research Community that distinguishes them from others. Additionally, the profile is also partially maintained by our team for better visibility and citation. All associates get a dedicated page on the website with their biography.

Career Credibility Reputation

FUTURE WORK

GET DISCOUNTS ON THE FUTURE PUBLICATIONS

Associates receive discounts on the future publications with Global Journals up to 60%. Through our recommendation programs, members also receive discounts on publications made with OARS affiliated organizations.

Career Financial

GJ ACCOUNT

UNLIMITED FORWARD OF EMAILS

Associates get secure and fast GJ work emails with unlimited storage of emails that they may use them as their primary email. For example, john [AT] globaljournals [DOT] org..

Career Credibility Reputation

PREMIUM TOOLS

ACCESS TO ALL THE PREMIUM TOOLS

To take future researches to the zenith, associates receive access to all the premium tools that Global Journals have to offer along with the partnership with some of the best marketing leading tools out there.

Financial

CONFERENCES & EVENTS

ORGANIZE SEMINAR/CONFERENCE

Associates are authorized to organize symposium/seminar/conference on behalf of Global Journal Incorporation (USA). They can also participate in the same organized by another institution as representative of Global Journal. In both the cases, it is mandatory for him to discuss with us and obtain our consent. Additionally, they get free research conferences (and others) alerts.

Career Credibility Financial

EARLY INVITATIONS

EARLY INVITATIONS TO ALL THE SYMPOSIUMS, SEMINARS, CONFERENCES

All associates receive the early invitations to all the symposiums, seminars, conferences and webinars hosted by Global Journals in their subject.

Exclusive

PUBLISHING ARTICLES & BOOKS

EARN 30-40% OF SALES PROCEEDS

Associates can publish articles (limited) without any fees. Also, they can earn up to 30-40% of sales proceeds from the sale of reference/review books/literature/publishing of research paper.

Exclusive Financial

REVIEWERS

GET A REMUNERATION OF 15% OF AUTHOR FEES

Associate members are eligible to join as a paid peer reviewer at Global Journals Incorporation (USA) and can get a remuneration of 15% of author fees, taken from the author of a respective paper.

Financial

AND MUCH MORE

GET ACCESS TO SCIENTIFIC MUSEUMS AND OBSERVATORIES ACROSS THE GLOBE

All members get access to 2 selected scientific museums and observatories across the globe. All researches published with Global Journals will be kept under deep archival facilities across regions for future protections and disaster recovery. They get 5 GB free secure cloud access for storing research files.

Associate	Fellow	Research Group	Basic
$4800	$6800	$12500.00	APC
lifetime designation	**lifetime designation**	**organizational**	**per article**
Certificate, LoR and Momento 2 discounted publishing/year **Gradation** of Research 10 research contacts/day 1 **GB** Cloud Storage **GJ** Community Access	**Certificate,** LoR and Momento **Unlimited** discounted publishing/year **Gradation** of Research **Unlimited** research contacts/day 5 **GB** Cloud Storage **Online Presense** Assistance **GJ** Community Access	**Certificates,** LoRs and Momentos **Unlimited** free publishing/year **Gradation** of Research **Unlimited** research contacts/day **Unlimited** Cloud Storage **Online Presense** Assistance **GJ** Community Access	**GJ** Community Access

PREFERRED AUTHOR GUIDELINES

We accept the manuscript submissions in any standard (generic) format.

We typeset manuscripts using advanced typesetting tools like Adobe In Design, CorelDraw, TeXnicCenter, and TeXStudio. We usually recommend authors submit their research using any standard format they are comfortable with, and let Global Journals do the rest.

Alternatively, you can download our basic template from https://globaljournals.org/Template.zip

Authors should submit their complete paper/article, including text illustrations, graphics, conclusions, artwork, and tables. Authors who are not able to submit manuscript using the form above can email the manuscript department at submit@globaljournals.org or get in touch with chiefeditor@globaljournals.org if they wish to send the abstract before submission.

BEFORE AND DURING SUBMISSION

Authors must ensure the information provided during the submission of a paper is authentic. Please go through the following checklist before submitting:

1. Authors must go through the complete author guideline and understand and *agree to Global Journals' ethics and code of conduct,* along with author responsibilities.
2. Authors must accept the privacy policy, terms, and conditions of Global Journals.
3. Ensure corresponding author's email address and postal address are accurate and reachable.
4. Manuscript to be submitted must include keywords, an abstract, a paper title, co-author(s') names and details (email address, name, phone number, and institution), figures and illustrations in vector format including appropriate captions, tables, including titles and footnotes, a conclusion, results, acknowledgments and references.
5. Authors should submit paper in a ZIP archive if any supplementary files are required along with the paper.
6. Proper permissions must be acquired for the use of any copyrighted material.
7. Manuscript submitted *must not have been submitted or published elsewhere* and all authors must be aware of the submission.

Declaration of Conflicts of Interest

It is required for authors to declare all financial, institutional, and personal relationships with other individuals and organizations that could influence (bias) their research.

POLICY ON PLAGIARISM

Plagiarism is not acceptable in Global Journals submissions at all.

Plagiarized content will not be considered for publication. We reserve the right to inform authors' institutions about plagiarism detected either before or after publication. If plagiarism is identified, we will follow COPE guidelines:

Authors are solely responsible for all the plagiarism that is found. The author must not fabricate, falsify or plagiarize existing research data. The following, if copied, will be considered plagiarism:

- Words (language)
- Ideas
- Findings
- Writings
- Diagrams
- Graphs
- Illustrations
- Lectures

- Printed material
- Graphic representations
- Computer programs
- Electronic material
- Any other original work

AUTHORSHIP POLICIES

Global Journals follows the definition of authorship set up by the Open Association of Research Society, USA. According to its guidelines, authorship criteria must be based on:

1. Substantial contributions to the conception and acquisition of data, analysis, and interpretation of findings.
2. Drafting the paper and revising it critically regarding important academic content.
3. Final approval of the version of the paper to be published.

Changes in Authorship

The corresponding author should mention the name and complete details of all co-authors during submission and in manuscript. We support addition, rearrangement, manipulation, and deletions in authors list till the early view publication of the journal. We expect that corresponding author will notify all co-authors of submission. We follow COPE guidelines for changes in authorship.

Copyright

During submission of the manuscript, the author is confirming an exclusive license agreement with Global Journals which gives Global Journals the authority to reproduce, reuse, and republish authors' research. We also believe in flexible copyright terms where copyright may remain with authors/employers/institutions as well. Contact your editor after acceptance to choose your copyright policy. You may follow this form for copyright transfers.

Appealing Decisions

Unless specified in the notification, the Editorial Board’s decision on publication of the paper is final and cannot be appealed before making the major change in the manuscript.

Acknowledgments

Contributors to the research other than authors credited should be mentioned in Acknowledgments. The source of funding for the research can be included. Suppliers of resources may be mentioned along with their addresses.

Declaration of funding sources

Global Journals is in partnership with various universities, laboratories, and other institutions worldwide in the research domain. Authors are requested to disclose their source of funding during every stage of their research, such as making analysis, performing laboratory operations, computing data, and using institutional resources, from writing an article to its submission. This will also help authors to get reimbursements by requesting an open access publication letter from Global Journals and submitting to the respective funding source.

PREPARING YOUR MANUSCRIPT

Authors can submit papers and articles in an acceptable file format: MS Word (doc, docx), LaTeX (.tex, .zip or .rar including all of your files), Adobe PDF (.pdf), rich text format (.rtf), simple text document (.txt), Open Document Text (.odt), and Apple Pages (.pages). Our professional layout editors will format the entire paper according to our official guidelines. This is one of the highlights of publishing with Global Journals—authors should not be concerned about the formatting of their paper. Global Journals accepts articles and manuscripts in every major language, be it Spanish, Chinese, Japanese, Portuguese, Russian, French, German, Dutch, Italian, Greek, or any other national language, but the title, subtitle, and abstract should be in English. This will facilitate indexing and the pre-peer review process.

The following is the official style and template developed for publication of a research paper. Authors are not required to follow this style during the submission of the paper. It is just for reference purposes.

Manuscript Style Instruction (Optional)

- Microsoft Word Document Setting Instructions.
- Font type of all text should be Swis721 Lt BT.
- Page size: 8.27" x 11'", left margin: 0.65, right margin: 0.65, bottom margin: 0.75.
- Paper title should be in one column of font size 24.
- Author name in font size of 11 in one column.
- Abstract: font size 9 with the word "Abstract" in bold italics.
- Main text: font size 10 with two justified columns.
- Two columns with equal column width of 3.38 and spacing of 0.2.
- First character must be three lines drop-capped.
- The paragraph before spacing of 1 pt and after of 0 pt.
- Line spacing of 1 pt.
- Large images must be in one column.
- The names of first main headings (Heading 1) must be in Roman font, capital letters, and font size of 10.
- The names of second main headings (Heading 2) must not include numbers and must be in italics with a font size of 10.

Structure and Format of Manuscript

The recommended size of an original research paper is under 15,000 words and review papers under 7,000 words. Research articles should be less than 10,000 words. Research papers are usually longer than review papers. Review papers are reports of significant research (typically less than 7,000 words, including tables, figures, and references)

A research paper must include:

a) A title which should be relevant to the theme of the paper.
b) A summary, known as an abstract (less than 150 words), containing the major results and conclusions.
c) Up to 10 keywords that precisely identify the paper's subject, purpose, and focus.
d) An introduction, giving fundamental background objectives.
e) Resources and techniques with sufficient complete experimental details (wherever possible by reference) to permit repetition, sources of information must be given, and numerical methods must be specified by reference.
f) Results which should be presented concisely by well-designed tables and figures.
g) Suitable statistical data should also be given.
h) All data must have been gathered with attention to numerical detail in the planning stage.

Design has been recognized to be essential to experiments for a considerable time, and the editor has decided that any paper that appears not to have adequate numerical treatments of the data will be returned unrefereed.

i) Discussion should cover implications and consequences and not just recapitulate the results; conclusions should also be summarized.
j) There should be brief acknowledgments.
k) There ought to be references in the conventional format. Global Journals recommends APA format.

Authors should carefully consider the preparation of papers to ensure that they communicate effectively. Papers are much more likely to be accepted if they are carefully designed and laid out, contain few or no errors, are summarizing, and follow instructions. They will also be published with much fewer delays than those that require much technical and editorial correction.

The Editorial Board reserves the right to make literary corrections and suggestions to improve brevity.

FORMAT STRUCTURE

It is necessary that authors take care in submitting a manuscript that is written in simple language and adheres to published guidelines.

All manuscripts submitted to Global Journals should include:

Title

The title page must carry an informative title that reflects the content, a running title (less than 45 characters together with spaces), names of the authors and co-authors, and the place(s) where the work was carried out.

Author details

The full postal address of any related author(s) must be specified.

Abstract

The abstract is the foundation of the research paper. It should be clear and concise and must contain the objective of the paper and inferences drawn. It is advised to not include big mathematical equations or complicated jargon.

Many researchers searching for information online will use search engines such as Google, Yahoo or others. By optimizing your paper for search engines, you will amplify the chance of someone finding it. In turn, this will make it more likely to be viewed and cited in further works. Global Journals has compiled these guidelines to facilitate you to maximize the web-friendliness of the most public part of your paper.

Keywords

A major lynchpin of research work for the writing of research papers is the keyword search, which one will employ to find both library and internet resources. Up to eleven keywords or very brief phrases have to be given to help data retrieval, mining, and indexing.

One must be persistent and creative in using keywords. An effective keyword search requires a strategy: planning of a list of possible keywords and phrases to try.

Choice of the main keywords is the first tool of writing a research paper. Research paper writing is an art. Keyword search should be as strategic as possible.

One should start brainstorming lists of potential keywords before even beginning searching. Think about the most important concepts related to research work. Ask, “What words would a source have to include to be truly valuable in a research paper?” Then consider synonyms for the important words.

It may take the discovery of only one important paper to steer in the right keyword direction because, in most databases, the keywords under which a research paper is abstracted are listed with the paper.

Numerical Methods

Numerical methods used should be transparent and, where appropriate, supported by references.

Abbreviations

Authors must list all the abbreviations used in the paper at the end of the paper or in a separate table before using them.

Formulas and equations

Authors are advised to submit any mathematical equation using either MathJax, KaTeX, or LaTeX, or in a very high-quality image.

Tables, Figures, and Figure Legends

Tables: Tables should be cautiously designed, uncrowned, and include only essential data. Each must have an Arabic number, e.g., Table 4, a self-explanatory caption, and be on a separate sheet. Authors must submit tables in an editable format and not as images. References to these tables (if any) must be mentioned accurately.

Figures

Figures are supposed to be submitted as separate files. Always include a citation in the text for each figure using Arabic numbers, e.g., Fig. 4. Artwork must be submitted online in vector electronic form or by emailing it.

Preparation of Eletronic Figures for Publication

Although low-quality images are sufficient for review purposes, print publication requires high-quality images to prevent the final product being blurred or fuzzy. Submit (possibly by e-mail) EPS (line art) or TIFF (halftone/ photographs) files only. MS PowerPoint and Word Graphics are unsuitable for printed pictures. Avoid using pixel-oriented software. Scans (TIFF only) should have a resolution of at least 350 dpi (halftone) or 700 to 1100 dpi (line drawings). Please give the data for figures in black and white or submit a Color Work Agreement form. EPS files must be saved with fonts embedded (and with a TIFF preview, if possible).

For scanned images, the scanning resolution at final image size ought to be as follows to ensure good reproduction: line art: >650 dpi; halftones (including gel photographs): >350 dpi; figures containing both halftone and line images: >650 dpi.

Color charges: Authors are advised to pay the full cost for the reproduction of their color artwork. Hence, please note that if there is color artwork in your manuscript when it is accepted for publication, we would require you to complete and return a Color Work Agreement form before your paper can be published. Also, you can email your editor to remove the color fee after acceptance of the paper.

Tips for Writing a Good Quality Engineering Research Paper

Techniques for writing a good quality engineering research paper:

1. Choosing the topic: In most cases, the topic is selected by the interests of the author, but it can also be suggested by the guides. You can have several topics, and then judge which you are most comfortable with. This may be done by asking several questions of yourself, like "Will I be able to carry out a search in this area? Will I find all necessary resources to accomplish the search? Will I be able to find all information in this field area?" If the answer to this type of question is "yes," then you ought to choose that topic. In most cases, you may have to conduct surveys and visit several places. Also, you might have to do a lot of work to find all the rises and falls of the various data on that subject. Sometimes, detailed information plays a vital role, instead of short information. Evaluators are human: The first thing to remember is that evaluators are also human beings. They are not only meant for rejecting a paper. They are here to evaluate your paper. So present your best aspect.

2. Think like evaluators: If you are in confusion or getting demotivated because your paper may not be accepted by the evaluators, then think, and try to evaluate your paper like an evaluator. Try to understand what an evaluator wants in your research paper, and you will automatically have your answer. Make blueprints of paper: The outline is the plan or framework that will help you to arrange your thoughts. It will make your paper logical. But remember that all points of your outline must be related to the topic you have chosen.

3. Ask your guides: If you are having any difficulty with your research, then do not hesitate to share your difficulty with your guide (if you have one). They will surely help you out and resolve your doubts. If you can't clarify what exactly you require for your work, then ask your supervisor to help you with an alternative. He or she might also provide you with a list of essential readings.

4. Use of computer is recommended: As you are doing research in the field of research engineering then this point is quite obvious. Use right software: Always use good quality software packages. If you are not capable of judging good software, then you can lose the quality of your paper unknowingly. There are various programs available to help you which you can get through the internet.

5. Use the internet for help: An excellent start for your paper is using Google. It is a wondrous search engine, where you can have your doubts resolved. You may also read some answers for the frequent question of how to write your research paper or find a model research paper. You can download books from the internet. If you have all the required books, place importance on reading, selecting, and analyzing the specified information. Then sketch out your research paper. Use big pictures: You may use encyclopedias like Wikipedia to get pictures with the best resolution. At Global Journals, you should strictly follow here.

6. Bookmarks are useful: When you read any book or magazine, you generally use bookmarks, right? It is a good habit which helps to not lose your continuity. You should always use bookmarks while searching on the internet also, which will make your search easier.

7. Revise what you wrote: When you write anything, always read it, summarize it, and then finalize it.

8. Make every effort: Make every effort to mention what you are going to write in your paper. That means always have a good start. Try to mention everything in the introduction—what is the need for a particular research paper. Polish your work with good writing skills and always give an evaluator what he wants. Make backups: When you are going to do any important thing like making a research paper, you should always have backup copies of it either on your computer or on paper. This protects you from losing any portion of your important data.

9. Produce good diagrams of your own: Always try to include good charts or diagrams in your paper to improve quality. Using several unnecessary diagrams will degrade the quality of your paper by creating a hodgepodge. So always try to include diagrams which were made by you to improve the readability of your paper. Use of direct quotes: When you do research relevant to literature, history, or current affairs, then use of quotes becomes essential, but if the study is relevant to science, use of quotes is not preferable.

10. Use proper verb tense: Use proper verb tenses in your paper. Use past tense to present those events that have happened. Use present tense to indicate events that are going on. Use future tense to indicate events that will happen in the future. Use of wrong tenses will confuse the evaluator. Avoid sentences that are incomplete.

11. Pick a good study spot: Always try to pick a spot for your research which is quiet. Not every spot is good for studying.

12. Know what you know: Always try to know what you know by making objectives, otherwise you will be confused and unable to achieve your target.

13. Use good grammar: Always use good grammar and words that will have a positive impact on the evaluator; use of good vocabulary does not mean using tough words which the evaluator has to find in a dictionary. Do not fragment sentences. Eliminate one-word sentences. Do not ever use a big word when a smaller one would suffice.

Verbs have to be in agreement with their subjects. In a research paper, do not start sentences with conjunctions or finish them with prepositions. When writing formally, it is advisable to never split an infinitive because someone will (wrongly) complain. Avoid clichés like a disease. Always shun irritating alliteration. Use language which is simple and straightforward. Put together a neat summary.

14. Arrangement of information: Each section of the main body should start with an opening sentence, and there should be a changeover at the end of the section. Give only valid and powerful arguments for your topic. You may also maintain your arguments with records.

15. Never start at the last minute: Always allow enough time for research work. Leaving everything to the last minute will degrade your paper and spoil your work.

16. Multitasking in research is not good: Doing several things at the same time is a bad habit in the case of research activity. Research is an area where everything has a particular time slot. Divide your research work into parts, and do a particular part in a particular time slot.

17. Never copy others' work: Never copy others' work and give it your name because if the evaluator has seen it anywhere, you will be in trouble. Take proper rest and food: No matter how many hours you spend on your research activity, if you are not taking care of your health, then all your efforts will have been in vain. For quality research, take proper rest and food.

18. Go to seminars: Attend seminars if the topic is relevant to your research area. Utilize all your resources.

19. Refresh your mind after intervals: Try to give your mind a rest by listening to soft music or sleeping in intervals. This will also improve your memory. Acquire colleagues: Always try to acquire colleagues. No matter how sharp you are, if you acquire colleagues, they can give you ideas which will be helpful to your research.

20. Think technically: Always think technically. If anything happens, search for its reasons, benefits, and demerits. Think and then print: When you go to print your paper, check that tables are not split, headings are not detached from their descriptions, and page sequence is maintained.

21. Adding unnecessary information: Do not add unnecessary information like "I have used MS Excel to draw graphs." Irrelevant and inappropriate material is superfluous. Foreign terminology and phrases are not apropos. One should never take a broad view. Analogy is like feathers on a snake. Use words properly, regardless of how others use them. Remove quotations. Puns are for kids, not grunt readers. Never oversimplify: When adding material to your research paper, never go for oversimplification; this will definitely irritate the evaluator. Be specific. Never use rhythmic redundancies. Contractions shouldn't be used in a research paper. Comparisons are as terrible as clichés. Give up ampersands, abbreviations, and so on. Remove commas that are not necessary. Parenthetical words should be between brackets or commas. Understatement is always the best way to put forward earth-shaking thoughts. Give a detailed literary review.

22. Report concluded results: Use concluded results. From raw data, filter the results, and then conclude your studies based on measurements and observations taken. An appropriate number of decimal places should be used. Parenthetical remarks are prohibited here. Proofread carefully at the final stage. At the end, give an outline to your arguments. Spot perspectives of further study of the subject. Justify your conclusion at the bottom sufficiently, which will probably include examples.

23. Upon conclusion: Once you have concluded your research, the next most important step is to present your findings. Presentation is extremely important as it is the definite medium though which your research is going to be in print for the rest of the crowd. Care should be taken to categorize your thoughts well and present them in a logical and neat manner. A good quality research paper format is essential because it serves to highlight your research paper and bring to light all necessary aspects of your research.

Informal Guidelines of Research Paper Writing

Key points to remember:

- Submit all work in its final form.
- Write your paper in the form which is presented in the guidelines using the template.
- Please note the criteria peer reviewers will use for grading the final paper.

Final points:

One purpose of organizing a research paper is to let people interpret your efforts selectively. The journal requires the following sections, submitted in the order listed, with each section starting on a new page:

The introduction: This will be compiled from reference matter and reflect the design processes or outline of basis that directed you to make a study. As you carry out the process of study, the method and process section will be constructed like that. The results segment will show related statistics in nearly sequential order and direct reviewers to similar intellectual paths throughout the data that you gathered to carry out your study.

The discussion section:

This will provide understanding of the data and projections as to the implications of the results. The use of good quality references throughout the paper will give the effort trustworthiness by representing an alertness to prior workings.

Writing a research paper is not an easy job, no matter how trouble-free the actual research or concept. Practice, excellent preparation, and controlled record-keeping are the only means to make straightforward progression.

General style:

Specific editorial column necessities for compliance of a manuscript will always take over from directions in these general guidelines.

To make a paper clear: Adhere to recommended page limits.

Mistakes to avoid:

- Insertion of a title at the foot of a page with subsequent text on the next page.
- Separating a table, chart, or figure—confine each to a single page.
- Submitting a manuscript with pages out of sequence.
- In every section of your document, use standard writing style, including articles ("a" and "the").
- Keep paying attention to the topic of the paper.

- Use paragraphs to split each significant point (excluding the abstract).
- Align the primary line of each section.
- Present your points in sound order.
- Use present tense to report well-accepted matters.
- Use past tense to describe specific results.
- Do not use familiar wording; don't address the reviewer directly. Don't use slang or superlatives.
- Avoid use of extra pictures—include only those figures essential to presenting results.

Title page:

Choose a revealing title. It should be short and include the name(s) and address(es) of all authors. It should not have acronyms or abbreviations or exceed two printed lines.

Abstract: This summary should be two hundred words or less. It should clearly and briefly explain the key findings reported in the manuscript and must have precise statistics. It should not have acronyms or abbreviations. It should be logical in itself. Do not cite references at this point.

An abstract is a brief, distinct paragraph summary of finished work or work in development. In a minute or less, a reviewer can be taught the foundation behind the study, common approaches to the problem, relevant results, and significant conclusions or new questions.

Write your summary when your paper is completed because how can you write the summary of anything which is not yet written? Wealth of terminology is very essential in abstract. Use comprehensive sentences, and do not sacrifice readability for brevity; you can maintain it succinctly by phrasing sentences so that they provide more than a lone rationale. The author can at this moment go straight to shortening the outcome. Sum up the study with the subsequent elements in any summary. Try to limit the initial two items to no more than one line each.

Reason for writing the article—theory, overall issue, purpose.

- Fundamental goal.
- To-the-point depiction of the research.
- Consequences, including definite statistics—if the consequences are quantitative in nature, account for this; results of any numerical analysis should be reported. Significant conclusions or questions that emerge from the research.

Approach:

- Single section and succinct.
- An outline of the job done is always written in past tense.
- Concentrate on shortening results—limit background information to a verdict or two.
- Exact spelling, clarity of sentences and phrases, and appropriate reporting of quantities (proper units, important statistics) are just as significant in an abstract as they are anywhere else.

Introduction:

The introduction should "introduce" the manuscript. The reviewer should be presented with sufficient background information to be capable of comprehending and calculating the purpose of your study without having to refer to other works. The basis for the study should be offered. Give the most important references, but avoid making a comprehensive appraisal of the topic. Describe the problem visibly. If the problem is not acknowledged in a logical, reasonable way, the reviewer will give no attention to your results. Speak in common terms about techniques used to explain the problem, if needed, but do not present any particulars about the protocols here.

The following approach can create a valuable beginning:

- Explain the value (significance) of the study.
- Defend the model—why did you employ this particular system or method? What is its compensation? Remark upon its appropriateness from an abstract point of view as well as pointing out sensible reasons for using it.
- Present a justification. State your particular theory(-ies) or aim(s), and describe the logic that led you to choose them.
- Briefly explain the study's tentative purpose and how it meets the declared objectives.

Approach:

Use past tense except for when referring to recognized facts. After all, the manuscript will be submitted after the entire job is done. Sort out your thoughts; manufacture one key point for every section. If you make the four points listed above, you will need at least four paragraphs. Present surrounding information only when it is necessary to support a situation. The reviewer does not desire to read everything you know about a topic. Shape the theory specifically—do not take a broad view.

As always, give awareness to spelling, simplicity, and correctness of sentences and phrases.

Procedures (methods and materials):

This part is supposed to be the easiest to carve if you have good skills. A soundly written procedures segment allows a capable scientist to replicate your results. Present precise information about your supplies. The suppliers and clarity of reagents can be helpful bits of information. Present methods in sequential order, but linked methodologies can be grouped as a segment. Be concise when relating the protocols. Attempt to give the least amount of information that would permit another capable scientist to replicate your outcome, but be cautious that vital information is integrated. The use of subheadings is suggested and ought to be synchronized with the results section.

When a technique is used that has been well-described in another section, mention the specific item describing the way, but draw the basic principle while stating the situation. The purpose is to show all particular resources and broad procedures so that another person may use some or all of the methods in one more study or referee the scientific value of your work. It is not to be a step-by-step report of the whole thing you did, nor is a methods section a set of orders.

Materials:

Materials may be reported in part of a section or else they may be recognized along with your measures.

Methods:

- Report the method and not the particulars of each process that engaged the same methodology.
- Describe the method entirely.
- To be succinct, present methods under headings dedicated to specific dealings or groups of measures.
- Simplify—detail how procedures were completed, not how they were performed on a particular day.
- If well-known procedures were used, account for the procedure by name, possibly with a reference, and that's all.

Approach:

It is embarrassing to use vigorous voice when documenting methods without using first person, which would focus the reviewer's interest on the researcher rather than the job. As a result, when writing up the methods, most authors use third person passive voice.

Use standard style in this and every other part of the paper—avoid familiar lists, and use full sentences.

What to keep away from:

- Resources and methods are not a set of information.
- Skip all descriptive information and surroundings—save it for the argument.
- Leave out information that is immaterial to a third party.

Results:

The principle of a results segment is to present and demonstrate your conclusion. Create this part as entirely objective details of the outcome, and save all understanding for the discussion.

The page length of this segment is set by the sum and types of data to be reported. Use statistics and tables, if suitable, to present consequences most efficiently.

You must clearly differentiate material which would usually be incorporated in a study editorial from any unprocessed data or additional appendix matter that would not be available. In fact, such matters should not be submitted at all except if requested by the instructor.

Content:

- Sum up your conclusions in text and demonstrate them, if suitable, with figures and tables.
- In the manuscript, explain each of your consequences, and point the reader to remarks that are most appropriate.
- Present a background, such as by describing the question that was addressed by creation of an exacting study.
- Explain results of control experiments and give remarks that are not accessible in a prescribed figure or table, if appropriate.
- Examine your data, then prepare the analyzed (transformed) data in the form of a figure (graph), table, or manuscript.

What to stay away from:

- Do not discuss or infer your outcome, report surrounding information, or try to explain anything.
- Do not include raw data or intermediate calculations in a research manuscript.
- Do not present similar data more than once.
- A manuscript should complement any figures or tables, not duplicate information.
- Never confuse figures with tables—there is a difference.

Approach:

As always, use past tense when you submit your results, and put the whole thing in a reasonable order.

Put figures and tables, appropriately numbered, in order at the end of the report.

If you desire, you may place your figures and tables properly within the text of your results section.

Figures and tables:

If you put figures and tables at the end of some details, make certain that they are visibly distinguished from any attached appendix materials, such as raw facts. Whatever the position, each table must be titled, numbered one after the other, and include a heading. All figures and tables must be divided from the text.

Discussion:

The discussion is expected to be the trickiest segment to write. A lot of papers submitted to the journal are discarded based on problems with the discussion. There is no rule for how long an argument should be.

Position your understanding of the outcome visibly to lead the reviewer through your conclusions, and then finish the paper with a summing up of the implications of the study. The purpose here is to offer an understanding of your results and support all of your conclusions, using facts from your research and generally accepted information, if suitable. The implication of results should be fully described.

Infer your data in the conversation in suitable depth. This means that when you clarify an observable fact, you must explain mechanisms that may account for the observation. If your results vary from your prospect, make clear why that may have happened. If your results agree, then explain the theory that the proof supported. It is never suitable to just state that the data approved the prospect, and let it drop at that. Make a decision as to whether each premise is supported or discarded or if you cannot make a conclusion with assurance. Do not just dismiss a study or part of a study as "uncertain."

Research papers are not acknowledged if the work is imperfect. Draw what conclusions you can based upon the results that you have, and take care of the study as a finished work.

- You may propose future guidelines, such as how an experiment might be personalized to accomplish a new idea.
- Give details of all of your remarks as much as possible, focusing on mechanisms.
- Make a decision as to whether the tentative design sufficiently addressed the theory and whether or not it was correctly restricted. Try to present substitute explanations if they are sensible alternatives.
- One piece of research will not counter an overall question, so maintain the large picture in mind. Where do you go next? The best studies unlock new avenues of study. What questions remain?
- Recommendations for detailed papers will offer supplementary suggestions.

Approach:

When you refer to information, differentiate data generated by your own studies from other available information. Present work done by specific persons (including you) in past tense.

Describe generally acknowledged facts and main beliefs in present tense.

THE ADMINISTRATION RULES

Administration Rules to Be Strictly Followed before Submitting Your Research Paper to Global Journals Inc.

Please read the following rules and regulations carefully before submitting your research paper to Global Journals Inc. to avoid rejection.

Segment draft and final research paper: You have to strictly follow the template of a research paper, failing which your paper may get rejected. You are expected to write each part of the paper wholly on your own. The peer reviewers need to identify your own perspective of the concepts in your own terms. Please do not extract straight from any other source, and do not rephrase someone else's analysis. Do not allow anyone else to proofread your manuscript.

Written material: You may discuss this with your guides and key sources. Do not copy anyone else's paper, even if this is only imitation, otherwise it will be rejected on the grounds of plagiarism, which is illegal. Various methods to avoid plagiarism are strictly applied by us to every paper, and, if found guilty, you may be blacklisted, which could affect your career adversely. To guard yourself and others from possible illegal use, please do not permit anyone to use or even read your paper and file.

CRITERION FOR GRADING A RESEARCH PAPER (COMPILATION) BY GLOBAL JOURNALS

Please note that following table is only a Grading of "Paper Compilation" and not on "Performed/Stated Research" whose grading solely depends on Individual Assigned Peer Reviewer and Editorial Board Member. These can be available only on request and after decision of Paper. This report will be the property of Global Journals.

Topics	Grades		
	A-B	**C-D**	**E-F**
Abstract	Clear and concise with appropriate content, Correct format. 200 words or below	Unclear summary and no specific data, Incorrect form Above 200 words	No specific data with ambiguous information Above 250 words
Introduction	Containing all background details with clear goal and appropriate details, flow specification, no grammar and spelling mistake, well organized sentence and paragraph, reference cited	Unclear and confusing data, appropriate format, grammar and spelling errors with unorganized matter	Out of place depth and content, hazy format
Methods and Procedures	Clear and to the point with well arranged paragraph, precision and accuracy of facts and figures, well organized subheads	Difficult to comprehend with embarrassed text, too much explanation but completed	Incorrect and unorganized structure with hazy meaning
Result	Well organized, Clear and specific, Correct units with precision, correct data, well structuring of paragraph, no grammar and spelling mistake	Complete and embarrassed text, difficult to comprehend	Irregular format with wrong facts and figures
Discussion	Well organized, meaningful specification, sound conclusion, logical and concise explanation, highly structured paragraph reference cited	Wordy, unclear conclusion, spurious	Conclusion is not cited, unorganized, difficult to comprehend
References	Complete and correct format, well organized	Beside the point, Incomplete	Wrong format and structuring

INDEX

save our planet

Global Journal of Researches in Engineering

Visit us on the Web at www.GlobalJournals.org | www.EngineeringResearch.org
or email us at helpdesk@globaljournals.org

ISSN 9755861